

Politecnico di Torino

Performance Optimization, Data Analysis and Simulation of a Formula SAE Electric Racing Car

Tesi di Laurea Magistrale in Automotive Engineering



Relatore

Prof. Andrea Tonoli

Candidato

Alessandro Girauda



Anno Accademico 2018-2019

Abstract

The following topics concern the role I had for 2 years in the Formula SAE team of the Politecnico di Torino, "Squadra Corse", which sees, every year, a group of young engineers intent on designing and building a high-performance electric vehicle, to compete at world level, against other universities, in Formula Student. This thesis is the collection of data analysis, projects and developments obtained during my period in the Team, in the vehicle dynamic and controls department, completed in the role of race telemetry responsible. The study addresses the issues of vehicle sensor instrumentation, data acquisition and analysis, vehicle simulation through CAE tools and finally the optimization of vehicle performance.

Torino,
2019

A. Giraudò

Summary

Chapter 1

| | |
|----------------------------------|---|
| 1.1 Formula SAE | 7 |
| 1.2 Squadra Corse – Polito | 9 |

Chapter 2

| | |
|---|----|
| 2.1 The Importance of Data Analysis | 11 |
| 2.2 The CAN Network | 12 |
| 2.3 Sensors and Data Logging | 12 |
| 2.4 The Bi-Directional Telemetry | 19 |

Chapter 3

| | |
|------------------------------|----|
| 3.1 Autocross Event | 23 |
| 3.2 Race Data Analysis | 27 |

Chapter 4

| | |
|--------------------------------------|----|
| 4.1 Vi-Grade CarRealTime | 40 |
| 4.2 Vehicle Model Creation | 42 |
| 4.3 Creation of the race track | 76 |
| 4.4 Static Lap Time Simulation | 77 |

Chapter 5

| | |
|---|-----|
| 5.1 Vehicle Performance Parameters | 79 |
| 5.2 Centre of Gravity Longitudinal Optimization | 80 |
| 5.3 Wheelbase Length Optimization | 89 |
| 5.4 Toe-in Toe-out angle Optimization | 95 |
| 5.5 Camber Angle Optimization | 102 |

Chapter 6

| | |
|--------------------------------------|-----|
| 6.1 Max Performance Simulation | 110 |
| 6.2 Evaluations and Results | 117 |

Chapter 7

| | |
|----------------------------|-----|
| 7.1 Conclusions.. | 120 |
| 7.2 Acknowledgements | 120 |

| | |
|--------------|------|
| Bibliography | 120 |
| APPENDIX | 1204 |

Chapter 1

Squadra Corse Polito – Formula SAE

1.1 Formula SAE

Testing yourself. This is the definition that I think is best suited to describe what the SAE formula is: one day, you realize that all the theory, equations, calculations and exercises that the professor assigns you, are no longer enough. You love the job you are learning, but at the same time you feel suffocated in a book. You are tired of following the lessons, copying notes and concentrating your studies only on achieving a grade, an exam that will unjustly determine your career and life. If you find yourself reflected in all this, well, you're in the right place.

Established in 1981, Formula SAE, or *Formula Student*, is an international university engineering design competition initially proposed by the Society of Automotive Engineers (SAE) that involves the design and production of a racing vehicle, evaluated during a series of tests based on its design qualities and engineering efficiency.

The aim of the initiative is to give university students the opportunity to participate in a competition that gives them the opportunity to put into practice what they have learned during their studies, deepening their knowledge but also learning other engineering fields (and not) that the student has never had the opportunity to know, because they belong to other university courses: the mechanical engineer will design and produce its components, but has also to assist his teammate, electrical engineer, in the wiring of the vehicle, as well as the designer will take care of the graphics of the car, but at the same time will have to mount the tires on the new rims, to get in time for track tests.

What is created in the Formula SAE, is a real team of colleagues, friends, people who support each other to reach a common goal: see their vehicle race on track and win.

This is one of the most important things in my opinion of the SAE formula: to teach the method to work together, to be tolerant, to help each other but at the same time to be respected by and respect your teammate. All this cannot be learned in a school book and often, today's university students come out of universities full of sacks and with a sheet of paper, presenting themselves at their first job without having understood what work is, how they work and without ever "getting their hands dirty".

This competition is spread all over the world, with several annual events, organized directly by SAE or by the various national associations of engineers and technicians of the automobile, thus allowing you to meet many people and colleagues in the field of engineering, making it possible to compare and exchange ideas and constructive opinions with realities different from ours.

Currently, the categories of each competition are 3: Class 1C (for petrol vehicles), Class 1E (for electric vehicles) and Class 1D (for driverless vehicles). In addition, there is a fourth one, called Class 3, in which teams that present only the design of the car participate, thus not participating in static and

dynamic events. Since 2017 Formula Student Germany, active as an official event of German SAE formula since 2005, has proposed its own version of the competition, renaming it "Formula Student", based on the same concept conceived by SAE, but with some minor changes in the regulations.

1.2 Squadra Corse – Polito

Squadra Corse is the name of the Formula SAE Team of the Polytechnic of Turin that has allowed, and allows every year, this incredible experience. The team, initially born with the design of internal combustion engine vehicles, has updated itself, for some years now, to the now most competitive and innovative world of the electric. The vehicle designed and treated in the following thesis, is a fully electric single-seater with the following main features:

- 4-wheel drive configuration with an electric motor mounted on each wheel;
- AMK motors with 35 kW peak power;
- Epicycloidal transmissions housed in the wheel hub;
- Carbon fibre monocoque;
- "Push rod" type suspension on both axles with a particular glass fibre knife antiroll bars;
- 13-inch Pirelli tyres;
- Aerodynamic package complete with front wing, rear wing, diffuser and sidepods;
- Battery pack made of lithium-polymer cells with a total capacity of 7.46 kWh;
- Bi-Directional telemetry.



The car has a power of 80 kW, limited by the regulations, which, thanks to its low weight, translates into a very high power-to-weight ratio, reaching 100 km/h starting from a standstill, in 2.5 seconds. The main objective of the project was to create a reliable vehicle, a feature that had been missing from the team for years. To do this, it was decided to use commercial electronic components, a choice that proved to be appropriate also due to the fact that there were 25 members in the team. This approach was successful: the team managed to make the car in the right time and participated in all three European races, taking third place in the over-all classification of the Italian race, a podium that had been missing for some time. This single-seater has achieved the best results since 2012, when the team began to design electric vehicles.

Chapter 2

Race Telemetry and Data Acquisition

2.1 The Importance of Data Analysis

In modern motor racing, data analysis is the basis for technological development and continuous progress. Designing a system without being able to know how it behaves, makes engineering developments very complex. The engineer has always needed to check and verify what happens in the built prototypes and in the outside world. In order to verify the behaviour of the vehicle and its components, it is necessary to use special sensors which, depending on their purpose, measure physical and chemical parameters, transmitting the data to the appropriate control unit which checks, orders and uses them. With special instruments, called data loggers, it is possible to record the signals coming from the vehicle control unit and from the sensors installed, thus allowing the engineer to study them. It is his task to develop the ability to analyze a system, looking and interpolating graphs and numbers.

2.2 The CAN Network

To allow communication and data exchange between all electronic devices on board, the most famous protocol in the automotive field has been used: the CAN BUS. CAN protocol (Controller Area Network) is a digital communication serial bus of the "broadcast" type. Introduced by Bosch in the early 1980s for automotive applications, it allows microcontrollers and devices communications with each other applications without a host computer, making it one of the most popular systems used in many industrial sectors. The spread of this protocol is due to its own characteristics:

- Simplicity and flexibility in wiring
- Response times
- High immunity to disturbances
- Errors confinement
- High reliability
- Cost
- Maturity of the Standard

On our racing vehicle, 4 CAN Bus lines was implemented, transmitting data at a speed of 1 MBaud. These lines are dedicated to different electronic systems:

- 2 lines for the Traction Control
- 1 line for the Data Collection only
- 1 line dedicated to the Energy Meter sensor

2.3 Sensors and Data Logging

The main characters on the network used by the data analysis are:

- ECU: the electronic control unit is a commercial *dSpace MicroAutobox II*,

installed behind the firewall. This unit collects data from all sensors, runs the control program and communicates with telemetry.



- IMU: the Inertial Measuring Unit is an electronic device that measures and reports a body's specific force, angular rate, orientation of the body, using a combination of accelerometers, gyroscopes, and magnetometers. In our vehicle, it is a *Bosch Acceleration Sensor MM5.10*, that includes MEMS measuring elements connected to an appropriate integrated circuit. A rotational acceleration around the integrated sensing elements generates a Coriolis force which changes the internal capacity of the micro machined sensing parts. Furthermore, a pure surface micro machined element is used to measure the vehicle linear acceleration in all 3 axis. This combination of rotational and lineal acceleration sensors enables a precise measurement of the vehicle dynamics. The main feature and benefit of this sensor is the combination of 3 linear and 2 rotational accelerometers and its high speed 1 Mbaud/s CAN-signal output.



| Parameter | Value |
|--|------------------------------|
| <u>APPLICATION A : 2-axis Rotation Rate</u> | |
| Measuring Range | ±160°/s (roll rate/yaw rate) |
| Over range limit | ± 1,000°/s |
| Absolute physical Resolution | 0.1°/s |
| Cut-off frequency (-3 dB) | 15 Hz; 30 Hz; 60 Hz |
| <u>APPLICATION B: 3-axis Accelerometer</u> | |
| Measuring Range | ±4.2 g |
| Over range limit | ±10 g |
| Absolute physical Resolution | 0.01 g |
| Cut-off frequency (-3 dB) | 15 Hz; 30 Hz; 60 Hz |
| <u>Common Characteristics</u> | |
| Operating Temperature Range | -20 to 85°C |
| Can Speed | 1 Mbaud/s or 500 kbaud/s |
| Power Supply | 7 to 18 V |
| Max input current | 90 mA |

- Brake Pedal sensor: in order to be able to know the percentage of request that the driver applies on the brake pedal, there may be different strategies:

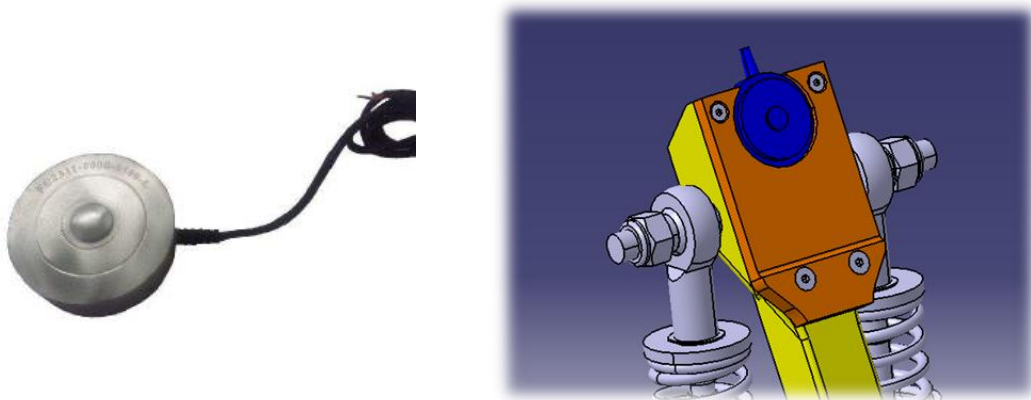
1. *Compression Load Cell*: it is an electronic component, called transducer, used to measure a force applied to an object (usually a mechanical component) by measuring an electrical signal that varies due to the deformation that this force produces on the component. With the application of that sensor on the brake pedal, we can measure the force applied by the driver to it and so, with a calibration of the component, his request. Our component is the *TE connectivity FC23 model*. The advantages of this type of sensor is related to

- Interchangeability
- Low noise
- Fast Response time

- Low weight

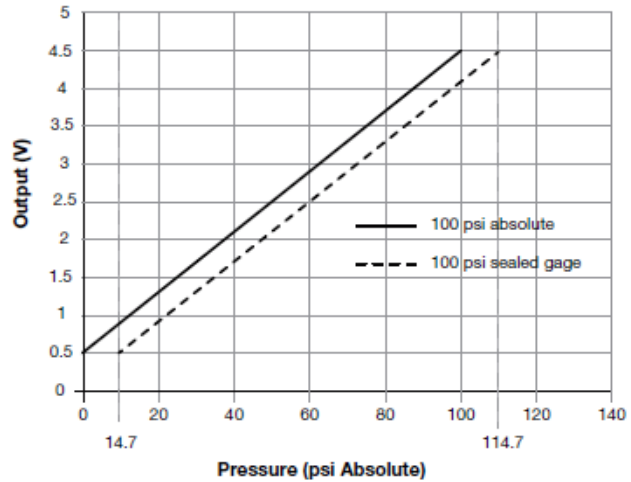
| Parameter | Value |
|-----------------------------|----------------|
| Measuring Range | 50 to 2000 lbf |
| Span | 3.8 to 4.2 V |
| Zero Force Output | 0.3 to 0.7 V |
| Accuracy | ±0.03 %FS |
| Response Time | 1.0 ms |
| Operating Temperature Range | -40 to 85°C |
| Power Supply | 4.5 to 5.5 V |

The functionality of the load cell, installed in the housing of the brake pedal, is also related to the implementation of a regenerative braking system: knowing the pressure of the driver on the pedal, allows you to divide the braking in 2 steps: the first, lighter, implemented only by electric motors that then, regenerate energy, sending it to the battery pack. Once a certain pressure threshold has been exceeded, a second hydraulic braking action is added.



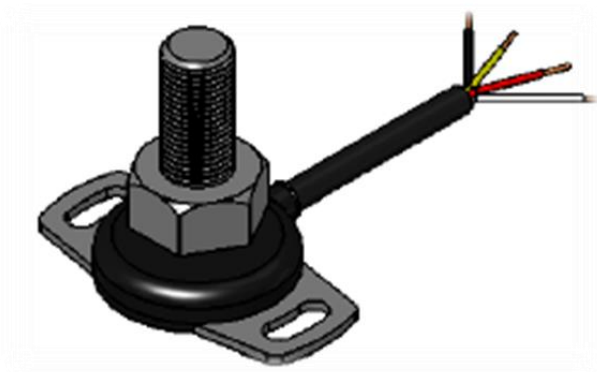
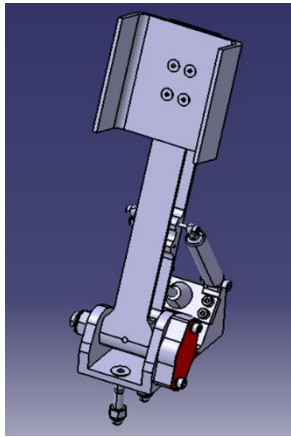
2. *Pressure sensor*: the second solution, to accurately measure the braking demand of the driver, is to install a pressure sensor directly on the braking circuit. In this case, we used *Honeywell's PX3 Series Pressure Transducers* that use piezoresistive sensing technology, with a pressure range from 1 to 46 bar, giving a

radiometric output from 0.5Vdc to 4.5Vdc, fully calibrated. In this case it is also possible to control in a better way the braking circuit, with a more expensive solution than the previous one. The image below shows the sensor used and the operating scale



| Parameter | Value |
|-----------------------------|--------------------|
| Measuring Range | 1 bar to 46 bar |
| Span | 0.5 Vdc to 4.5 Vdc |
| Response Time | <2 ms |
| Operating Temperature Range | -40 °C to 125 °C |
| Power Supply | 5 Vdc ±0.25 Vdc |
| Max input current | 3.5 mA |

- Throttle Pedal sensor: in order to acquire the driver's accelerator request percentage, the solution with last year's estensimeter was improved, replacing it with a *Magnetic Hall effect sensor*, with high accuracy (12 bit signal in a 20° range) which made possible to improve the signal and the packaging of the pedal box.



- **Steering Sensor:** in order to measure the driver's request on the steering wheel, it is necessary to install a sensor on the steering column, which is sensitive to the rotation around its axis. We used a *Rotary sensor with Hall effect*, from *Avio Race*, suitable for use in the motorsport field thanks to its immunity to disturbances and temperature stability.



| Parameter | Value |
|-----------------------------|-------------|
| Measuring Range | 0÷360° |
| Response Frequency | >250Hz |
| Accuracy | ±0,03 %FS |
| Operating Temperature Range | -40 to 85°C |
| Power Supply | 5 Vdc |
| Max Input Current | 20 mA |

In addition to all the sensors installed specifically on the vehicle, all the signals coming from the sensors already present in some fundamental components must also be considered:

- Electric Motors: *AMK* electric motors, installed directly on the wheel hub, have sensors that measure the rotational speed generated. These signals, one for each wheel, were used to calculate the speeds of the 4 wheels, and then derive the estimated speed of the vehicle. In the same way, the torques that the motors deliver to each individual wheel are obtained.
- Inverter: a key element capable of converting an input direct current (that of the battery pack) into an output alternating current (required by the motors), sends useful information such as current flow and possible errors, which can create malfunctions in the system.
- BMS: battery management system, powered by *Podium Engineering* is the electronic heart of the battery pack. It manages the charge and discharge of individual cells and modules, ensuring their operation. The BMS sends data on residual voltage in the battery pack, SOC, state of charge of the cells and especially their temperature, in order to monitor a proper functioning of the same.
- Data Logger: all the signals described so far, sent to the electronic control unit, are collected and saved in a device, mounted on the vehicle, called *Data Logger Vector GL type*, which records everything that the sensors detect on an SD card. This technique is an excellent way to record everything that happens on the vehicle during testing, but it has limits: it is impossible to have real-time information on the status of the vehicle (because it must necessarily be extracted the SD card).

Moreover, during tests and races, it is not possible to act from the pits on the vehicle parameters. The driver is therefore left alone.



2.4 The Bi-Directional Telemetry

A bi-directional telemetry system has been adopted to obtain information on the vehicle in real time, during tests and races, in order to optimise its performance and reliability. The telemetry system consists of a 2.4 Ghz wifi modem, mounted on the vehicle and connected directly to the dSpace control unit. It communicates by sending and receiving data with the wifi modem to the boxes. Being of bi-directional type, besides the analysis of the data sent by the vehicle, it is possible to act on the control parameters directly on the vehicle. This improvement has allowed a total control of the vehicle from the pits, with the possibility to vary the race strategy in an active way. Real Time data analysis is carried out using the *dSpace Control Desk* software, which allows customization to facilitate immediate reading of the basic parameters, which were filtered.

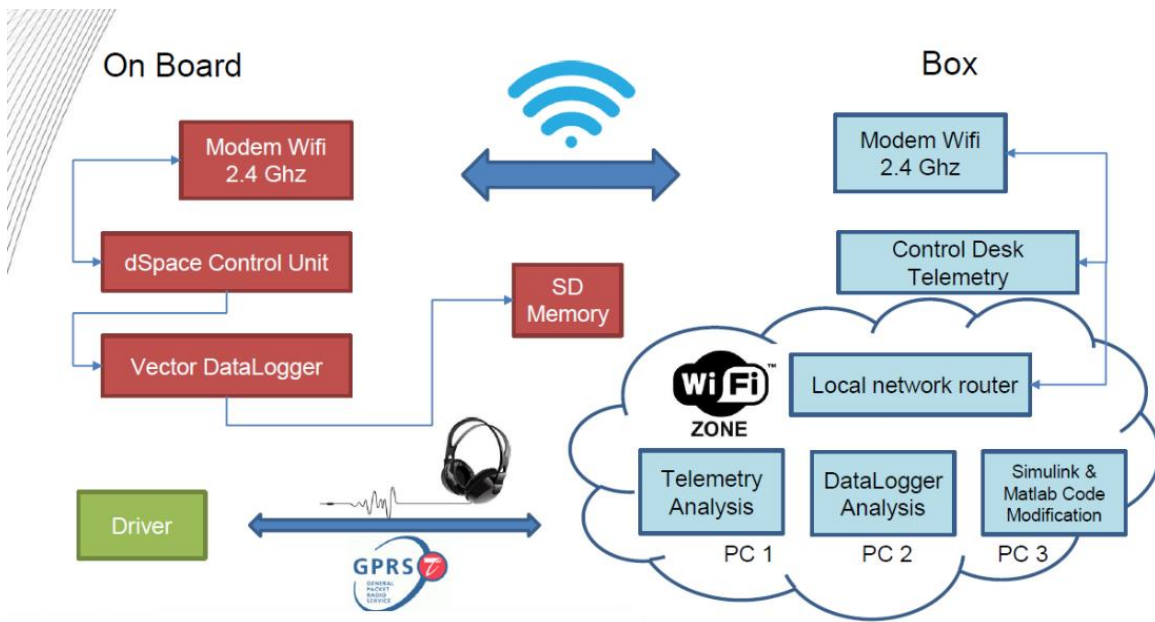
| | | | | | |
|---------------------------------------|---------------------|---------------------|---------------------|----------------------------------|----------------------------|
| START | BMS_eCtorSts | Throttle | mapTop | CAN_LV_dash_lapTime/dash_lapTime | |
| 1 | 4 | 0 | 1 | 14.74 | |
| Energy | | Temperatures | | Velocities | |
| energyMeter_voltage | energyMeter_current | FL/AMK_TempMotor | FR/AMK_TempMotor | FL/AMK_ActualVelocity | FR/AMK_ActualVelocity |
| 526.8 | -2.2 | 53.5 | 62.7 | 5906 | 6896 |
| Instant Power | avgPowerFromStart | RL/AMK_TempMotor | RR/AMK_TempMotor | RL/AMK_ActualVelocity | RR/AMK_ActualVelocity |
| 1.8 | 1117.1 | 68 | 93 | 5917 | 6950 |
| power integral (consumed energy)/Out1 | | FL/AMK_TempInverter | FR/AMK_TempInverter | PRE-TC Torques | |
| 2654.8 | | 45.4 | 47.5 | OLD Control System/Torque2 | OLD Control System/Torque1 |
| | | RL/AMK_TempInverter | RR/AMK_TempInverter | 0.0 | 0.0 |
| | | 44.8 | 48.2 | OLD Control System/Torque3 | OLD Control System/Torque4 |
| | | FL/AMK_TempIGBT | FR/AMK_TempIGBT | 0.0 | 0.0 |
| | | 57.4 | 55.6 | | |
| | | RL/AMK_TempIGBT | RR/AMK_TempIGBT | | |
| | | 67.5 | 62.3 | | |
| | | BMS_TTabAvg | BMS_TTabHi | | |
| | | -19.8 | 36.0 | | |
| Inverter Status | | | | | |
| FL/ROX_delta time | FR/ROX_delta time | | | | |
| 0.00299 | 0.00300 | | | | |
| RL/ROX_delta time | RR/ROX_delta time | | | | |
| 0.00299 | 0.00300 | | | | |
| FL/AMK_ErrorInfo | FR/AMK_ErrorInfo | | | | |
| 0 | 0 | | | | |
| RL/AMK_ErrorInfo | RR/AMK_ErrorInfo | | | | |
| 0 | 0 | | | | |

The main parameters and data analyzed in real time during the race are listed and described below:

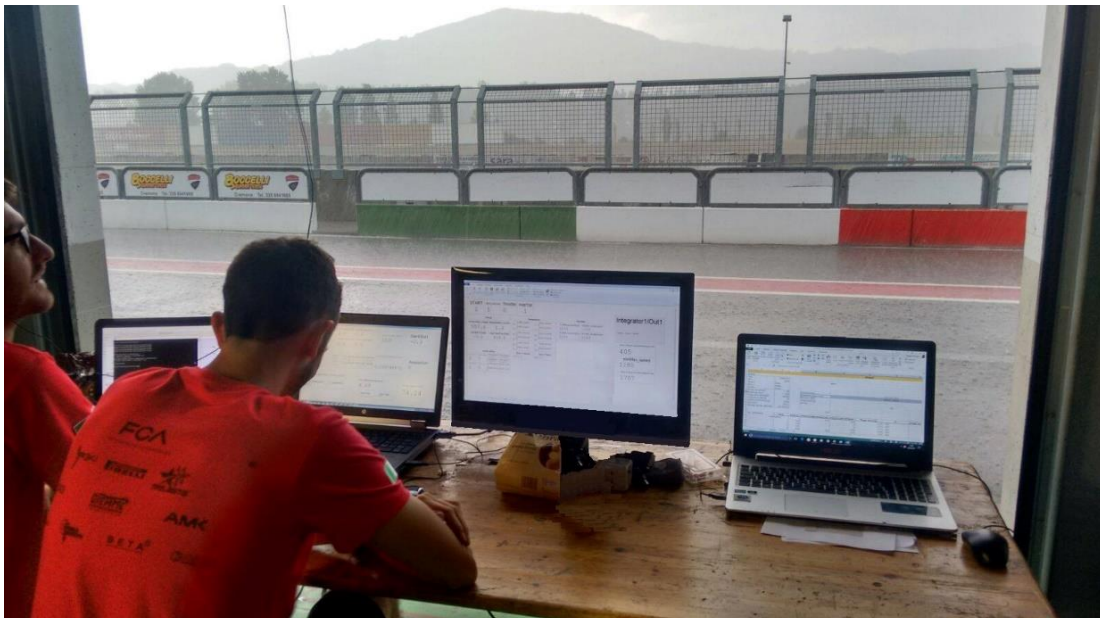
- *Power on/off Status*
- *BMS Status*: indicate the state of the battery management system
- *Inverter Status*: indicate the function code of the inverter and, in case of errors, permits to identify what is the problem
- *Throttle Percentage*: Gas pedal request
- *Control Unit Map*: indicate what is the driver control unit selected on the steering wheel. We have created different maps for all the 4 different race tests.
- *Energy Consumption*: allows you to know the amount of energy consumed by the vehicle, so you can calculate the remaining energy and manage the endurance race in the best way, without running out of power.
- *Battery State of Charge*: allows you to know the percentage of charge remaining in the battery pack.

- *Motors Temperature:* allows you to keep one of the most delicate parameters of our vehicle under control. Engine temperature management is essential to avoid failures that can lead to engine shutdown.
- *Inverter Temperature:* in the same way as the motors, it is necessary to monitor the operation of the inverter and its dedicated cooling circuit.
- *Battery Pack Temperature:* the temperature of the battery pack must be monitored to ensure correct use of the cells. This component has been a big problem for years, as a good flow of fresh air inside the battery pack was not guaranteed, in order to cool the cells. They have relatively low ideal operating temperatures.
- *Motors instantaneous Velocity & Torque:* parameters directly coming from the electric motor sensors
- *Traction Control & Torque Vectoring Parameters:* parameters integrated in the Simulink code of the electronic controls present on the vehicle. These parameters are gains that allows to adjust the behavior of the control according to the driver's requests.
- *Errors Message/Code*

These parameters were analyzed in the pits, dividing the various roles between car status control, consumption calculation and race management, performance analysis and electronic control tuning. In addition, the driver was in constant connection with the pits, and was informed of the machine status, with the consequent updating of the race strategy and could at the same time make requests to change the behavior of electronic controls. In the diagram below the structure of the system is illustrated.



The image below was taken during an event in Varano de Melegari, where data analysis and telemetry of the vehicle, running in the rain, was carried out.



Chapter 3

Data Analysis

3.1 Autocross Event

Autocross tests the vehicle's overall dynamic performance by running the car through a series of tight obstacles. Setup for the event is driven by guidelines within the rules. The track setup can vary widely depending upon the facilities available and the track designer's prerogative. Generally the track should be 805 meters in length with average speeds in the range of 40 to 48 kilometers per hour. Track design elements may be any of the following outlined in the rules but are not limited to these alone.

- Straights: No longer than 60 m (200 feet) with hairpins at both ends (or) no longer than 45 m (150 feet) with wide turns on the ends.
- Constant Turns: 23 m (75 feet) to 45 m (148 feet) diameter.
- Hairpin Turns: Minimum of 9 m (29.5 feet) outside diameter (of the turn).
- Slaloms: Cones in a straight line with 7.62 m (25 feet) to 12.19 m (40 feet)

spacing.

- Miscellaneous: Chicanes, multiple turns, decreasing radius turns, etc. The minimum track width will be 3.5 m (11.5 feet)

Each driver gets 2 runs, which may be run in succession. The vehicle is staged 6 meters behind the starting line where it starts from a stand still. Penalties of 20 seconds and 2 seconds are applied for going off course and hitting cones respectively. Scores are determined from the team's corrected run time, the minimum run time for the event, and the calculated maximum time. The maximum time is 125% of the minimum time; teams that exceed the max time score 7.5 points for completing the event. Times within the scoring range receive points by the following equation.

$$Score_{Autocross} = 142.5 \times \frac{(T_{Max}/T_{Your}) - 1}{(T_{Max}/T_{Min}) - 1} + 7.5$$

$$T_{Max} = 1.25 \times T_{Min}$$

Autocross course layout has similar performance affecting characteristics as the endurance event, which will host the discussion of those attributes. Special considerations that distinguish autocross from endurance are the lack of energy economy judging and limited run time to reach steady state conditions. For vehicle performance, motor mapping should provide maximum power when demanded without consideration for fuel economy. The transient nature of the runs, which is comparable to both skidpad and acceleration, puts an emphasis on the heat in the tires. Tire temperature and thus performance should increase throughout the lap and start at a higher temperature for the second lap. Setup changes and driver aggressiveness can induce more heat into the tires by scrubbing them; these changes will effectively take engine power to cause faster heat generation in the tires.

The performance of the vehicle in an autocross style course can be categorized

under two types of behavior, steady state and transient. Steady state behavior can be generalized as occurring when yaw acceleration is zero and the vehicle is fully settled. Three types of maneuvers can satisfy this stipulation. Steady state acceleration under power is seen in power or traction limited acceleration down straights. This characteristic was already demonstrated in the acceleration event. After acceleration of the vehicle, braking decelerates the vehicle in a steady state behavior during limit braking. During both acceleration and deceleration yaw rate should be zero as well. The last steady state characteristic was seen in the skidpad event, cornering. Depending upon the setup of the corner, the behavior will differ in length. During a long sweeper turn, steady state cornering will occur for an extended time. In shorter maneuvers, it will occur between transients at the peak yaw rate. An apt definition of this behavior is constant non-zero yaw rate which incurs the condition of zero yaw acceleration. Transients make up the remainder of the track. They connect all events that are deemed steady state. Consecutive transients may occur, while steady state conditions may not. Transients can be seen as the entry and exit from a steady state cornering situation. The entry may be from either a previous turn or a braking zone. In the case of braking, the corner entry will consist of trail braking accompanied by yaw acceleration increasing in magnitude to start to build yaw rate. This is followed by mid corner entry where yaw acceleration is decreasing in magnitude and yaw rate continues to increase towards the peak yaw rate at steady state cornering. After the steady state portion, mid corner exit will begin. Yaw acceleration will start to build in magnitude with opposite sign; yaw rate will start to decrease. Finally, at corner exit, either another corner or a straight will follow. In the case of a straight, yaw rate and yaw acceleration will both become zero and power will start to be applied as traction becomes available. One transient not covered under cornering behavior is the transition from acceleration to braking in a straight, which is characterized by the pitch dynamics of the vehicle as longitudinal load transfer shifts normal force from the vehicle's rear to its front. Due to the constraints of the event a new set of transient aspects affecting performance will also take place. With the continuous running, tire temperatures can increase beyond the performance limits of the tire compound. A single compound must be run for the

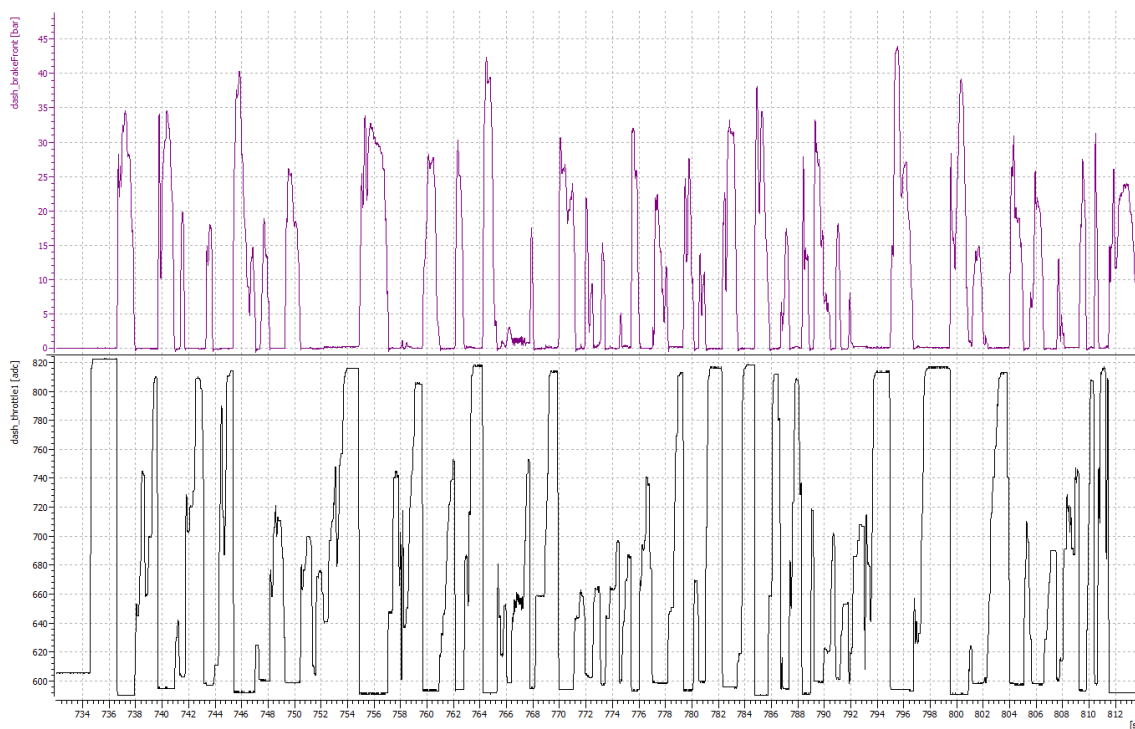
entire competition; a soft compound will be advantageous for short duration running but lose capability under the continuous running in the Endurance event. The mass of the vehicle and its location change due to the effects of fuel burn off and the changing of the driver; these changes affect the tuning of the vehicle's suspension and chassis. Unlike every other event during the competition, tuning changes cannot be made by the team between the two drivers. Only cockpit adjustable tuning devices accessible by the driver can be changed to adapt to the driver change. Changes to the seat and the pedal cluster position can be made by the team to allow the safe operation of the vehicle by both drivers.



3.2 Race Data Analysis

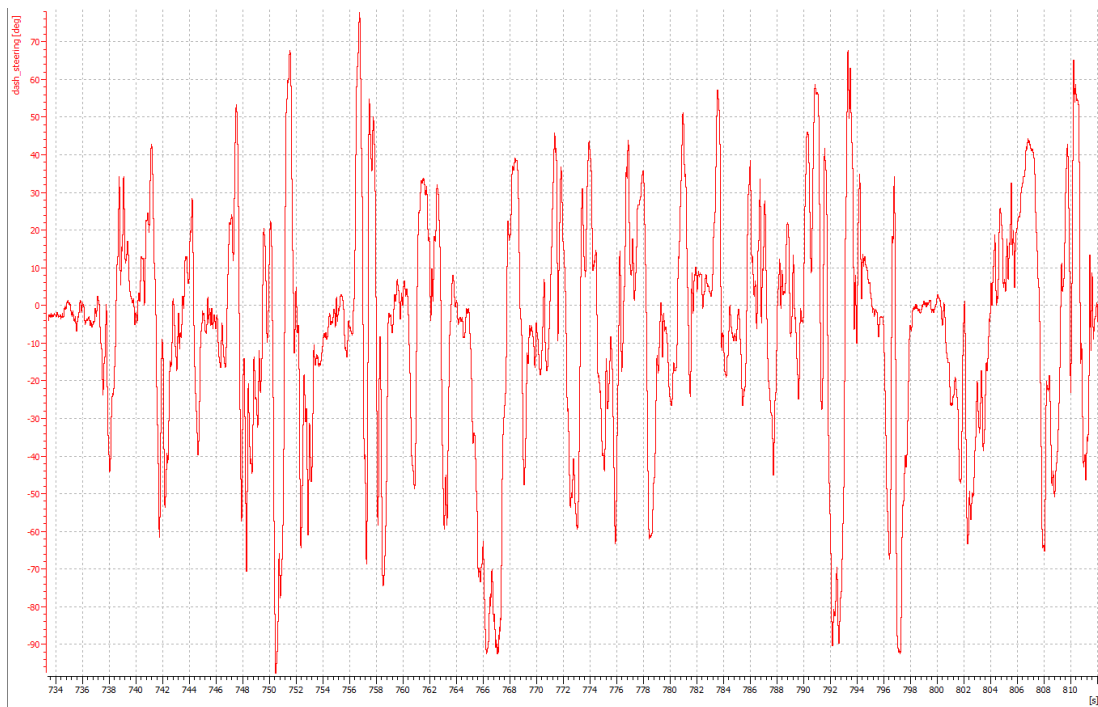
Once the test was carried out on the track, it was therefore possible to proceed to the accurate analysis of the data. In our case, the data available are as follows:

- Brakes: Front [bar], Rear [bar], Pedal [%]
- Accelerator: Throttle Pedal [%]



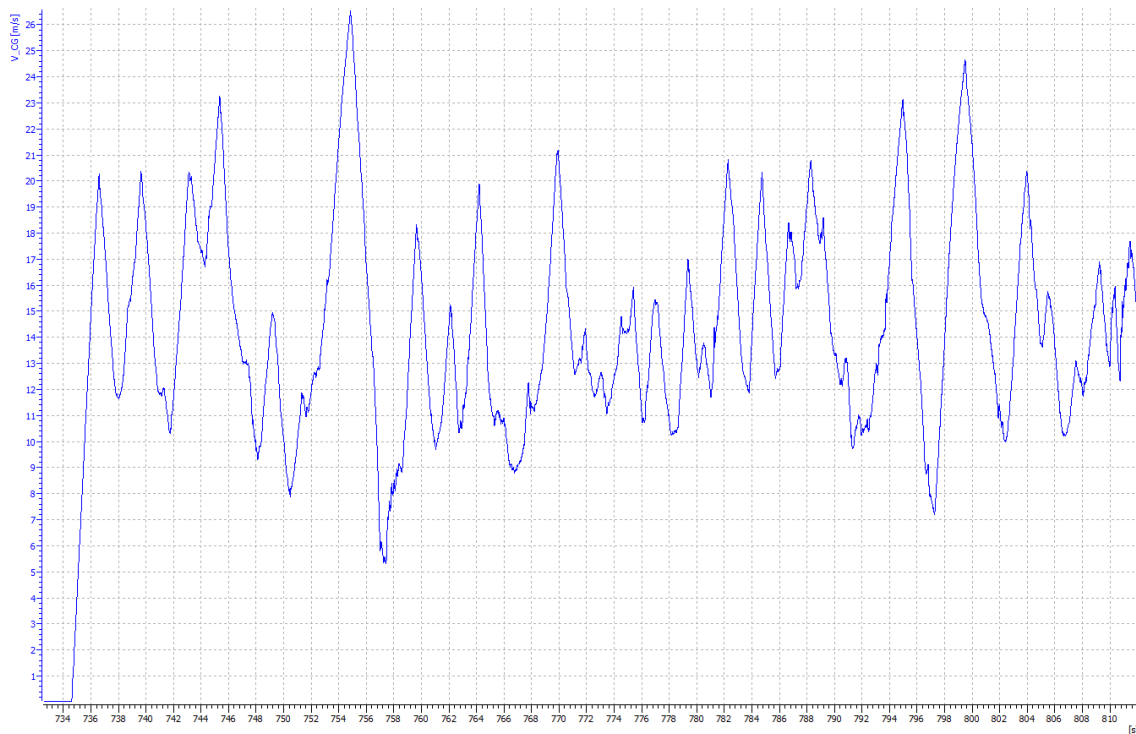
In the data above, you can notice the question of the driver on the brake pedal and accelerator. It is evident how the two requests are opposite, and how the driver often tends to require 100% gas during the acceleration phases. With these graphs it is also possible to divide the track into acceleration and braking sectors, so as to assess the importance of these two performance factors. The throttle scale in [adc] has not been converted, but its maximums and minimums correspond to values between 0 and 100% of the pedal stroke. The braking request is instead directly expressed in brake system pressure [bar].

- Steering Wheel Angle [deg]



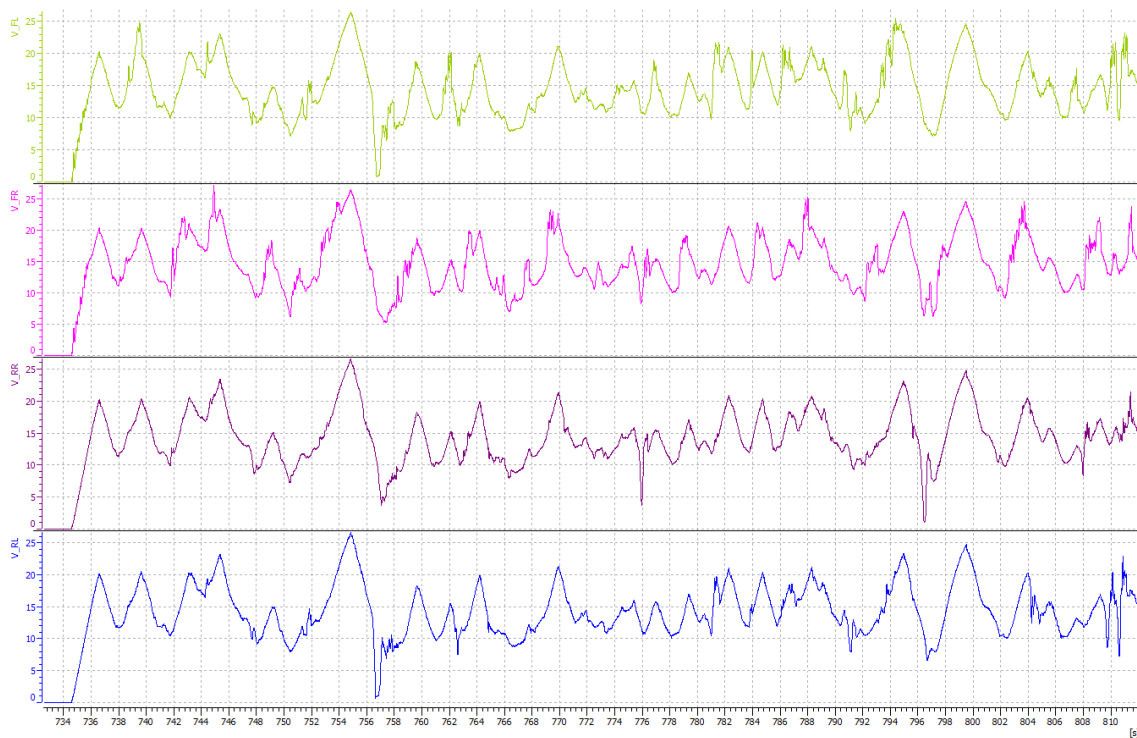
The steering graph gives us a clear idea of the complexity of the track, with a lot of abruptly change of direction. From this graph it is possible to obtain information on the maximum peaks required and also to identify all the situations in which the vehicle had oversteering, where the sudden counter-steering correction of the driver on the steering wheel can be noticed.

- Vehicle Speed [m/s]



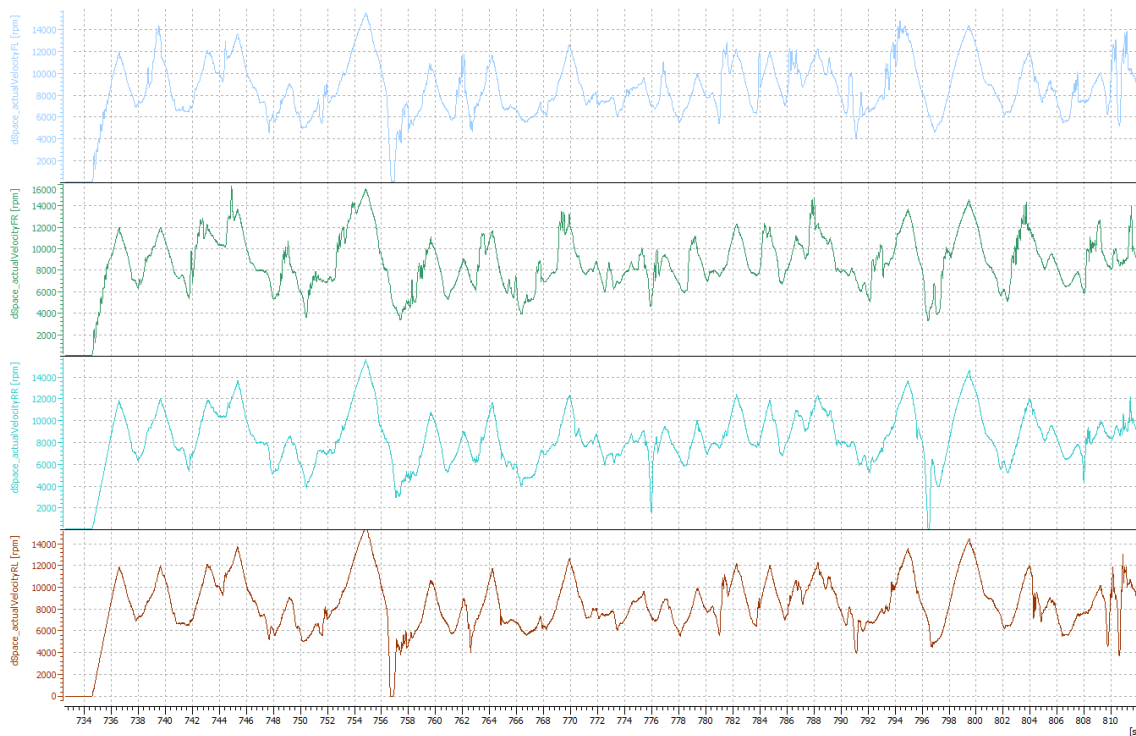
The speed graph is one of the most important in the performance optimization phase. In fact, it provides us with the trend of the instantaneous speed of the vehicle for the whole circuit. In addition to the maximum speeds reached, it is very important to go and evaluate the sections where the vehicle maintains constant speed or is in the coast down phase. It is therefore necessary to calculate from this signal, the average speed maintained by the vehicle from the beginning to the end of the test. In this case the vehicle reaches a maximum peak speed along the straight of about 94 km/h, maintaining an average speed of 50.06 km/h during the race. The lap time during this test was measured at 76.32 s. It should be noted that this time also takes into account some errors made by the driver during the race.

- Wheel Speed: FL, FR, RR, RL [m/s]



The graph above shows the instantaneous speeds of the 4 individual wheels, supplied by the sensors on the motors. The analysis of these speeds is useful to understand the slip or blocking of the individual wheels and their behavior in curves, acceleration and braking. From these 4 speeds is then obtained the overall speed of the vehicle, shown in the previous graph. All speeds are measured in [m/s].

- Wheel velocity [rpm]



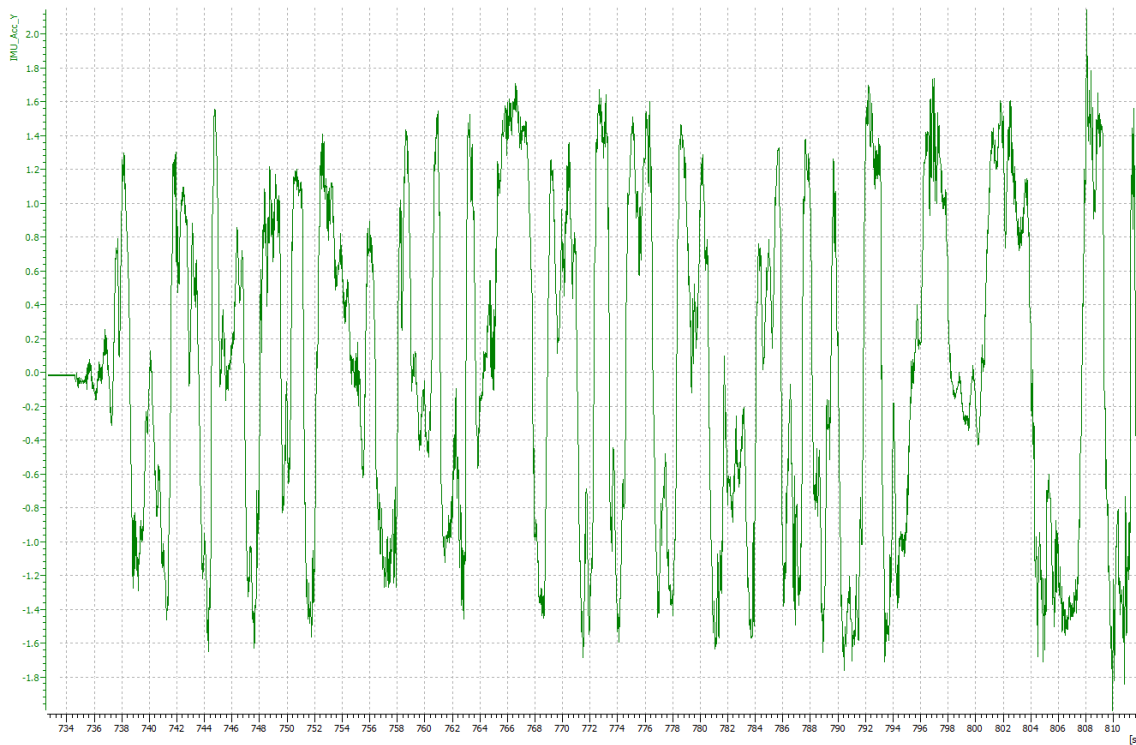
In the same way as the previous one, the speeds in [rpm] of the single wheels supplied by the same sensors present on the engine are shown above. From these, it is possible to understand the behaviour of the controls present in the control unit, such as traction control, and to see their effectiveness. In some sections of acceleration, it is in fact possible to notice how the wheel would tend to acquire greater rotational speed, because in the phase of slip, but the action of the traction control goes to reduce the speed itself, going to bring the rubber back in conditions of grip and avoiding losing seconds in slip.

- Longitudinal Acceleration: IMU X [g], Estimated [g]



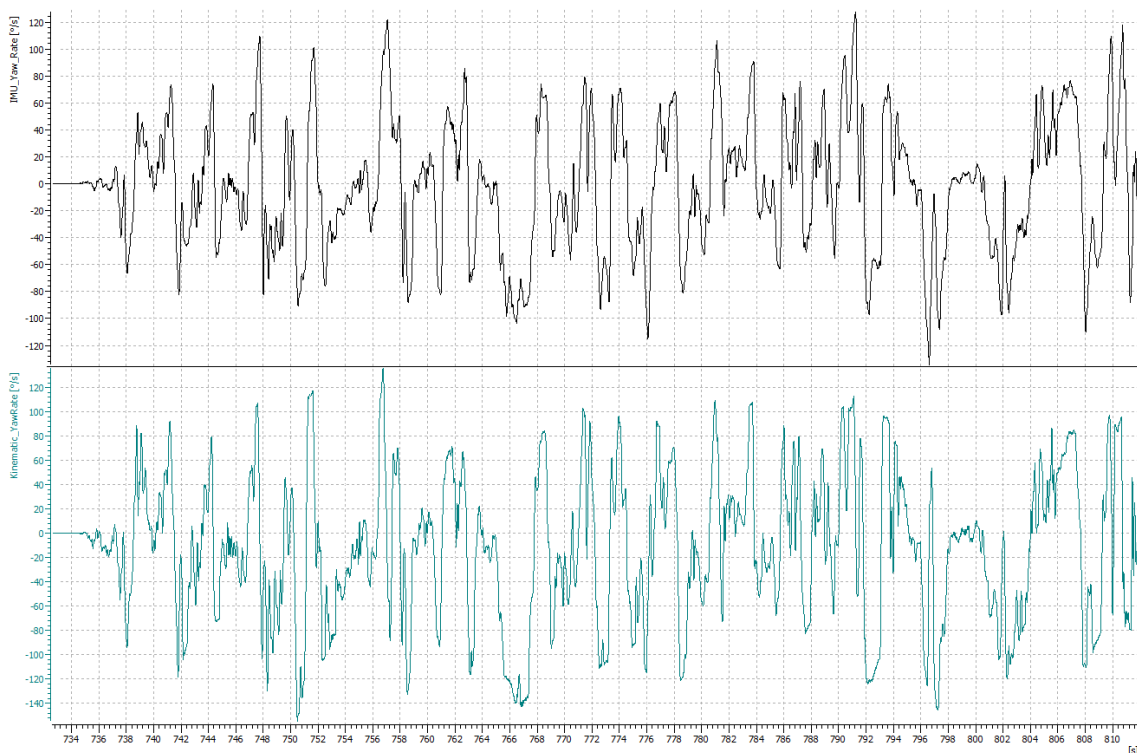
A parameter to be taken into account for the pure performance achieved by the vehicle is the longitudinal acceleration. It is measured through the inertial platform installed on the vehicle, and provides the main information of the longitudinal performance of the vehicle. The highest graph represents the signal taken directly from the platform (in this case with negative signs during acceleration, probably due to incorrect post-processing of the signal, while the second, lower, represents only the longitudinal acceleration (positive sign) without counting the braking section, in which the vehicle decelerates. This signal has been obtained and cleaned from the inertial platform, and used in onboard electronic controls. The signals are measured in [g] and the acceleration and deceleration peaks that the vehicle can reach in these conditions can be highlighted. Also from this graph it is possible to obtain a segmentation of the track in braking, acceleration and coasting phases.

- Lateral Acceleration: IMU Y [g]



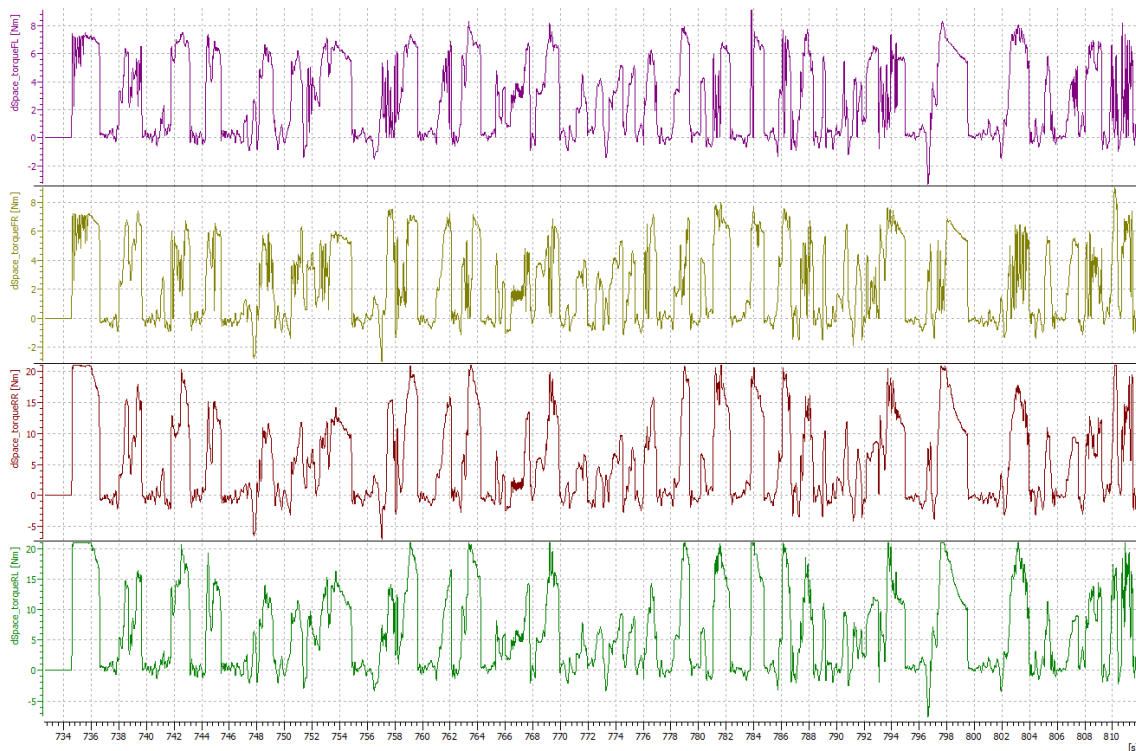
The graph above indicates the lateral acceleration signal, measured in [g] from the inertial platform. In it it is possible to obtain the curve performance of the vehicle, analysing its curve entry, its distance and its exit. It is also possible to notice the maximum peak reached and also in this case, the sudden changes of sign, which indicate a track rich in curves and changes of direction.

- Yaw Rate: IMU Sensor and Kinematic [deg/s]



In the two graphs is represented the trend of the Yaw rate, measured in [deg/s], also obtained from the inertial platform. Its behaviour is directly correlated to the course of the flying angle and consequently to the signal of the lateral acceleration that is produced. In this case, it is used as input to a second electronic control present on the vehicle, the torque vectoring. The signal below, in fact, shows the estimate of the kinematic yaw rate, which the vehicle should have to accurately travel the curve considered, which is calculated and estimated according to the steering angle that the driver requires. When the two signals overlap, when there is a difference between the current yaw rate and the required yaw rate, the torque vectoring system increases or decreases the torque on the engines outside or inside the curve, in order to allow the vehicle to obtain a better distribution of the forces acting on the ground and a better performance in curves.

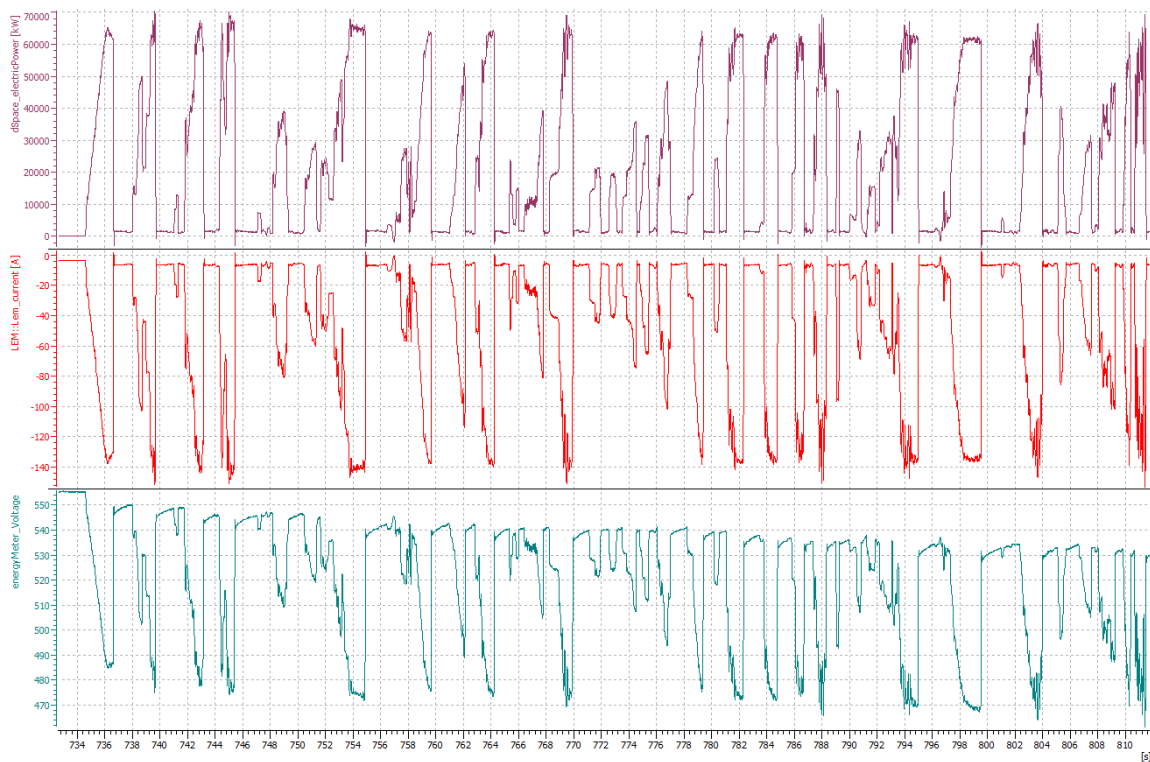
- Wheel Torque: FL,FR,RR,RL [Nm]



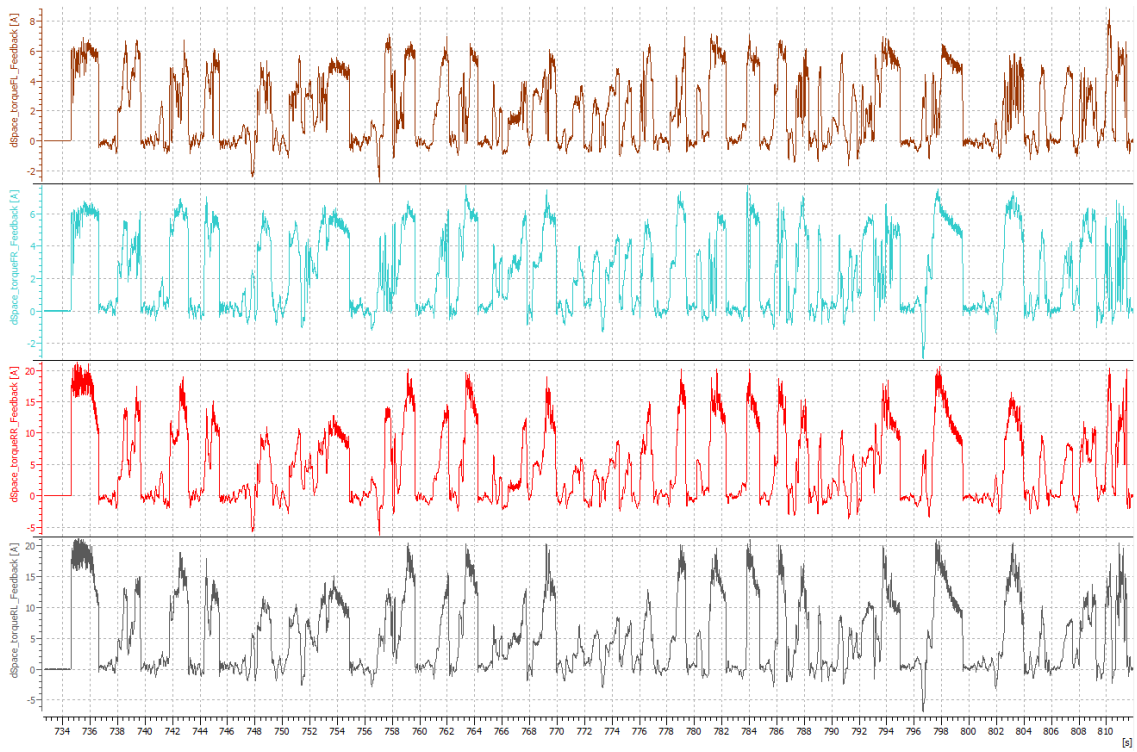
From the 4 graphs above, it is possible to analyse the torques generated by the electric motors and then distributed directly to the wheel. In this case, it is possible to notice very well the action of torque vectoring control in curves, which reduces the torque of the internal wheels to increase the torque of the external wheels. In the same way the traction control is analysed, which during acceleration, with the transfer of load to the rear, increases the torque on the rear axle reducing that of the front wheels, so as to avoid slipping. As can be seen, during the following accelerations, the torque of the engines at the rear is maximum, at 21 Nm, while the torque at the front is around 7 Nm, thus reaching a value of 1/3 of the maximum.

In addition to the signals inherent to the dynamics of the vehicle, it is possible to obtain all the other control signals, such as temperatures and currents, which will not be dealt with in detail in this thesis. They are listed below:

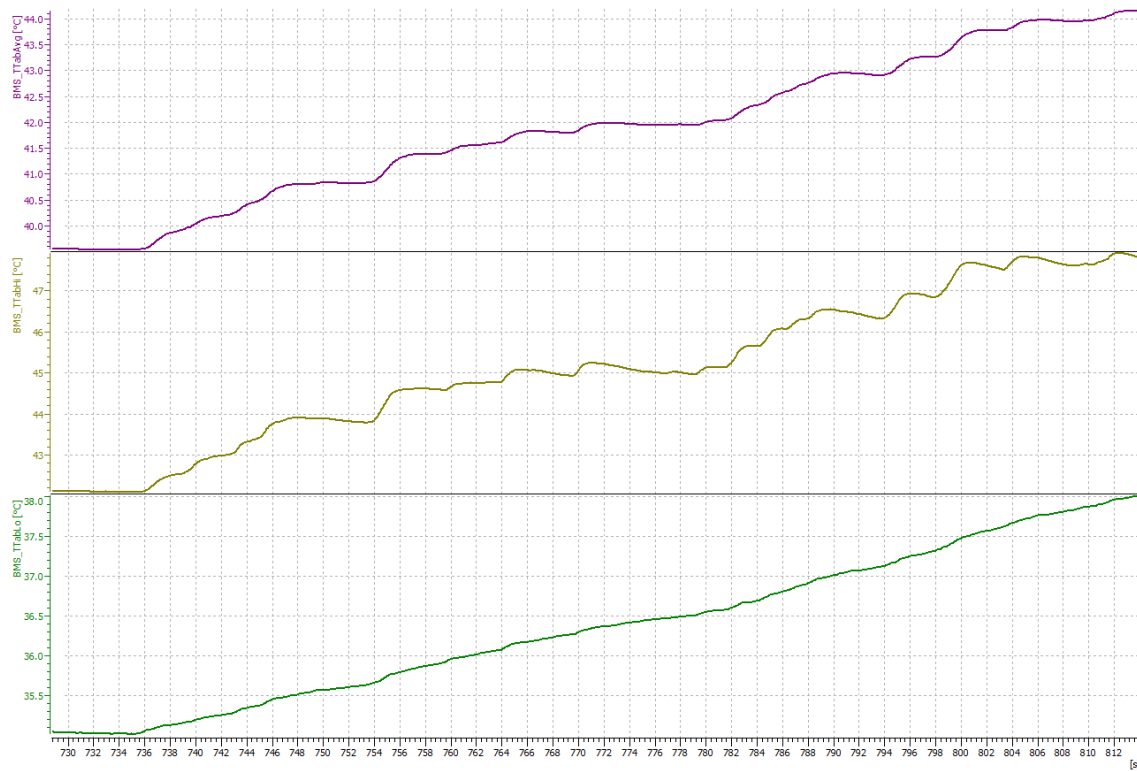
- Electric Power [kW]
- LEM Current [A]
- Battery Pack Voltage [V]



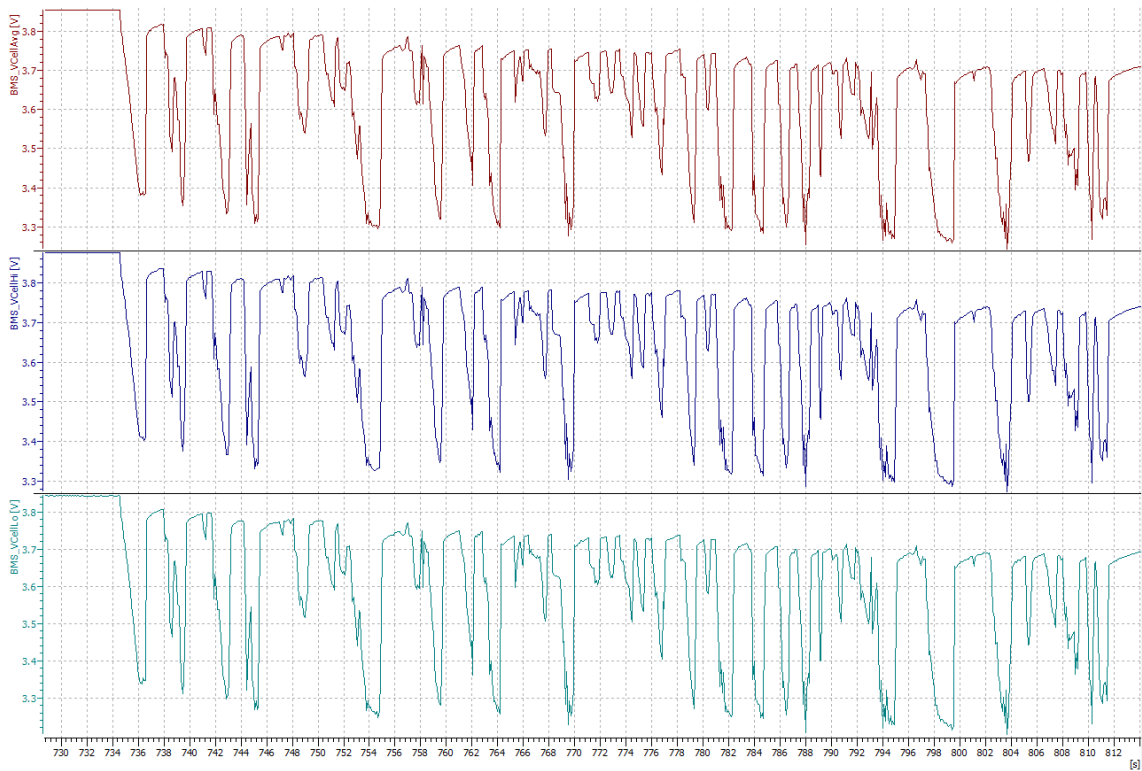
- Motor Current: FL, FR, RR, RL [A]



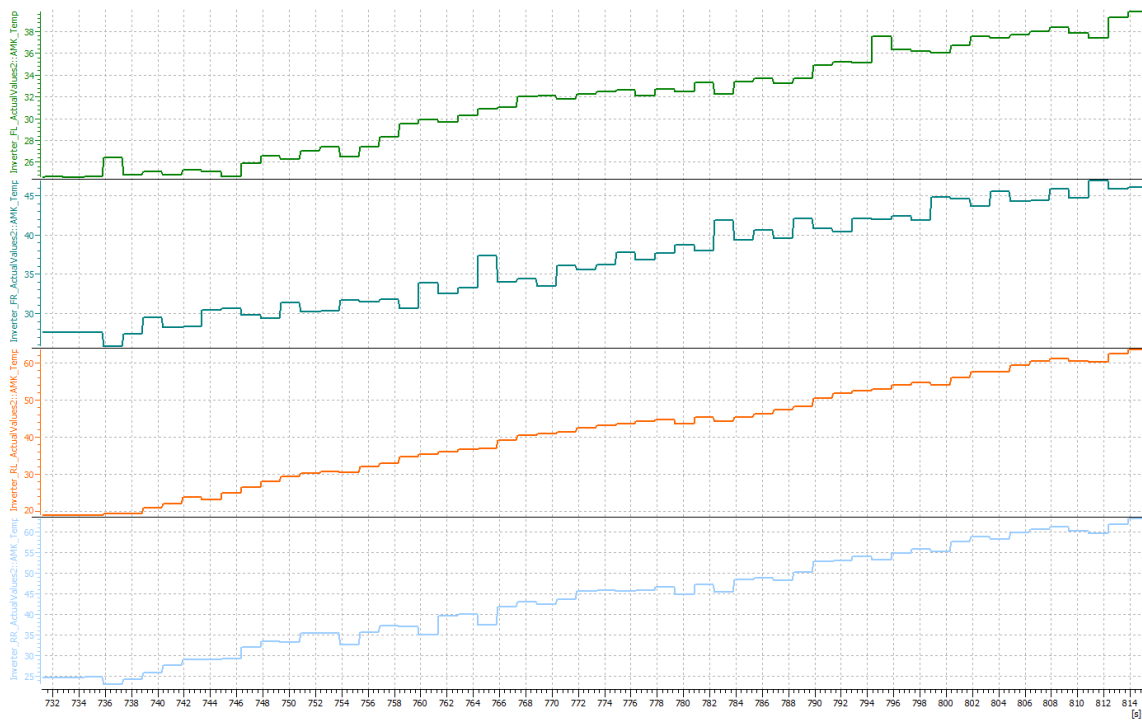
- Battery Cells Temperature: Average, Highest, Lowest [°C]



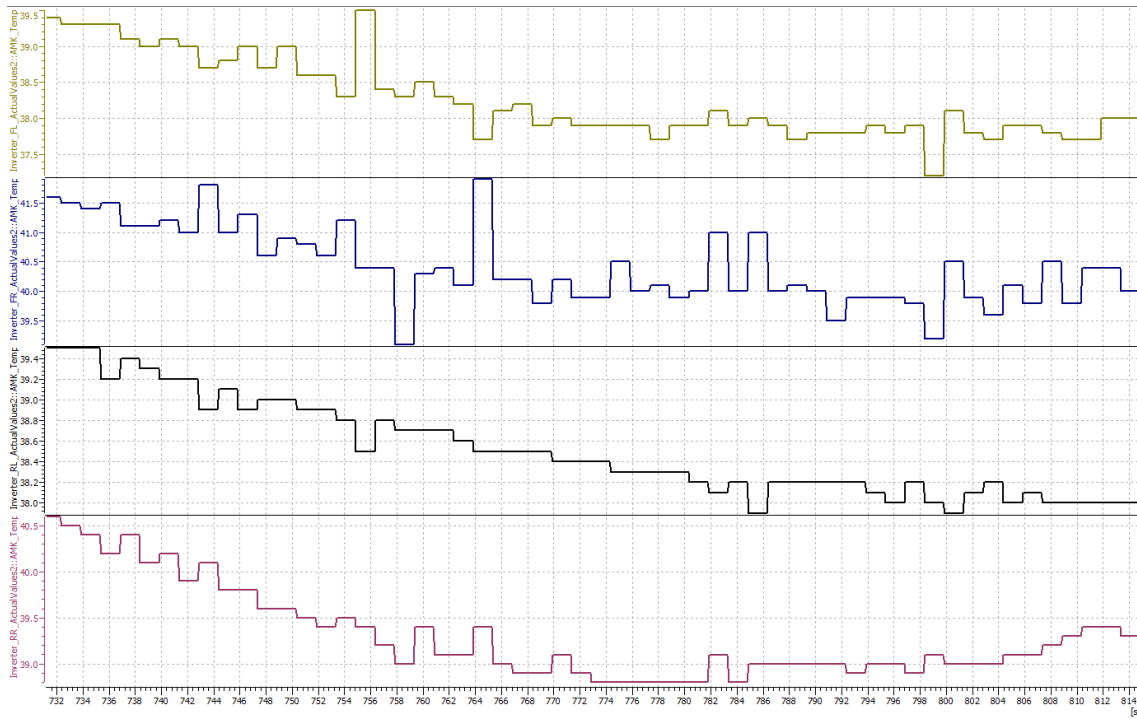
- Battery Cells Voltage: Average, Highest, Lowest [V]



- Motor Temperature: FL, FR, RR, RL [°C]



- Inverter Temperature: FL, FR, RR, RL [°C]



Chapter 4

Vehicle Simulation

4.1 Vi-Grade CarRealTime

In order to be able to study the behaviour of the vehicle under certain conditions, starting from the design and development phase, continuing with the optimisation of performance and tuning, it is absolutely necessary to use CAE systems in order to be able to reduce the costs and times of the testing phase. As a reference point for the analysis of vehicle dynamics, one of the most popular software in the world is the Vi-Grade suite, especially the CarRealTime.

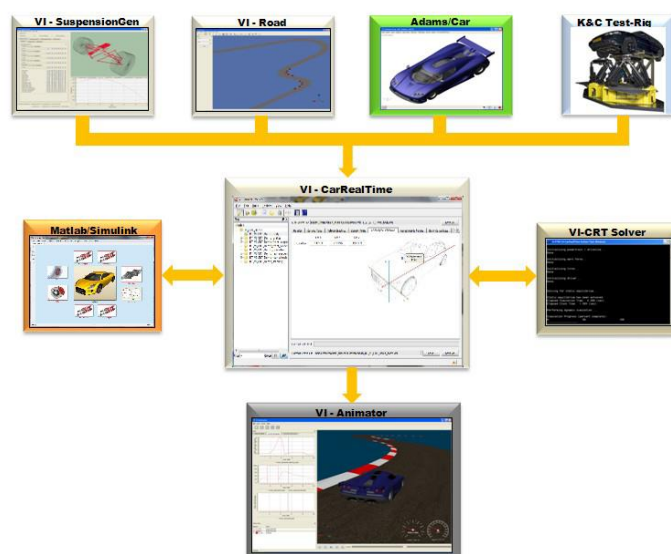
VI-CarRealTime is a virtual modeling and simulation environment based on a simplified 4-wheeler model. Its main function is to support the engineer, allowing the entire assemble of a vehicle by dividing it into subsystems connected each other. In this way it is possible to create a simplified virtual model of the vehicle during the design and development phase.

Once created, it is possible to define the dynamic maneuver to be carried out by the vehicle, with different options and configurations of Open Loop or Closed

Loop, under different conditions and tracks, simulating the behavior of the vehicle and allowing a rapid post-processing of the necessary data. The environment is based on different types of solvers, which essentially consist of symbolically derived parameterized equations of motion, Pacejka tire model and a sophisticated virtual driver model. The vehicle model can be created directly by introducing the vehicle data into the default models or, if the Adams Car software is used, it is possible to directly import the model with the appropriate plugins. In this thesis, we will not go into the Adams Car environment and its use. In order to allow the total customization of the simulation, in addition to the main software (CarRealTime) there are some tools, which allow you to deepen in detail the personalization of the simulation:

- VI-Road: a tool for generating roads and driver paths.
- VI-Animator: post-processing tool for plots and animations
- VI-SuspensionGen: suspension curves generation utility.
- VI-TireLimits: a tool for evaluating the force envelope given an input tire property file.

In this project, we will use the main software CarRealTime, Vi-Road and Vi-Animator.



Our goal was to recreate, as faithfully as possible, the FSAE electric vehicle that performed the Autocross test in the Spanish Race, in order to improve its performance on that single track.

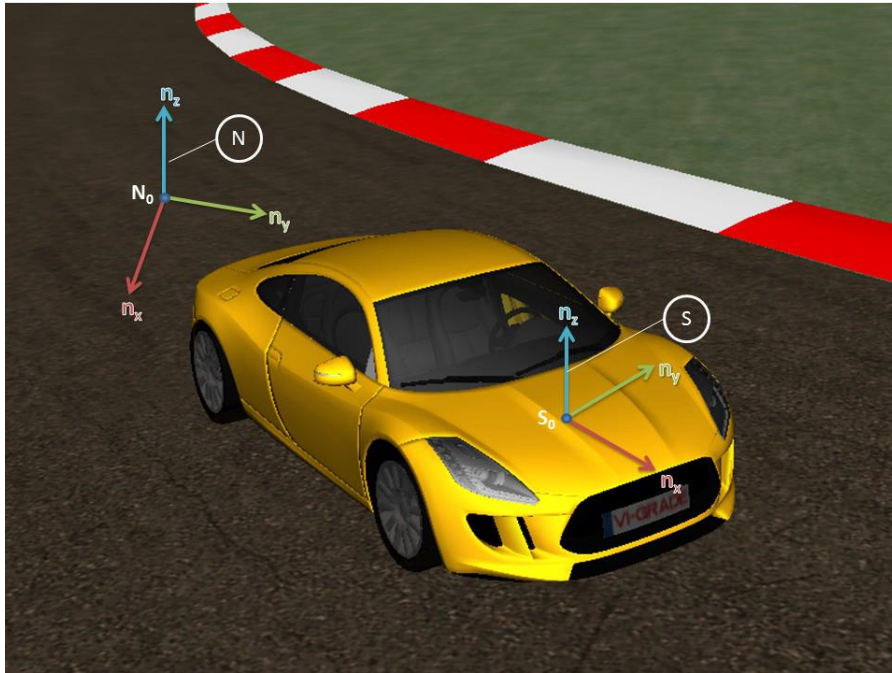
4.2 Vehicle Model Creation

In order to reproduce our vehicle model, it is necessary to know the structure of the virtual model Vi-Grade. It is a simplified model of 4-wheeled vehicle based on 14 DOFs distributed in 5 rigid parts: the chassis of the vehicle (sprung mass) and the 4 wheels (unsprung masses).

The model is splitted into different fundamental subsystems:

1. Body
2. Front Suspensions
3. Rear Suspensions
4. Front Wheels
5. Rear Wheels
6. Brakes
7. Steering
8. Powertrain

The system also allows the possibility to increase the DOFs of the model, adding for example an additional stiffness in series to the main spring of each suspension (4 more DOFs) or also includes the body chassis torsional compliances (up to 6 DOFs) obtaining a 20 DOFs model. Before creating the model, it is important to know the coordinate system accurately, consistent with ISO 8855 and SAE Recommended Practice J670f, differentiating the Global Reference System from the Vehicle Reference system (as shown in the figure below).



We can now start with the analysis and creation of all the subsystems of the vehicle.

1. BODY

The main sub-system is the body. It contains all vehicle information such as mass, inertia, suspended mass information, aerodynamic forces and all model setups.

Sprung Masses: In our vehicle, the wheelbase measures 1525 mm and all parameters of mass and inertia, have been measured or calculated by the CAD model (Catia) of our entire assembly. For the inertia, all major components was evaluated by considering their real mass and their position in the CAD assembly and approximating their shape to that of either a cylinder or a parallelepiped. Then, all of these, were evaluated respect to a local reference frame in the COG of the object and parallel to that of the car. We divided the components into cylindrical shaped and parallelepipeds, calculating the inertias with the following equations:

Cylindrical Shape

$$I_{xx} = \frac{1}{4}mr^2 + \frac{1}{12}ml^2$$

$$I_{yy} = \frac{mr^2}{2}$$

$$I_{zz} = \frac{1}{2}mr^2$$

Parallelepipeds Shape

$$I_{xx} = \frac{m(a^2 + l^2)}{12}$$

$$I_{yy} = \frac{m(b^2 + l^2)}{12}$$

$$I_{zz} = \frac{m(a^2 + b^2)}{12}$$

The inertia of components with more complex shapes was obtained directly from the CAD model. The inertias obtained this way were then translated first to the intersection between the firewall, midplane and monocoque floor, then to the car's COG utilizing the Huygens-Steiner inertia translation formula for parallel axes:

$$I_{xxCOG} = I_{xx} * m * x^2$$

$$I_{yyCOG} = I_{yy} * m * y^2$$

$$I_{zzCOG} = I_{zz} * m * |z|^2$$

The figure below shows the final inertia calculation sheet with inertias of major components in both local and inertial reference frames.

| CALCOLO INERZIE | | | | | | | | | | | | | | | | |
|------------------------------|---------------|----------------------|--------|-------|-------------------------------|----------------------|-------|------------------------------|-----------------|-----------------|--------------|---------------|---------------|--|--|-----------------------------------|
| | | | | | NOTA | G=baricentro veicolo | | G'=baricentro componente | | | | | | | | O=intersezione firewall/fondo/pia |
| COMPONENTE | MASS[kg] | POSIZIONE G'(risp O) | | | INERZIA RISPETTO A G'[kg*m^2] | | | INERZIA RISPETTO A G[kg*m^2] | | | | | | | | |
| | | G'x | G'y | G'z | I'xx | I'yy | I'zz | Ixx | Iyy | Izz | Ixy | Ixz | Iyz | | | |
| Pilota | 75,00 | 72,6 | 0 | 249,6 | | | | 2,767 | 10,928 | 10,429 | 0,074 | 1,373 | -0,016 | | | |
| Inverter sx | 6,00 | -62 | 286 | 111 | 0,026 | 0,199 | 0,181 | 0,621 | 0,305 | 0,674 | 0,029 | -0,013 | 0,226 | | | |
| Inverter dx | 6,00 | -62 | -286 | 111 | 0,026 | 0,199 | 0,181 | 0,621 | 0,305 | 0,674 | -0,029 | -0,013 | 0,226 | | | |
| Battery pack | 42,00 | -557 | 0 | 79 | 0,706 | 1,503 | 2,079 | 1,831 | 13,632 | 13,083 | 0 | -3,518 | 0 | | | |
| Front wing | 2,50 | 1474 | 0 | 95 | 0,403 | 0,051 | 0,044 | 0,458 | 5,875 | 6,21 | 0 | 0,561 | 0 | | | |
| Rear Wing | 3,50 | -899 | 0 | 897 | 0,975 | 0,255 | 0,431 | 1,874 | 4,305 | 2,983 | 0 | 1,956 | 0 | | | |
| Wheel FL | 8,11 | 763 | 600 | 237 | 0,142 | 0,228 | 0,142 | 3,063 | 5,526 | 8,361 | -3,933 | 0,037 | 0,028 | | | |
| Motor+Transm FL | 5,30 | 763 | 522,5 | 237 | 0,039 | 0,008 | 0,039 | 1,486 | 3,47 | 4,947 | -2,238 | 0,024 | 0,016 | | | |
| Wheel FR | 8,11 | 763 | -600 | 237 | 0,142 | 0,228 | 0,142 | 3,063 | 5,526 | 8,361 | 3,933 | 0,037 | -0,028 | | | |
| Motor+Transm FR | 5,30 | 763 | -522,5 | 237 | 0,039 | 0,008 | 0,039 | 1,486 | 3,47 | 4,947 | 2,238 | 0,024 | -0,016 | | | |
| Wheel RL | 7,91 | -762 | 600 | 237 | 0,139 | 0,223 | 0,139 | 2,986 | 4,286 | 7,049 | 3,401 | -0,032 | 0,027 | | | |
| Motor+Transm RL | 5,30 | -762 | 522,5 | 237 | 0,039 | 0,008 | 0,039 | 1,486 | 2,732 | 4,209 | 1,985 | -0,022 | 0,016 | | | |
| Wheel RR | 7,91 | -762 | -600 | 237 | 0,139 | 0,223 | 0,139 | 2,986 | 4,286 | 7,049 | -3,401 | -0,032 | -0,027 | | | |
| Motor+Transm RR | 5,30 | -762 | -522,5 | 237 | 0,039 | 0,008 | 0,039 | 1,486 | 2,732 | 4,209 | -1,985 | -0,022 | -0,016 | | | |
| Monocoque | 47,00 | 68 | 0 | 242,2 | | | | 3,51 | 15,95 | 16,095 | 0 | -0,34 | 0 | | | |
| Damper front | 3,50 | 737 | 0 | 302 | 0,102 | 0,002 | 0,102 | 0,115 | 2,156 | 2,244 | 0 | -0,162 | 0 | | | |
| Damper rear | 3,50 | -757 | 0 | 291 | 0,14 | 0,002 | 0,14 | 0,148 | 1,784 | 1,914 | 0 | 0,12 | 0 | | | |
| VEICOLO[kg*m^2] | 242,24 | | | | | | | 29,987 | 87,268 | 103,438 | 0,074 | -0,022 | 0,436 | | | |
| MASSE SOSPESE[kgmm^4] | 189,00 | | | | | | | 11945000 | 55240000 | 54306000 | 74000 | -36000 | 436000 | | | |

In the figure below are listed one by one. In the analysis we carried out, no chassis compliance was activated. For this reason, our model does not see the division into 2 parts of the sprung masses. The center of gravity of the vehicle was instead measured directly on our prototype, by weighing the vehicle on a level road, at the front and rear axles. Considering F_{z1} and F_{z2} the vertical forces of the 2 axles, the equilibrium equations for translations in the z direction can be written as:

$$\begin{cases} F_{z1} + F_{z2} = mg \\ lF_{z1} = bmg, \end{cases}$$

And then:

$$\begin{cases} a = l \frac{F_{z2}}{F_{z1} + F_{z2}} \\ b = l \frac{F_{z1}}{F_{z1} + F_{z2}}. \end{cases}$$

If the center of mass does not lie in the symmetry plane, it is possible to compute the transversal position of the center of mass by measuring the forces under the right and left wheels. It is more difficult to determine the height of the center of mass. Once the longitudinal position is known (once a and b have been determined) it is possible to measure again the forces on the ground after the front (or the rear) axle has been raised from the ground. Let the front axle be set on a platform with height h with respect to the platform on which the rear axle is located. If the height of the center of mass h_G is greater than the radius under load of the wheels, the force F_{z1} measured at the front axle will be smaller than that measured on level road. It is possible to write:

$$F'_{z1} = F_{z1} - \Delta F_z.$$

$$F'_{z2} = F_{z2} + \Delta F_z.$$

In this way, the equilibrium equation for rotations about the center of the front axle is:

$$\begin{aligned} mg [a \cos (\alpha) + (h_G - R_{l_1}) \sin (\alpha)] &= \\ &= (F_{z_2} + \Delta F_z) [l \cos (\alpha) + (R_{l_2} - R_{l_1}) \sin (\alpha)]. \end{aligned}$$

And so the height of center of mass is then:

$$h_G = \frac{F_{z_2} + \Delta F_z}{mg} \left[\frac{l}{\tan (\alpha)} + R_{l_2} - R_{l_1} \right] - \frac{a}{\tan (\alpha)} + R_{l_1}.$$

Remembering that:

$$\frac{F_{z_2}}{mg} = \frac{a}{l},$$

It follows that:

$$h_G = \frac{a}{l} [R_{l_2} - R_{l_1}] + R_{l_1} + \frac{\Delta F_z}{mg} \left[\frac{l}{\tan (\alpha)} + R_{l_2} - R_{l_1} \right].$$

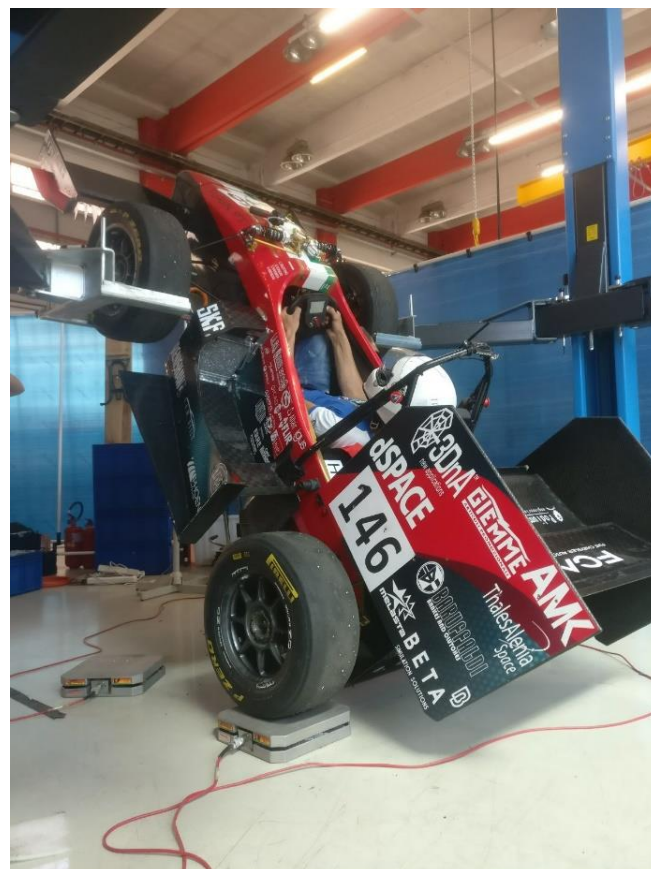
If the loaded radius of the wheels is the same, as it is usually the case, the calculation can be simplified as:

$$\begin{aligned} h_G &= R_l + \frac{\Delta F_z}{mg} \frac{l}{\tan (\alpha)}, \\ h_G &= R_l + \frac{\Delta F_z}{mg} \frac{l \sqrt{l^2 - h^2}}{h}. \end{aligned}$$

To measure accurately the height of the center of mass, the wheels must be completely free (brakes released) and the vehicle must be restrained from rolling by chocks at one of the axles. Moreover, the suspensions must be locked at a height corresponding to the load distribution on level road, and the tires must be equally compressed. This last condition can be obtained in an approximate way by increasing the inflation pressure. It is then possible to take several measurements of ΔF_z at different values of $\tan(\alpha)$ and to plot ΔF_z versus $\tan(\alpha)$. If the radii of the wheels are all equal, such a curve is a straight line, whose slope

$$\frac{\Delta F_z}{\tan(\alpha)} = \frac{mg}{l} (h_G - R_l)$$

allows one to finally compute the height of the center of mass. The image below shows the process of measuring the centre of gravity.



Front Downforce:

$$F_z = k \cdot \frac{\rho}{k_\rho} \cdot (F_z^{table} + k_{shift}^f) \cdot \left(\frac{V}{V_{ref}}\right)^2$$

Rear Downforce:

$$F_z = k \cdot \frac{\rho}{k_\rho} \cdot (F_z^{table} + k_{shift}^r) \cdot \left(\frac{V}{V_{ref}}\right)^2$$

Drag Force:

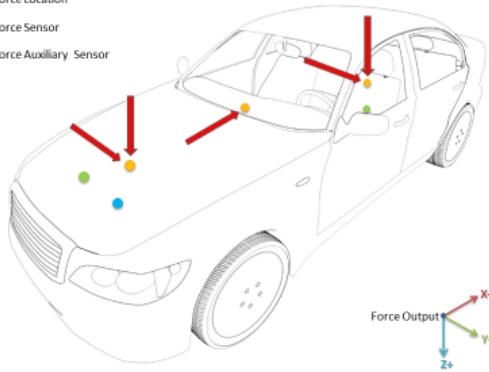
$$F_x = k \cdot \frac{\rho}{k_\rho} \cdot (F_d^{table} + k_{shift}^d) \cdot \left(\frac{V}{V_{ref}}\right)^2$$

Property File   Active

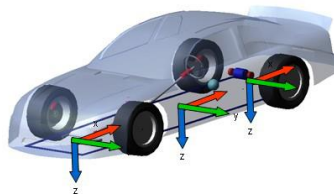
| | X | Y | Z |
|----------------------------|--|----------------------------------|------------------------------------|
| Front Downforce Location * | <input type="text" value="0.0"/> | <input type="text" value="0.0"/> | <input type="text" value="240.0"/> |
| Rear Downforce Location * | <input type="text" value="1525.0"/> | <input type="text" value="0.0"/> | <input type="text" value="240.0"/> |
| Drag Force Location * | <input type="text" value="-619.1891"/> | <input type="text" value="0.0"/> | <input type="text" value="460.0"/> |

| | X | Y | Z |
|---|-------------------------------------|----------------------------------|------------------------------------|
| Front Sensor Location * | <input type="text" value="0.0"/> | <input type="text" value="0.0"/> | <input type="text" value="329.0"/> |
| Rear Sensor Location * | <input type="text" value="1525.0"/> | <input type="text" value="0.0"/> | <input type="text" value="360.0"/> |
| <input type="checkbox"/> Front Aux Downforce Sensor * | <input type="text" value="0.0"/> | <input type="text" value="0.0"/> | <input type="text" value="0.0"/> |

* Location expressed according to ISO 8855:2011 reference system



The description of all parameters is given in the nomenclature. The reference system used for the calculation is the following

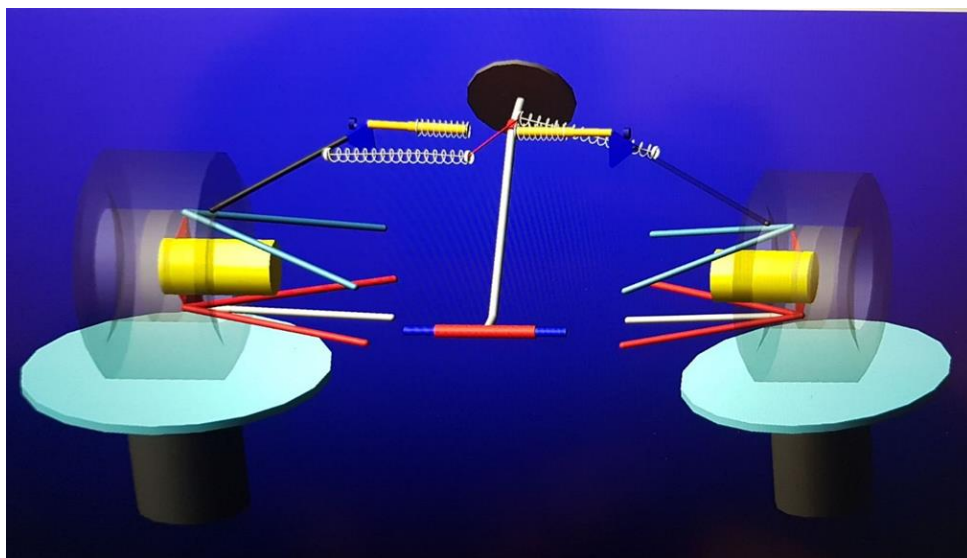


Other body subsystems including Body Setup Data, Cross Weight Adjustment, Ride Height Maps, User Sensor, Skidplate Point and Sensor Point have been set by default. An FSAE vehicle model has been imported for the model graphics.

2. FRONT SUSPENSION

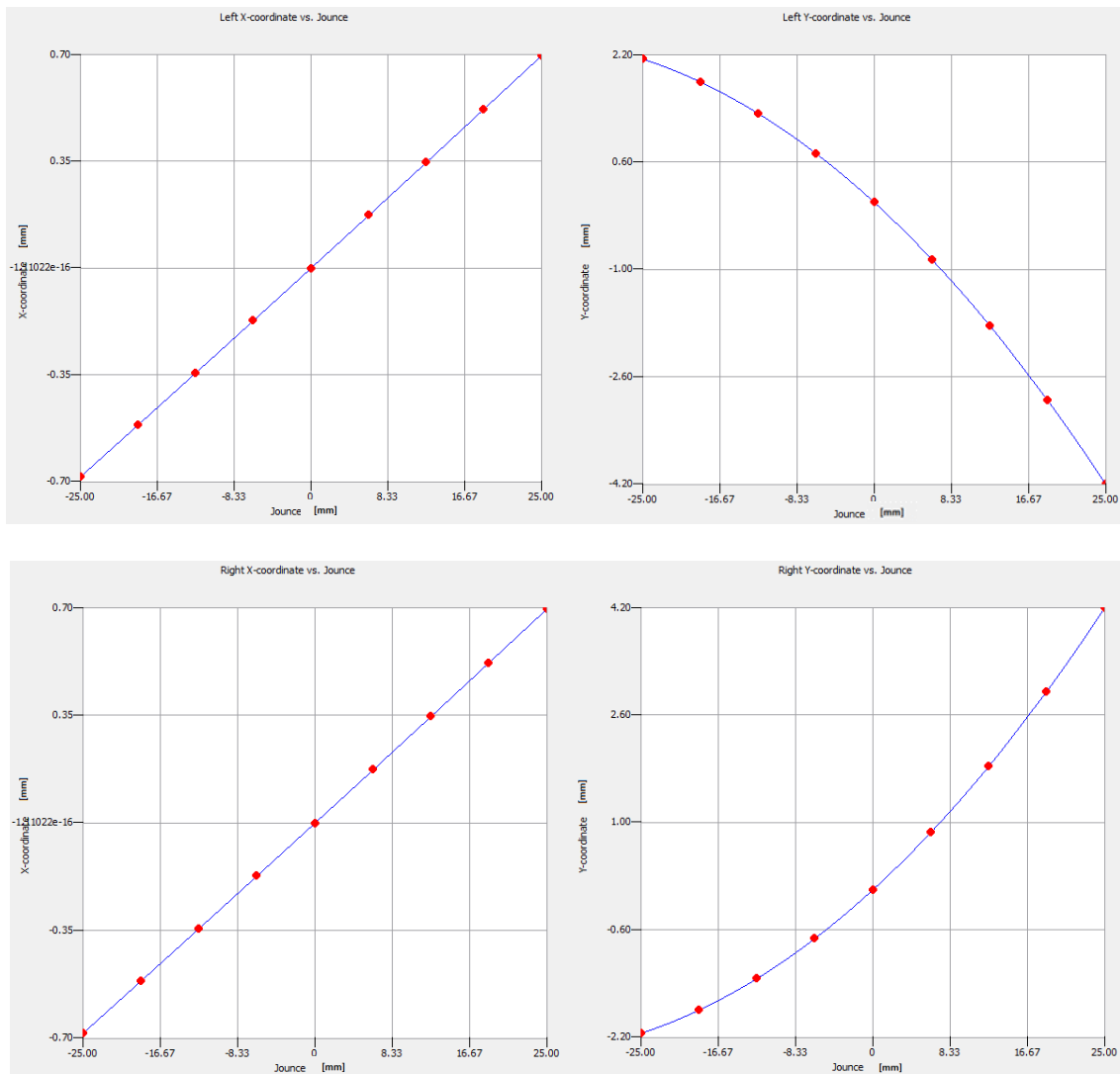
For the modeling of the suspensions, the software adopts a conceptual approach. They are not in fact composed of physical parts connected to each other and the wheel moves in vertical jounce using a special constraint that defines the position and orientation (5 DOF) using lookup tables. The effect of suspension components like springs, dampers, etc. is projected onto wheels and computed by applying motion ratio from wheel to suspension component travel, use component lookup tables to get element forces and use motion ratio to compute equivalent force at wheel center.

In our case, the suspension to model is the classic Formula SAE vehicle type: a Push/Pull type suspension, equivalent to a short-long arm double wishbone layout.



The first step in modelling the suspension is to define the **Wheel Location**, using the measure of the track width and the wheel center X-coordinate vs Z (right and left), that is the wheel base variation in wheel location reference system as a function of wheel jounce. The same for Y-coordinate vs Z. These are described by spline data editable via the Curve Editor. Important is to remember that The Wheel Location Reference System is defined by a triad positioned at wheel center (left and right, at design time) with same orientation of global reference system with X positive forward, Z positive vertical up, Y positive left. Here below are

presented our reference curves.

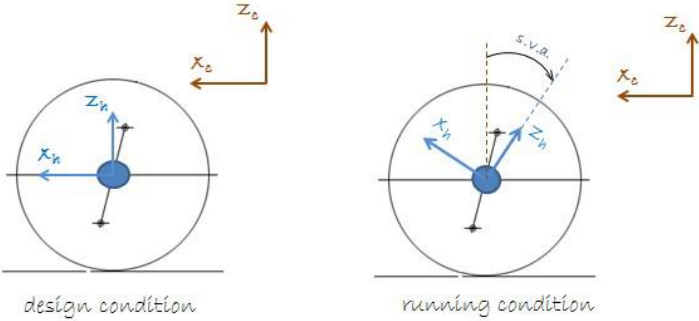


The Track Width of our vehicle is 1200 mm.

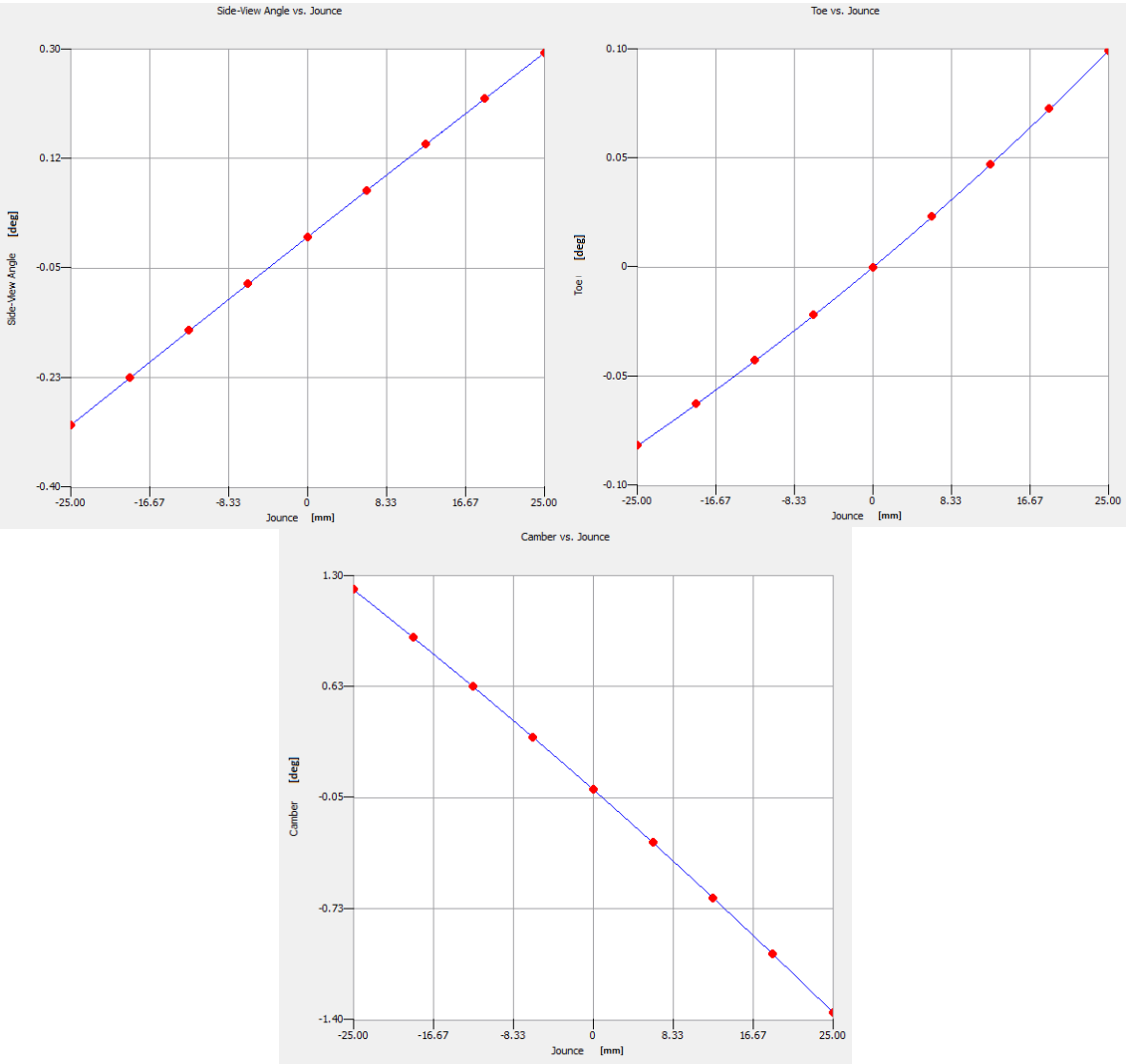
Second step is definition of **Wheel Orientation** using the following parameters:

- **Side View Angle** : is the variation of the wheel carrier side-view rotation angle with respect to the caster angle at design time. It is positive for a clockwise rotation, as seen from the left side of the vehicle.
- **Toe Angle**: is the angle between the longitudinal axis of the vehicle and the line of intersection of the wheel plane and the vehicle's XY plane. It is positive if the wheel front is rotated in towards the vehicle body.

- Camber Angle:** is the angle the wheel plane has with respect to the vehicle's vertical axis. It is positive when the top of the wheel leans outward from the vehicle body.



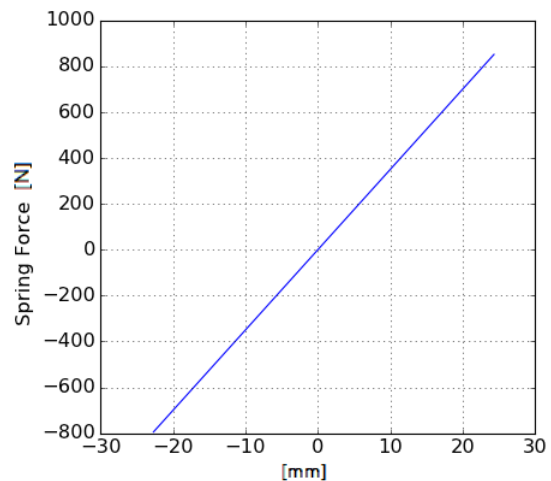
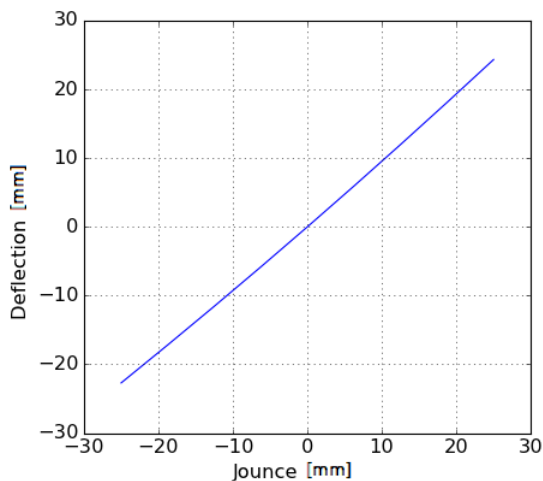
For all these parameters it is possible to define the dependency with the suspension jounce as constant rate or to introduce data from the table, also defining possible left and right symmetries.



For what concern **Compliance**, in our study have not been analyzed and therefore the parameter has been set by default as constant Zero Value and has not been deepened.

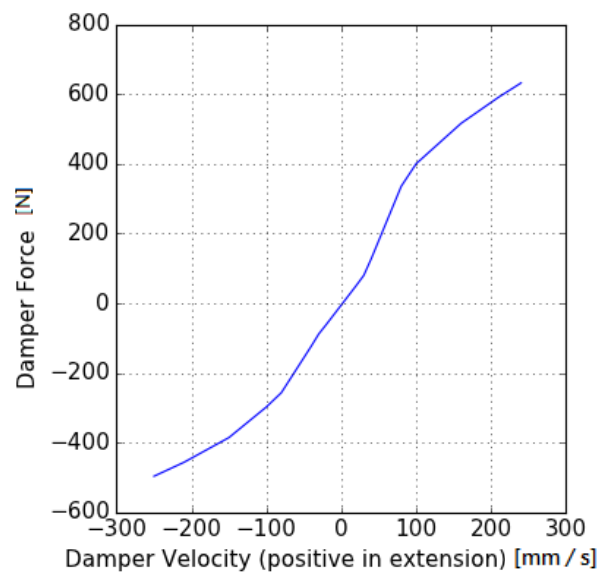
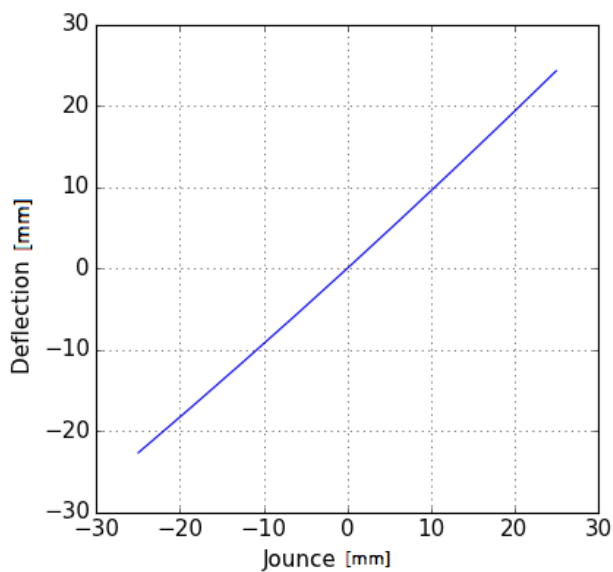


Instead, the behaviour of the **Springs** has been modelled in detail. It is possible to model two types of springs: coil springs or air springs. In our case, a coil spring was modeled, starting from the installation method, specifying the *Installed length* of the spring (at design time). In this way, the preload is computed depending on spring free length. In addition to this, the compression ratio method is also used: it convert the spring component deformation to the equivalent wheel jounce. Also



in this case are available the constant rate values or data input using the curve editor table. We use the second case, applying a curve with wheel jounce as independent variable (X) expressing the spring deflection (Y).

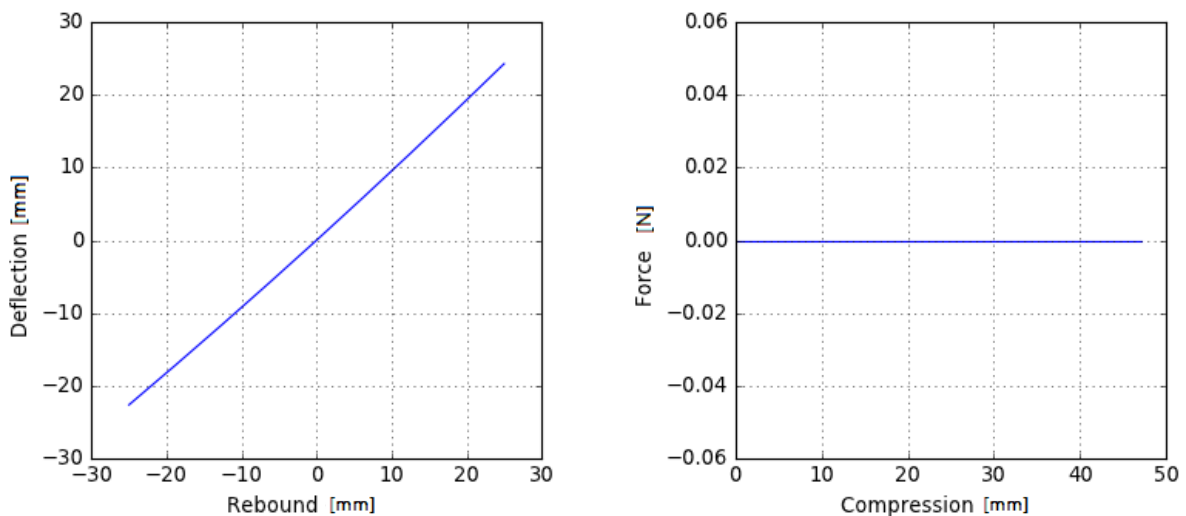
In our installation, the spring length is 112,8 mm. We apply a linear characteristic of the component, with a free length of 125,0 mm and a linear rate of about 35,03 mm.



After modelling the spring element, it is possible to switch to **dampers**, a key element in the suspension behaviour. After many years in which the behaviour of the dampers was underestimated, in order to make a correct design of the suspension and to allow a correct simulation and tuning of the element, we performed the characterization of the dampers on a test bench, going to characterize in detail their behavior and refining their tuning. In this way it was possible to obtain the characterization curves that we went to insert in the model Vi-CRT.

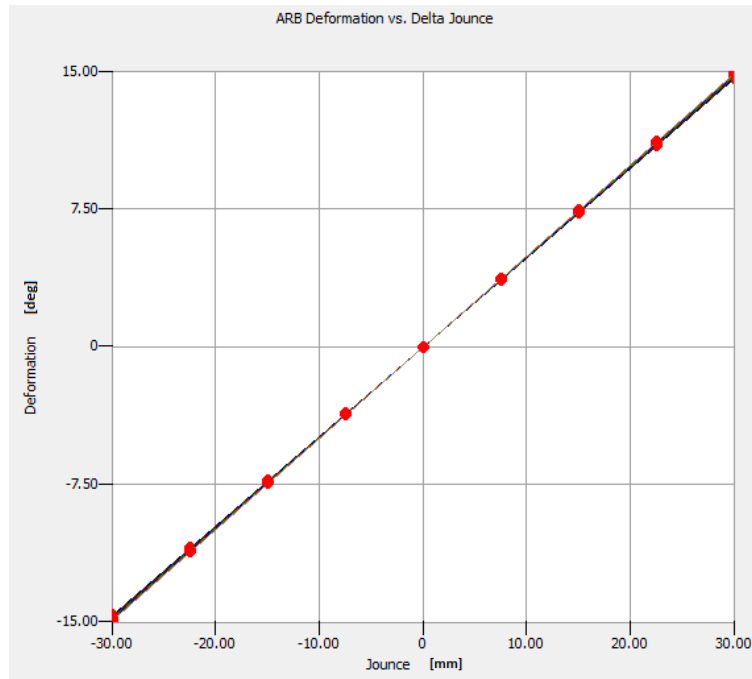
In this case, the Damper Force vs Damper Velocity has a Nonlinear behaviour.

When modelling, **bumper** elements are used to limit the jounce and rebound of the suspension. To describe their behavior, first they are divided into two: one per jounce and the other rebound. They are modelled by entering their clearance value, that describes the deformation that the component must undergo before engaging and applying a force. For models including suspension adjustments the value refers to conditions after the setup, in the other cases to design conditions.



After that, it is necessary the description with the compression ratio method, using the table as before for the spring elements. In our case, the Bumber Clearance is set to zero.

Another importance subsystem, is the **Anti-Roll Bar** component. It is an elastic element that connects left and right paired wheels. Depending on the conceptual suspension model the force is projected at the wheels as a pair of opposite vertical forces acting between the wheel (unsprung mass) and the body chassis. In this case, the behaviour is described with a compression ration curve. The next step in modeling the front suspension is to set the Suspension Setup Data correctly.



The next step in modeling the front suspension is to set the ***Suspension Setup Data*** correctly. This is useful for racing application, in which it's necessary to modify some parameters that changes after static equilibrium of the vehicle. These parameters are Ride Height, Toe Angle, Camber Angle, Pin Height, Bumper Clearance Setup and Reboundstop clearance setup. In our case, we decide to not investigate about these detailed parameters.

The same considerations have been made for the additional settings concerning:

- Installation Stiffness, used to model the vertical compliance of the suspension oh hub side
- Auxiliary Translational DOF, to insert an additional degree of freedom between unsprung mass and chassis, in order to capture the dynamics of the wheel and its vibration phenomena along x direction

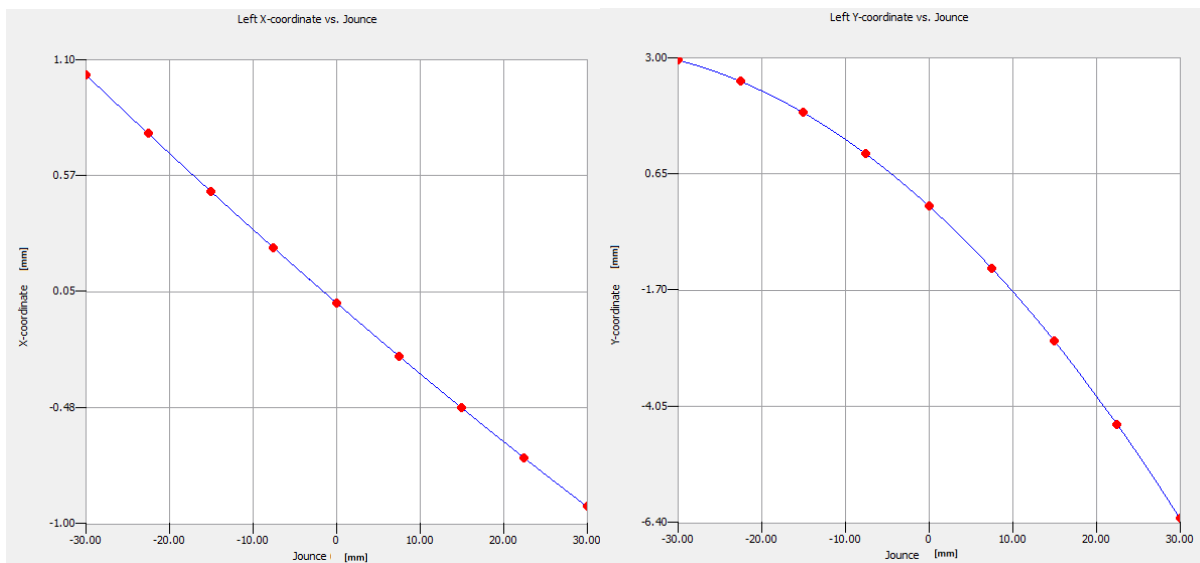
All these subsystems have been set by default and no detailed analysis of their development has been made.

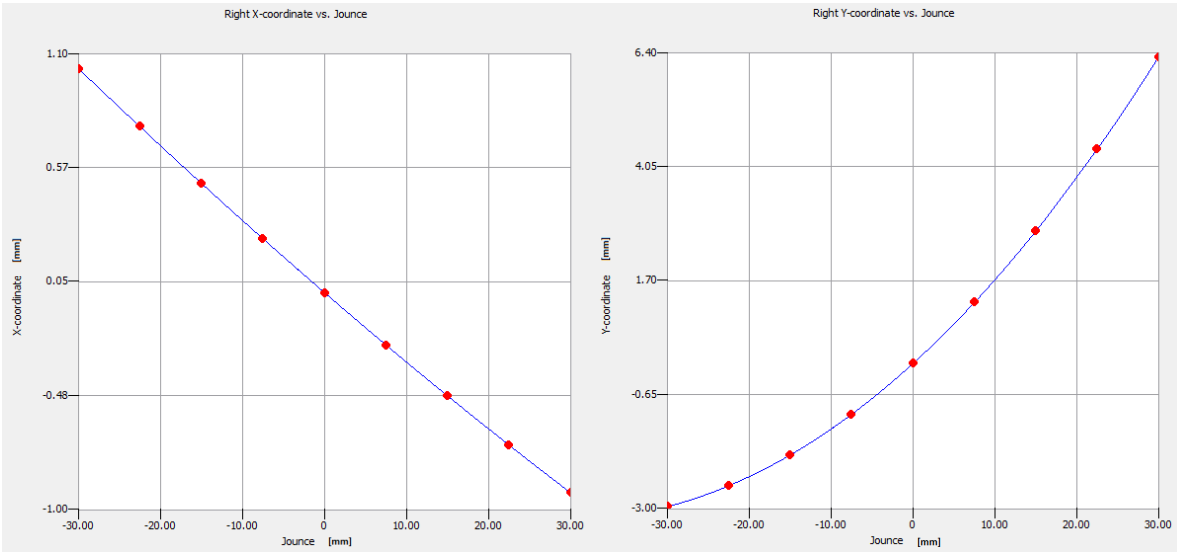


3. REAR SUSPENSION

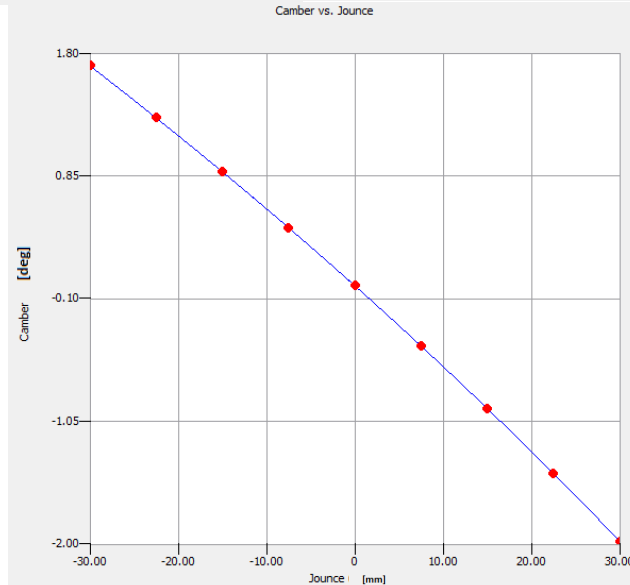
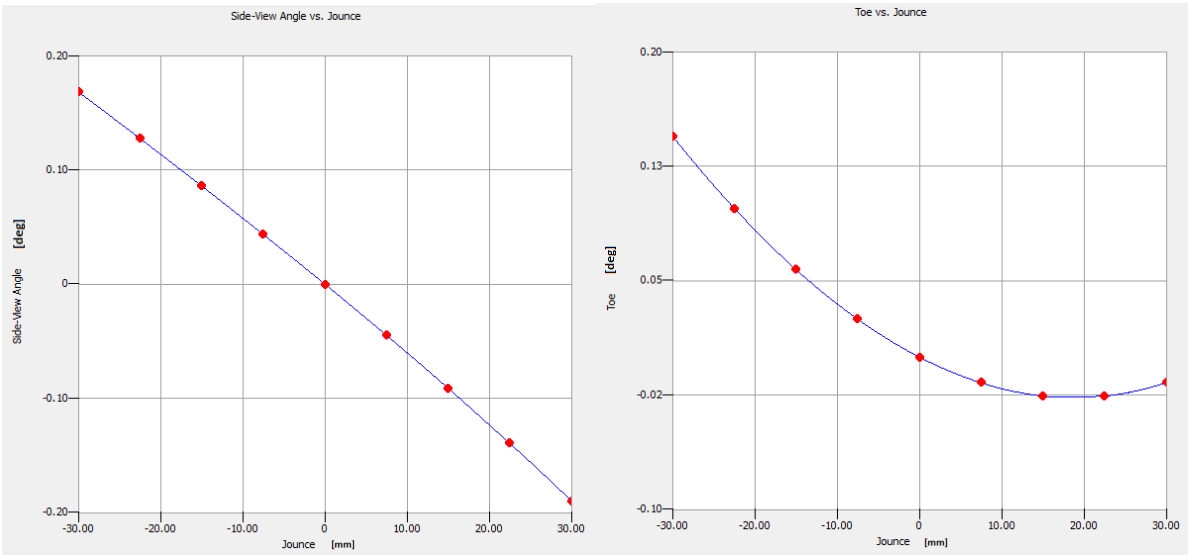
For rear suspensions, the procedure is the same as for front suspensions. For this reason, I shall confine myself to introducing only the characteristic graphs of interest.

- Wheel Location (Left and Right)

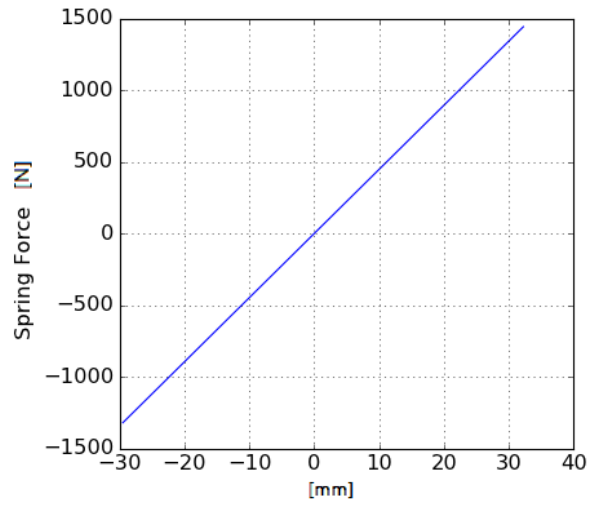
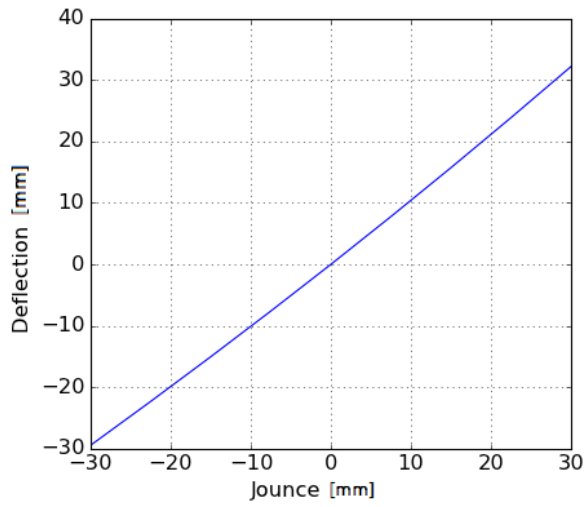




Wheel Orientation

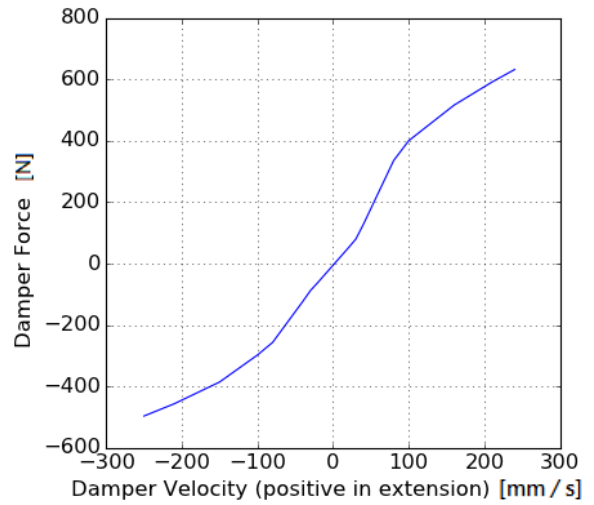
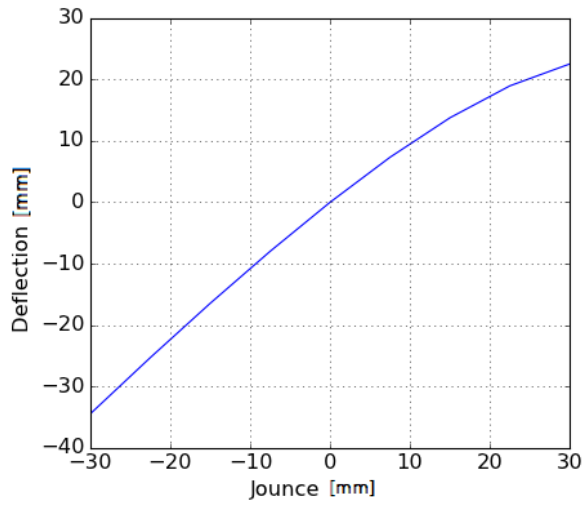


Springs



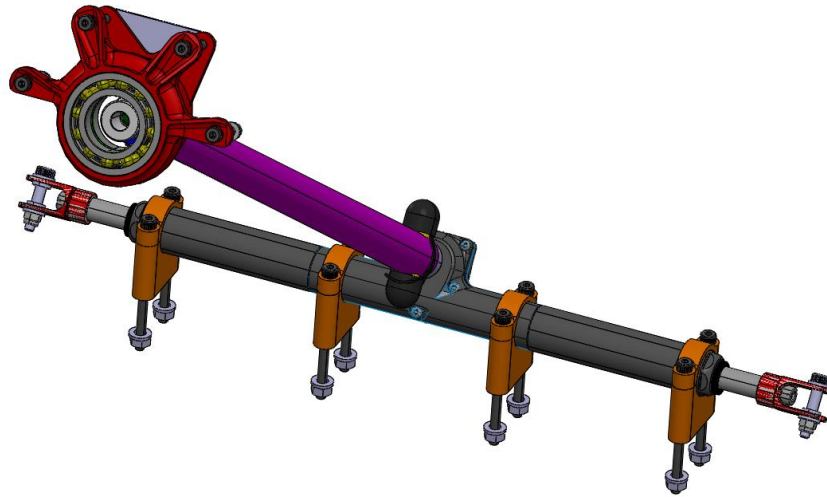
Installed Length 115,0 mm , Free Length 125,0 mm, Linear Rate 44,78

Dampers



4. STEERING SYSTEM

The steering subsystem has to be modeled using different approaches. In a basic formulation no physical part or linkage is present in the model; the steering and other movements of the wheels are related to steering wheel (or rack) motion and wheel jounce by lookup tables, like the suspension. For what concern compliance effect of the steering column, in our model we have not considered their effect. It is also possible to use an advanced rack-pinion steering model which physically models the steering in terms of mechanical and electric/hydraulic components, but is not our case of study.



Our steering mechanism is composed of a steering wheel support, a steering column that works with a rackbox component. To model its behaviour it is needed to start from the description of steering kinematics using lookup tables as usual. The data stored in the curves introduce the dependency on steering wheel angle (or rack travel) of the following quantities:

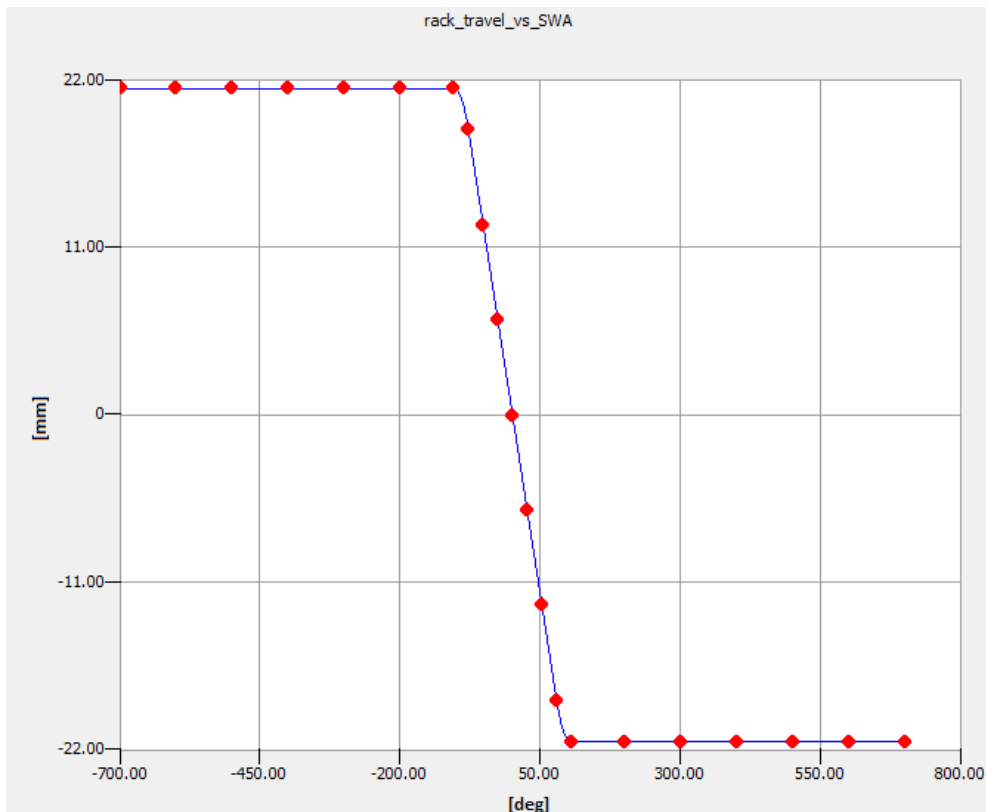
- **Steer At Ground** (Left/Right): is the angle measured from the vehicle heading to the line formed by the intersection of the wheel plane with the ground plane. The Steer At Ground angle is positive when a wheel is rotated to the left as if the vehicle were making a left turn.
- **Camber angle** (Left/Right) is the angle the wheel plane has with respect

to the vehicle's vertical axis. It is positive when the top of the wheel leans outward from the vehicle body.

- **Side view angle** (Left/Right) is the variation of the wheel carrier side-view rotation angle with respect to the caster angle at design time. It is positive for a clockwise rotation, as seen from the left side of the vehicle.
- **Wheel center x-coordinate variation** (Left/Right) describes wheel base variation in wheel location reference system as a function of wheel jounce.
- **Wheel center y-coordinate variation** (Left/Right) describes wheel track variation in wheel location reference system as a function of wheel jounce.

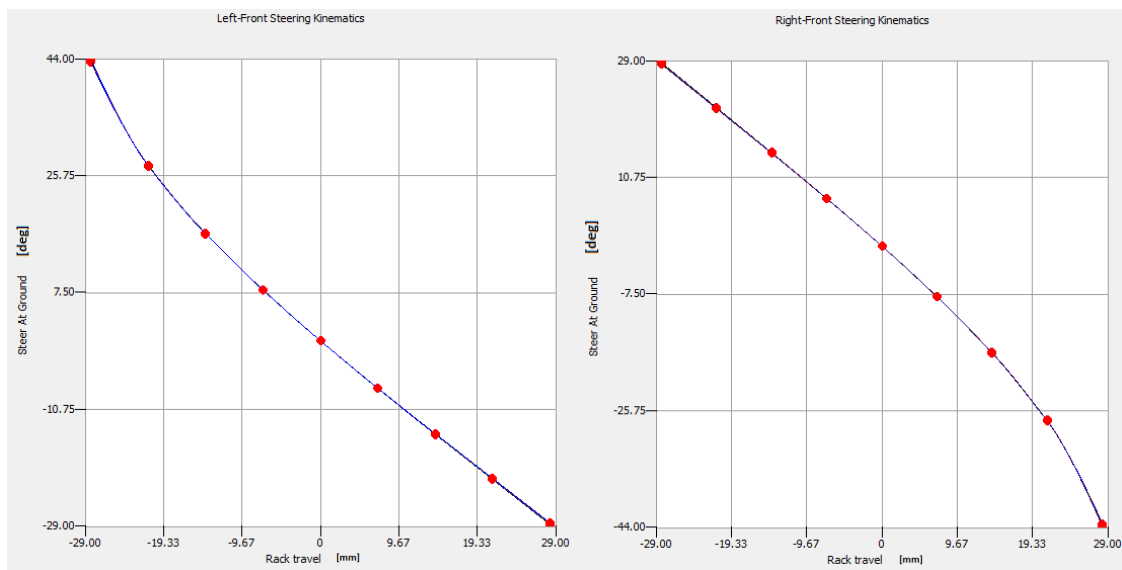
In particular, it's necessary to define:

- **Rack Travel vs Steering Wheel Angle:** it relates the steering wheel input to rack travel kinematics; all the splines which define the steering kinematic are defined as a function of the rack displacement.



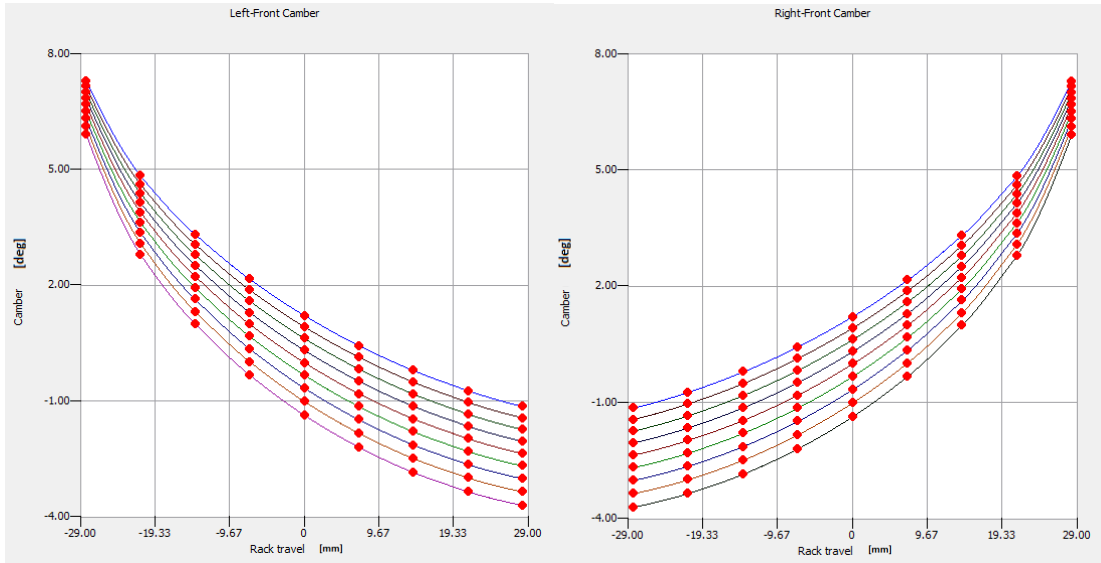
- **Steer at ground vs Input Steer** used to set properties for the steer angle method. The option we have selected is the **Steer Input and Jounce** defining the steer angle by a 3D spline having the steering wheel angle as first independent variable and the wheel jounce as second independent variable. Total Steer at Ground can be expressed as:

$$\delta_{SaG} = \delta(\text{steering_wheel_angle}/\text{rack_travel}, \text{jounce})$$



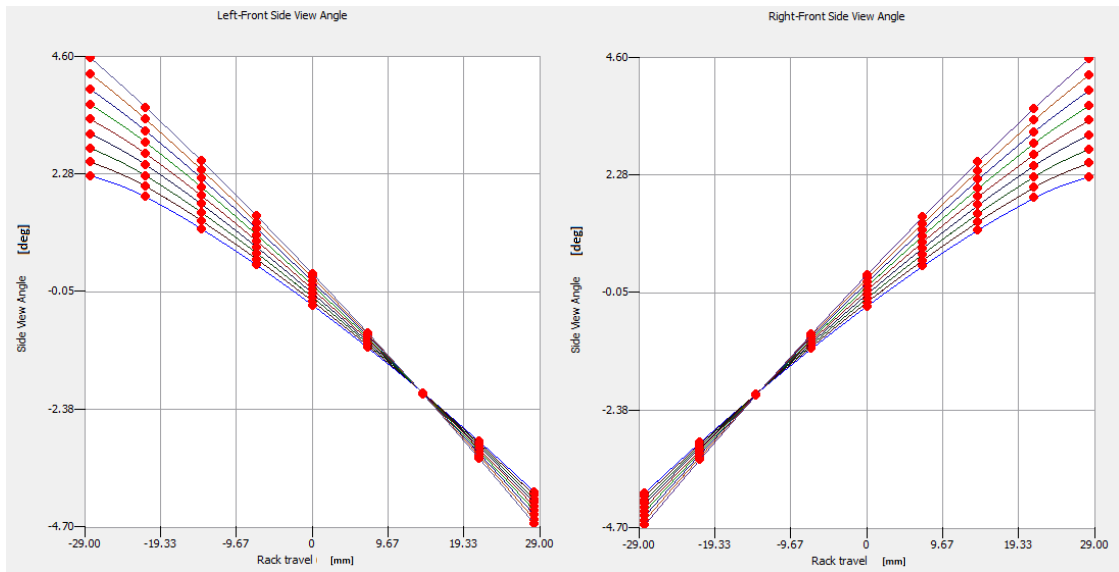
- **Camber Angle vs Input Steer vs Jounce**, gives information about camber angle dependency on steering wheel angle, having the latter as first independent variable and the wheel jounce as second independent variable. Camber angle can be expressed as:

$$\kappa = \kappa(\text{steering_wheel_angle}/\text{rack_travel}, \text{jounce})$$



- **Side View Angle vs Input Steer vs Jounce**, representing the curves for side view angle dependency on steering wheel angle. In this case, as in the previous one, the first two variables are unchanged while the third one is the side view angle, expressed as:

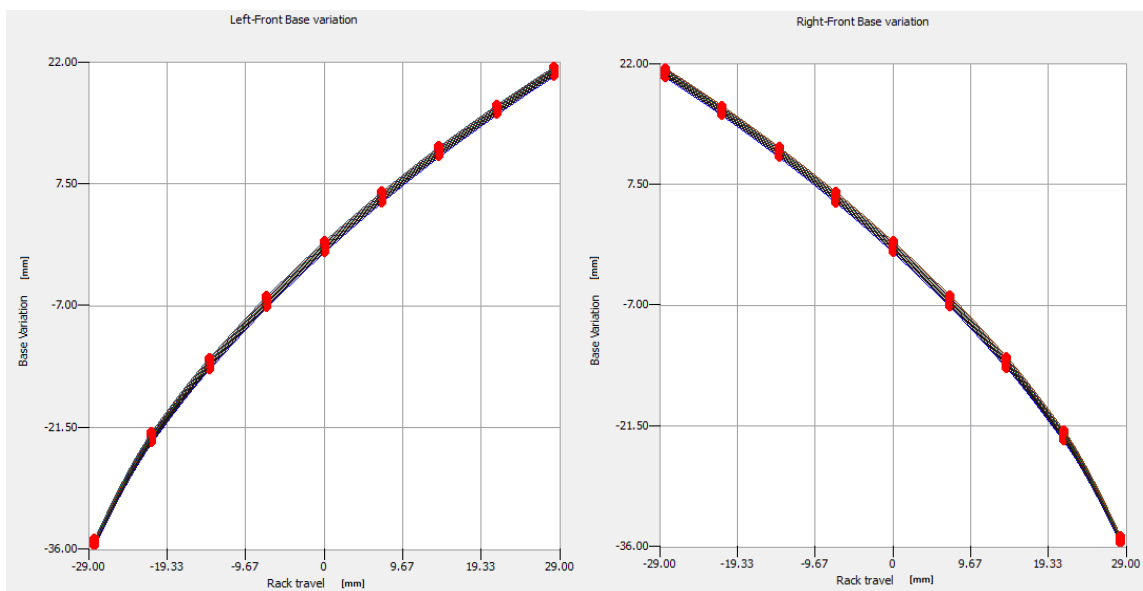
$$\theta = \theta(\text{steering_wheel_angle}, \text{jounce})$$



- **Steering dependent wheel location**, that indicates the dependency of track and base variation (kinematics) on steering wheel angle (or rack displacement). They are divided into 2:

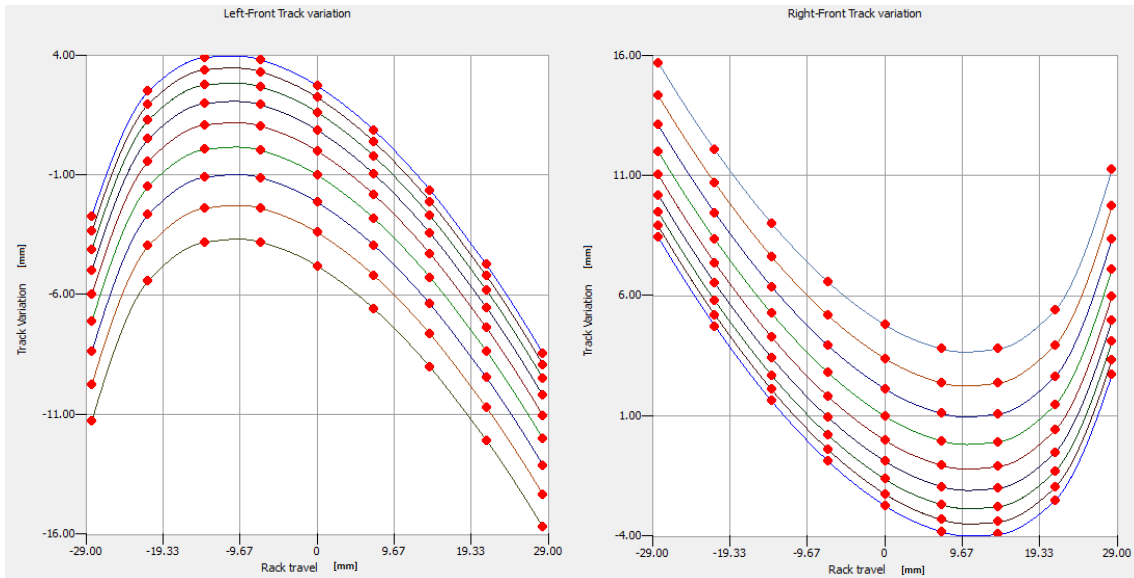
- **X-coord variation vs Input Steer vs Jounce**, shows the curves for wheelbase dependency on steering wheel angle as 3D spline. The wheelbase variation can be expressed as:

$$x = x(\text{steering_wheel_angle}, \text{jounce})$$



- **Y-coord variation vs Input Steer vs Jounce**, for wheel track dependency on steering wheel angle. The wheel track variation expressed as:

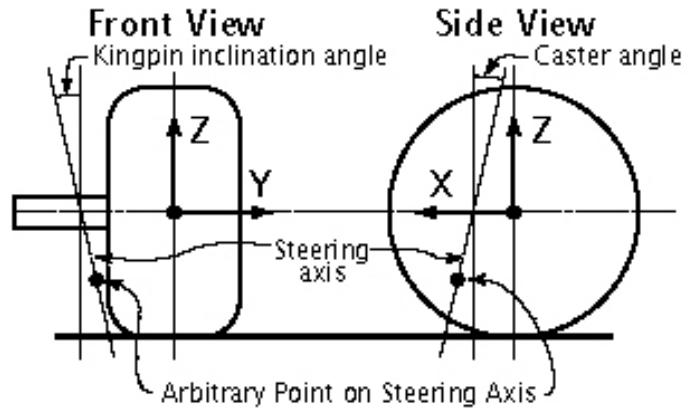
$$y = y(\text{steering_wheel_angle}, \text{jounce})$$



In order to compute the steering wheel torque feedback, it is also important to introduce the Kingpin Geometry, that defines the steering axis position using the following quantities:

- **Caster Angle:** is the angle in the side elevation (vehicle XZ plane) between the steering (kingpin) axis and the vehicle's vertical axis. It is positive when the steer axis is inclined upward and rearward. The Caster Angle is mapped as a function of Steering Wheel Angle (or Rack Travel) and Suspension Jounce.
- **Kingpin Inclination:** is the angle in the front elevation between the steer axis (the kingpin axis) and the vehicle's vertical axis. It is positive when the steer axis is inclined upward and inward. The Kingpin Inclination Angle is mapped as a function of Steering Wheel Angle (or Rack Travel) and Suspension Jounce.
- **Arbitrary Point on Steer Axis** in order to fully define the kingpin axis it is needed to identify a point belonging to the axis. The X,Y,Z locations of the point are mapped as a function of Steering Wheel Angle (or Rack Travel) and Suspension Jounce.

Coordinates of the point on kingpin axis are expressed in wheel location reference system.



The calculation of Kingpin Geometry was performed using the data available in the Steering and Front Suspension Subsystems. The method for calculation is to compute the instant axis of rotation of the wheel carrier parts. In case of independent suspensions, it calculates Base, Track, Toe, Camber, Side View Angle derivatives using kinematics data from Steering Subsystem as:

$$\frac{\partial x(\delta, J)}{\partial t} = \frac{\partial x(\delta, J)}{\partial \delta} \cdot \frac{\partial \delta}{\partial t} + \frac{\partial x(\delta, J)}{\partial J} \cdot \frac{\partial J}{\partial t}$$

and locking the spring travel it's possible to write:

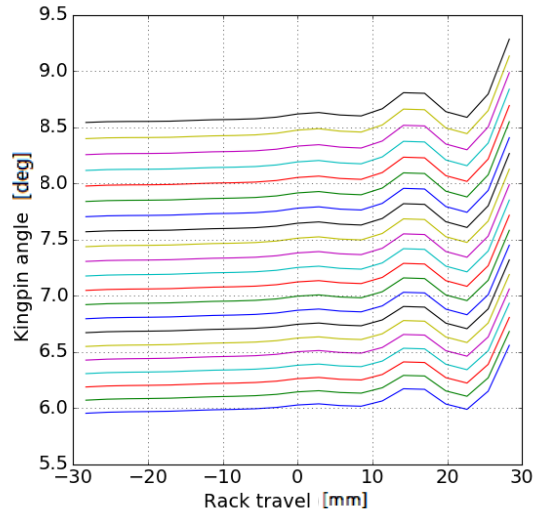
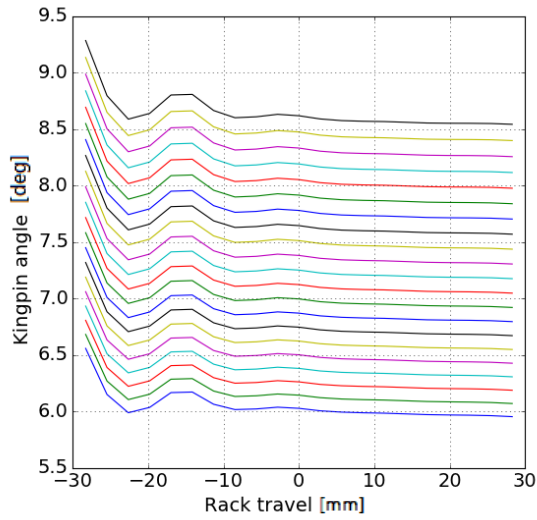
$$\frac{\partial f(J)}{\partial t} + \frac{\partial g(\delta, J)}{\partial t} = \frac{\partial f(J)}{\partial J} \cdot \frac{\partial J}{\partial t} + \frac{\partial g(\delta, J)}{\partial \delta} \cdot \frac{\partial \delta}{\partial t} + \frac{\partial g(\delta, J)}{\partial J} \cdot \frac{\partial J}{\partial t} = 0$$

where f and g are the motion ratios of the spring function of Jounce and SWA. Substituting the second equation into the first one is obtained:

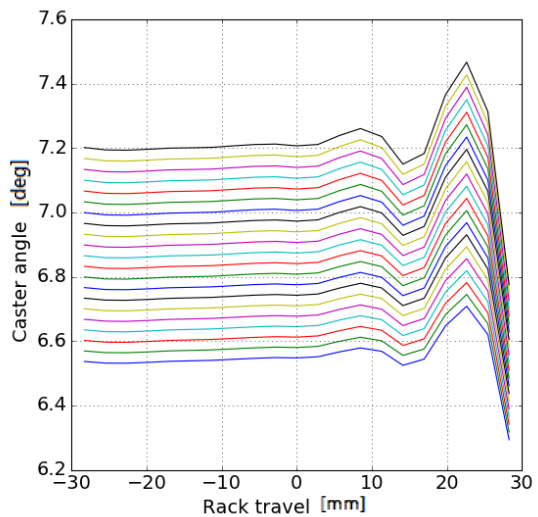
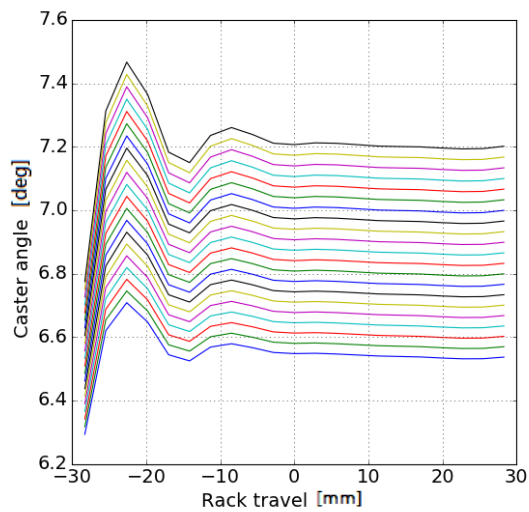
$$\partial x = \left(\frac{\partial x(\delta, J)}{\partial \delta} - \frac{\partial x(\delta, J)}{\partial J} \cdot \frac{\frac{\partial g(\delta, J)}{\partial \delta}}{\frac{\partial f(J)}{\partial J} + \frac{\partial g(\delta, J)}{\partial J}} \right) \partial \delta$$

With these steps, we can obtain information about:

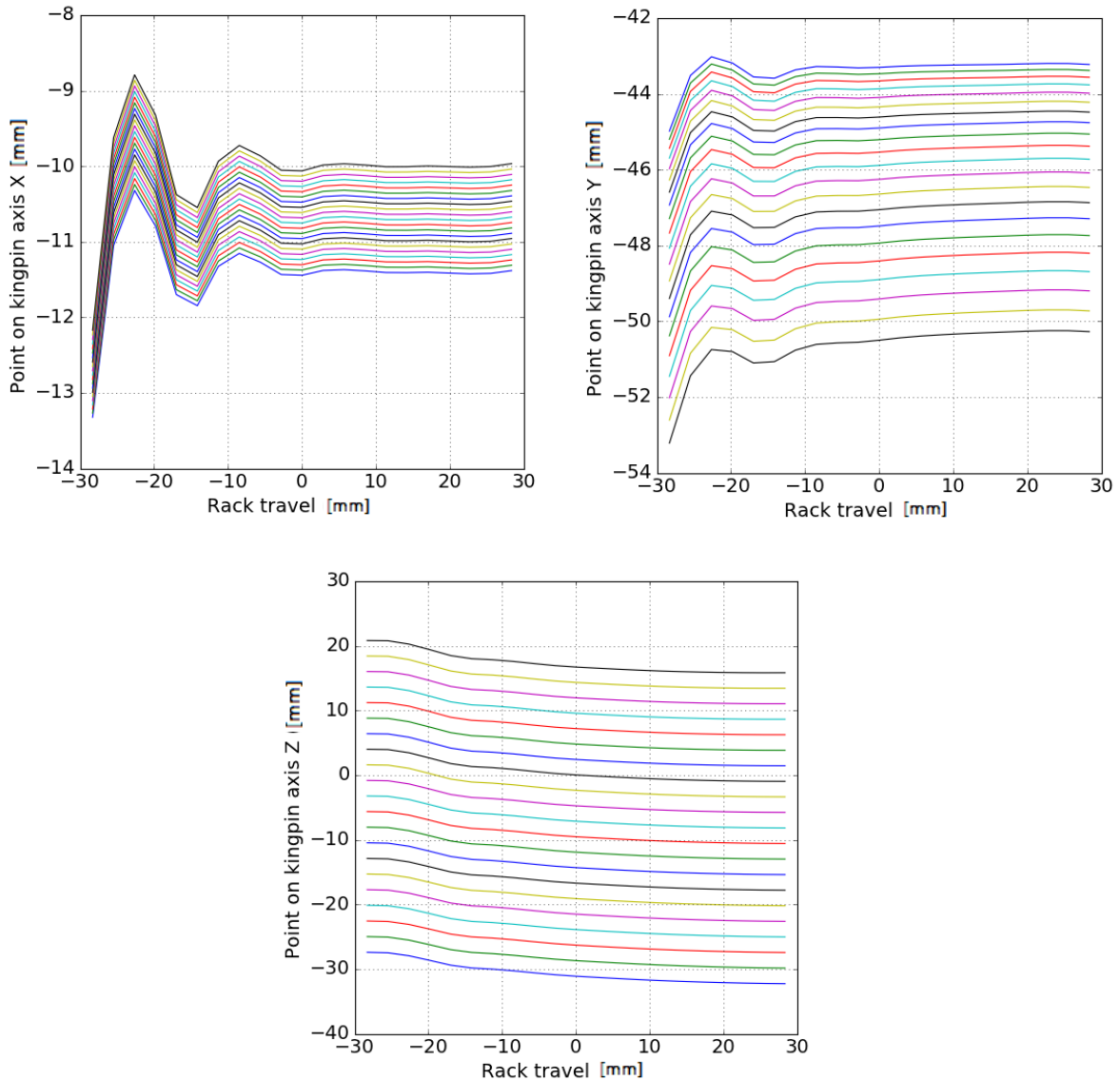
- **Kingpin Inclination** (Left/Right)



- **Caster Angle** (Left/Right)



- **Point X, Y, Z of Kingpin Axis (Left/Right)** (here reported only for the Left side, for a symmetric reason)



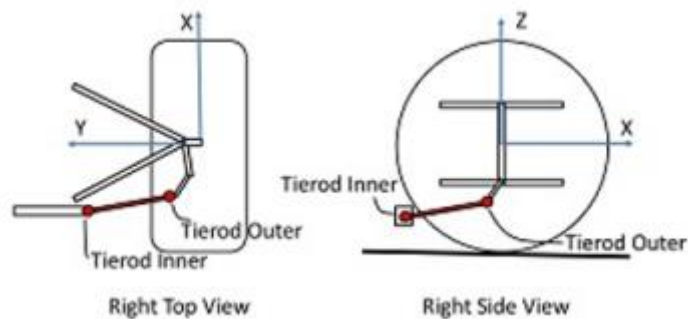
Continuing with the modelling, it is necessary to define the parameters for the calculation of the steering wheel torque (or rack force). They are supported 2 alternative methods: the Tie-rod geometry based computation and the Steering Feedback maps. In our case, we use the first one.

- **Tie-rod geometry:** require the input of the geometry of left and right tie-rod in terms of locations of their inner and outer hardpoints. In this way, the steering torque is computed under the assumption of ideal mechanical transmission of motion (eventually including compliance), from steering wheel to tierods. Friction are not considered. The geometry require the

following parameters:

- **Left Tierod Outer:** X,Y,Z coordinates of the left tie-rod outer hardpoint, with respect to a reference frame located in the wheel center and oriented as vehicle reference frame.
- **Left Tierod Inner** X,Y,Z coordinates of the left tie-rod inner hardpoint, with respect to a reference frame located in the wheel center and oriented as vehicle reference frame.
- **Right Tierod Outer** X,Y,Z coordinates of the right tie-rod outer hardpoint, with respect to a reference frame located in the wheel center and oriented as vehicle reference frame.
- **Right Tierod Inner** X,Y,Z coordinates of the right tie-rod inner hardpoint, with respect to a reference frame located in the wheel center and oriented as vehicle reference frame.

| Tierod Geometry | | | |
|--------------------|-------|--------|--------|
| | X | Y | Z |
| Left Tierod Outer | -50.0 | -56.0 | -120.3 |
| Left Tierod Inner | -50.0 | -379.0 | -134.7 |
| Right Tierod Outer | -50.0 | 56.0 | -120.3 |
| Right Tierod Inner | -50.0 | 379.0 | -134.7 |



In this way, in order to compute torque and forces, the instantaneous torque acting about the instantaneous kingpin axis is put in equilibrium with the force acting along the tie-rod direction, according to the following equation:

$$M_K = r \times F_t$$

where r is the distance between the instantaneous kingpin axis and the tie-rod outer point. The X,Y,Z components of the tie-rod force are evaluated by projecting F_t vector with respect to the vehicle location reference system.

The rack force is then evaluated as the sum of the left and right tie-rod force:

$$F_{rack} = F_{tL} + F_{tR}$$

and it is used to evaluate the **Steering Wheel Torque** according to:

$$T_{swa} \cdot \partial\theta_{swa} = F_{rack} \cdot \partial\tau$$

where:

- T_{swa} is the Steering Wheel Torque;
- θ_{swa} is the rotation angle of the steering wheel angle;
- F_{rack} is the rack force;
- τ is the rack displacement (displacement along the Y direction)



The Steering Wheel Torque is then computed as:

$$T_{swa} = F_{rack} \cdot \frac{\partial \tau}{\partial \theta_{swa}}$$

The steering system modeling is thus completed, leaving all other settings for more complex systems by default. We can therefore proceed with the next subsystem.

5. WHEELS

This subsystem collect mass, inertia, **tire property** of unsprung masses of our vehicle model. First of all, it is imported the .tir file of our specific tire. This is used to compute the tire forces, with different method and format like MF_05, PAC2002, PAC_CT, FTire, MF-Tyre/MF-Swift. The file with all parameters of our tires is included into the Index section of this thesis. In addition to this, the spin inertia properties of the parts rotating with the wheel must be added, which are: rim, tire, brake disk, driveshaft. In addition, the moments of inertia of the unsprung masses, measured in the wheel location reference frame, must be specified. Finally, the mass of the individual wheel and of the suspension part that is not counted in the suspended masses is inserted. Together with it, the vertical position of the wheel centre is introduced.

| Wheel Properties | |
|---------------------------|--|
| Tire Property File | mdids://SC17/tires.tbl/Pirelli_52_32457_.tir   |
| Spin inertia (one wheel) | 187500.0 |
| Ixx (hub carrier + wheel) | 228000.0 |
| Iyy (hub carrier + wheel) | 230000.0 |
| Izz (hub carrier + wheel) | 368000.0 |
| Unsprung mass | 16.75 |
| Wheel center height | 260.0 |

This process is to be carried out for each individual vehicle corner.



6. BRAKES

For the description of the braking subsystem, the vehicle model allows open or closed-loop brake torques to be specified at the wheels. The brake model represents a four-wheel disk brake configuration. All brake parameters associated with the brake on one wheel can be specified independently. The parameters are:

- **bias_front:** gives the portion of braking system pressure going to front wheels.
- **master_cylinder_pressure_gain:** is the scalar relating the driver brake demand to master cylinder pressure.
- **mu** (front/rear) friction coefficient
- **effective_piston_radius** (front/rear) radius for applying friction force.
- **piston_area** (front/rear)
- **lockup_natural_frequency** (front/rear) the brake model includes a 1DOF spring-damper system to model the wheel lockup; the parameter sets system natural frequency.

- **lockup_damping_ratio** (front/rear) the parameter sets lockup model damping.
- **lockup_speed** (front/rear) the parameter sets the lockup speed.

| Name | Left Value | Right Value |
|-------------------------------|------------|-------------|
| bias_front | 0.7 | |
| master_cylinder_pressure_gain | 0.1 | |
| mu | 0.4 | 0.4 |
| effective_piston_radius | 180.0 | 180.0 |
| piston_area | 2300.0 | 2300.0 |
| lockup_natural_frequency | 10.0 | 10.0 |
| lockup_damping_ratio | 1.0 | 1.0 |
| lockup_speed | 139.0 | 139.0 |
| mu | 0.4 | 0.4 |
| effective_piston_radius | 180.0 | 180.0 |
| piston_area | 2300.0 | 2300.0 |
| lockup_natural_frequency | 10.0 | 10.0 |
| lockup_damping_ratio | 1.0 | 1.0 |
| lockup_speed | 139.0 | 139.0 |

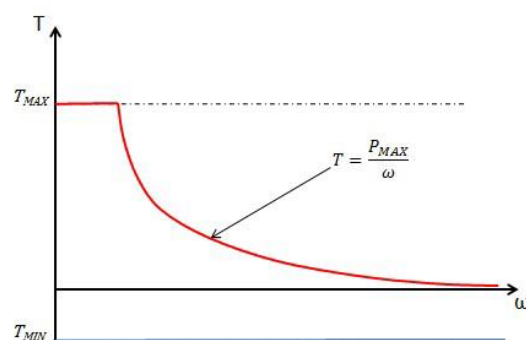
7. POWERTRAIN

Last but vital subsystem is engine modelling. Or rather, in our case, the 4 motors. In fact, the introduction in Vi-CarRealTime of the possibility to model electric motors directly coupled to the wheels was of vital importance. Until now, the behaviour of the 4 electric motors was in fact modeled as a single thermal motor, with AWD configuration with 30% drive front bias. The torque curve of the motor was given by the sum of the curves of the 4 motors, and relative inertia. This model was working but did not allow a precise modelling of the real component. Now, the flexibility and modularity of the new driveline allows the user to easily configure powertrain subsystem in terms of main engine (internal combustion or electric), 8 different motors (internal combustion or electric), gearbox (automatic/manual), clutch (standard, dual), torque converter, differentials (FWD, RWD, AWD).

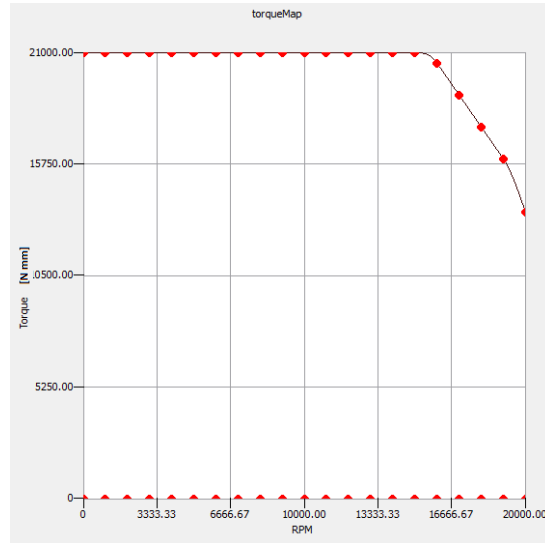
First of all the driveline layout has to be set properly. This is our case:

Then, depending on what we have selected on the layout , it's necessary to describe the motors (for all 4 corners). We can choose between 2 types of model: Simple Engine or Standard Engine. A simple engine is modeled as follow:

At full throttle (100%), the engine provides a torque equal to T_{MAX} until the product between T and Ω is less than P_{max} ; then it provides a torque equals to the ratio of P_{max} and ω . During coasting (throttle 0%), it generates a constant T_{MIN} .



In this case, the parameters to be entered are simplified. In our case, however, having all the characteristics of the AMK engines used, we can describe the model in detail, the Standard Model, with the Torque Map Data, the curve that provides the torque produced by the engine as a function of RPM.



All the others parameters are the following:

- **Inertia** of the engine rotating parts.
- **Efficiency**, defines the efficiency of the engine rotating parts.
- **Stall RPM** is the engine rpm speed at which the driver disengages the clutch.
- **Idle RPM**, Idle rotational speed of the engine.
- **Rev Limit RPM**, Maximum rotational speed of the engine.
- **Torque scaling**, Engine torque scaling factor.
- **Transmission Ratio**, it is the transmission ratio between the engine crankshaft and the clutch input plate.

| Mechanical Properties | | Controllers | |
|---|----------------|------------------------------|--------------------|
| Model Type | standard | Transmission Ratio | 14.82 |
| Torque Map Data | Plot/Edit Data | Simple Engine Minimum Torque | 0.0 |
| <input type="checkbox"/> Torque Map Property File | | Simple Engine Maximum Torque | 1.0 |
| Inertia | 274.0 | Simple Engine Maximum Power | 1.0 |
| Efficiency | 1.0 | Simple Engine Tau | 0.0 |
| Idle RPM | 0.0 | Torque Scaling | 1.0 |
| Rev Limit RPM | 19200.0 | Torque Reaction Direction | No Torque Reaction |

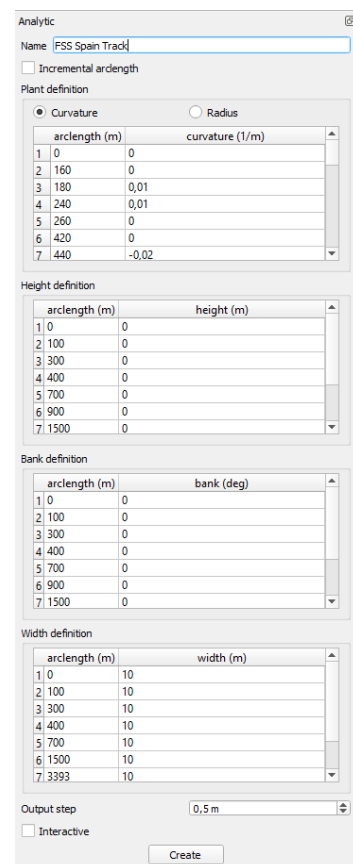
At this point all subsystems have been modeled, and our vehicle model is complete. The next engineering step, once the model is completed, would be to validate it. Model validation is a key process that bridges the virtual world of simulations with the real world. It is in fact necessary to carry out some typical manoeuvres to be able to verify that the model reflects exactly, or almost, what happens in the real world. However, in this specific thesis, the validation of the model is not treated, which would provide so much material to write another thesis. So, at this point, let's consider the model validated.

4.3 Creation of the race track

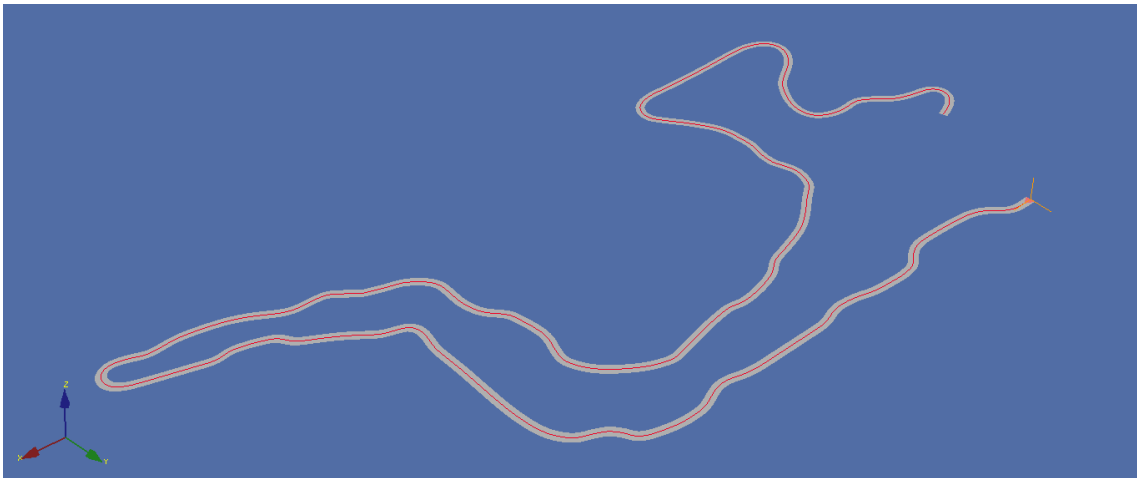
At this point, created the vehicle model is necessary to proceed to the creation of the path. In our case, we want to submit our model to follow the same track of the autocross test in Spain, in order to verify its performance, compare data with telemetry and then proceed to an optimization of the vehicle.

To proceed, it is necessary to have the correct information of the track, in our case collected with a GPS device directly on the road during the safe walk before the race, and build the racetrack using the Vi-Road software of the same suite Vi-Grade. This process, shown on the image here on the right, was carried out in an analytical way, creating first the centerline that the vehicle will have to take as a reference and follow, to then complete the track with the road and in case of need enter details such as curbs, irregularities and friction.

After that, it is possible to modify the Path that the vehicle has to follow. In fact, the real trajectories that a driver would make, for example the corner cutting,



can be considered. There is a section within the software in which it is possible to evaluate the size of the vehicle, compare it with the available dimensions of the road travelled and recalculate a trajectory with the cut of the curves (without leaving the road) with an index of effectiveness and maximum offset distance from the central trajectory generated at the start. In our case, however, since the GPS data collected already simulated the "real" distance chosen by the driver, no changes were made, even considering the approximation of the measurement made.



4.4 Static Lap Time Simulation

After the preparation of the model and layout and having correctly set the solver and all the parameters of interest, it is possible to proceed with the first simulation.

Static Lap Time:

This event is used to define static limit velocity profile on a given track. It uses a specific static solver (SpeedGen) and a simplified model respect to the one used in other events. Basically, the vehicle has no suspensions and inherits all the properties from the full VI-CarRealTime model.

The effect of aero forces is considered and the effect of suspension jounce is taken into account by the presence of ride height maps. The solver, based on vehicle model and specified lateral and longitudinal grip, computes the limit velocity profile and produces it as output tabular data for simplified vehicle state and a Driving Machine event file which can be used to verify if the vehicle can reach the limit set by VI-SpeedGen static solver in a dynamic simulation. Into the setting parameters of this event, the user has the option to scale the grip in some regions of the track when verifying that the performance computed by VI-SpeedGen cannot be reached in dynamics. It is possible to introduce a constant performance factor or also a table. This is possible for:

- **Longitudinal Acceleration Performance**
- **Longitudinal Braking Performance**
- **Lateral Performance**

An important feature in this type of simplified model is the possibility to consider the limits of the tires. Tire Limits tool is used to evaluate the force envelope produced by each tire. Such envelopes are used by VI-SpeedGen solver to compute the maximum lateral and longitudinal acceleration of the simplified vehicle. In general it allows the solver to estimate speed profiles closer to the dynamic simulation ones, thus reducing the overestimation of the speed profile.

In our case, taking into account of tire limits and considering a performance factors of 1.0 for all 3 cases, we reach a lap time of 74.60 sec.

Chapter 5

Performance Parameters Evaluation

5.1 Vehicle Performance Parameters

The framework of the FSAE competition is defined by a small, open set of rules limiting possibilities for vehicle development. They also set up performance metrics in the form of the competition itself. In our specific case, the Autocross event contains all the performance parameter important to evaluate a racecar excepting the fuel consumption. Our evaluation and optimization criteria concern the vehicle behaviour in:

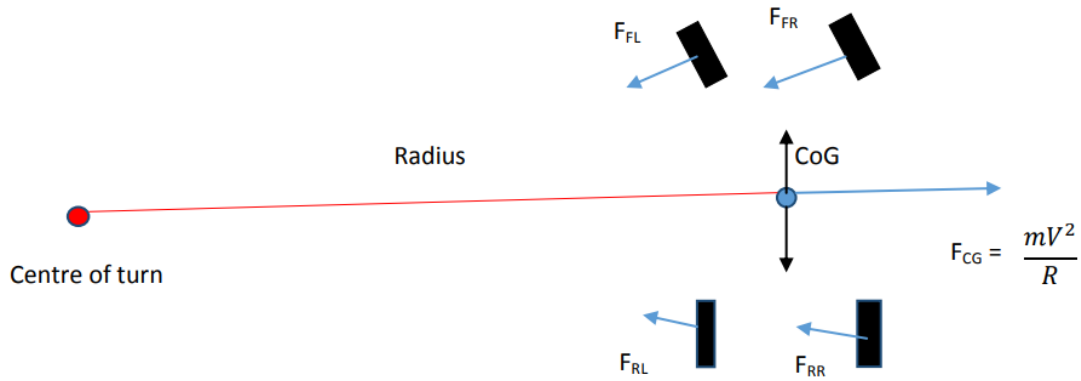
- Acceleration: taking into account the steady state condition but also all the transient aspects like the traction limited acceleration on corner exit
- Braking: steady state braking and transient behaviour like trail braking
- Cornering: steady state cornering and all the transient behaviour like corner entry, corner exit, cornering control

5.2 Centre of Gravity Longitudinal Optimization

The location of the centre of gravity (CoG) of a race car is one of the most fundamental determinants of performance because tire cornering force capability is very dependent on the vertical (or normal) load applied to the tire. Most chassis changes that are made in an attempt to tune handling performance of race cars have, in one way or another, an effect on wheel loads. This may be either through CG position changes or changes that affect the weight transfer distribution during cornering. The first important fact in calculating the vertical individual wheel loads in steady state cornering, accelerating and braking is the determination of CG position.

In our case, considering the Autocross event, it is really important to investigate about the effects that the centre of gravity has on its ability to negotiate corners of varying radii at different velocities. Our objective is to gain the most advantage on vehicle handling, understanding how to optimize the weight distribution so that the velocity the vehicle can negotiate the various turns is maximized.

During a corner, The overarching force that has to be opposed is the centripetal force acting through the centre of gravity of the vehicle. This requires the sum of the lateral forces created by the tyres to be equal and opposite to this force. It is easier to see visually that when the centre of gravity location is varied then the required angle of the front tyres is going to change due to the rear tyres being fixed. This is where the toe in/toe out angle of the rear tyres would be changed in order to try and create the most beneficial setup. This is typically easier to do when looking at either small or large radius turns but not a combination of both. A graphical representation of these forces can be seen in the following figure.



This produces the following balance equation:

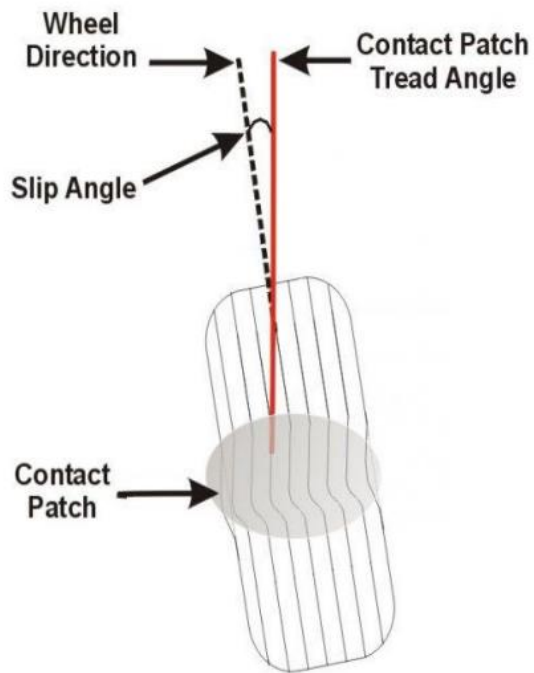
$$F_{CG} + F_{FL} + F_{FR} + F_{RL} + F_{RR} = 0$$

In order to determine whether there is a feasible solution this force equation has to be satisfied. This is done by determining if the required angle of the front wheels to produce the most beneficial slip angle depending on the vertical load experienced by each tyre is within the steering limit. The equation may not be satisfied which would mean that the vehicle would not be able to negotiate a turn of that radius at the given velocity for that particular location of the centre of gravity due to tyre slip i.e., the traction in the tyres cannot produce enough lateral force to counter the centripetal force of the vehicle.

The magnitude of the individual forces is largely dependent on the overall weight of the vehicle, but most importantly where the centre of that weight is located. This centre of gravity determines the distribution of the vertical forces placed on the front versus rear wheels and the height of the centre of gravity affects the weight transfer to the outside tyres whilst cornering. During this evaluation, it is very important to understand the difference in the behavior of the individual tire with the road. In our case, the analysis was carried out using our supplier's Pirelli tyre data. Therefore, the possibility of changing tyres was not evaluated.

These factors are relevant when discussing allowable slip angles for certain tyres. The slip angle on a tyre is the angle between the direction the tyre is facing compared to the actual direction the tyre is travelling and the optimum

slip angles on different tyres vary with different vertical loads. This is due to a higher coefficient of friction for lower vertical loads at smaller slip angles. This is illustrated in figure below depicting a tyre that is turning to the left. The tyre follows the red path due to the deformation in the tyre as it rotates around.

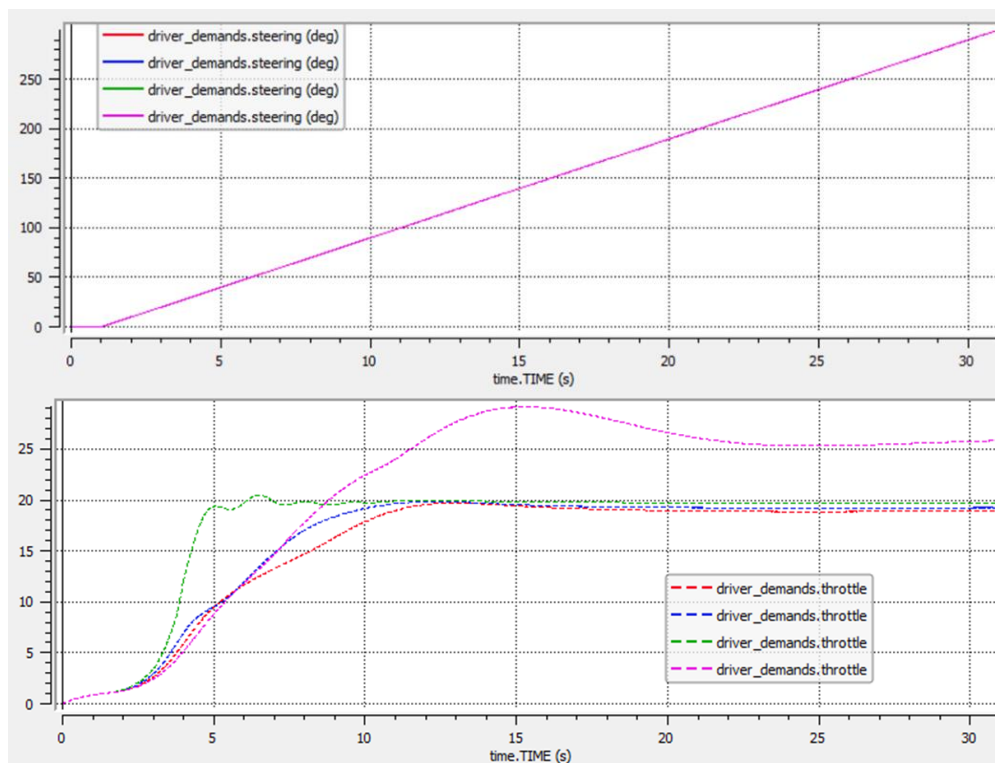


In our evaluation we focused on the variation of the longitudinal position of the centre of gravity, performing a typical Ramp Steer manoeuvre to verify the behaviour, before implementing it in the max performance event.

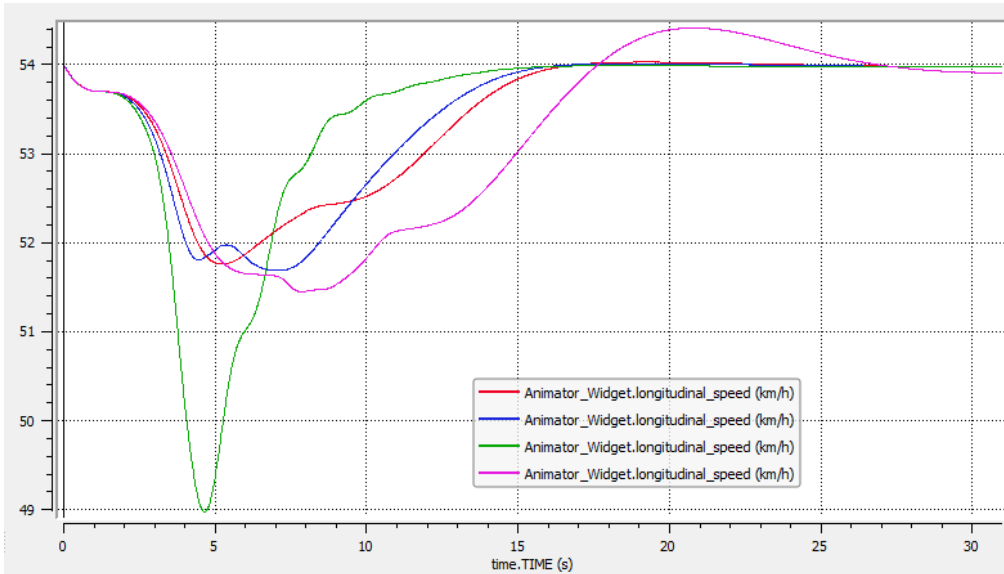
| Ramp Steer | |
|--|---------|
| End Time | 31.0 |
| Initial Velocity | 15000.0 |
| Initial Gear | 1 |
| Start Time | 1.0 |
| Ramp Duration | 30.0 |
| Initial Steer | 0.0 |
| Slope | 10.0 |
| <input checked="" type="checkbox"/> Cruise control | |
| <input type="checkbox"/> Steer Release Time | 5.0 |

The original position of the CG was measured at 809 mm. According to our analysis, we will perform tests by varying the longitudinal position, on the following target values:

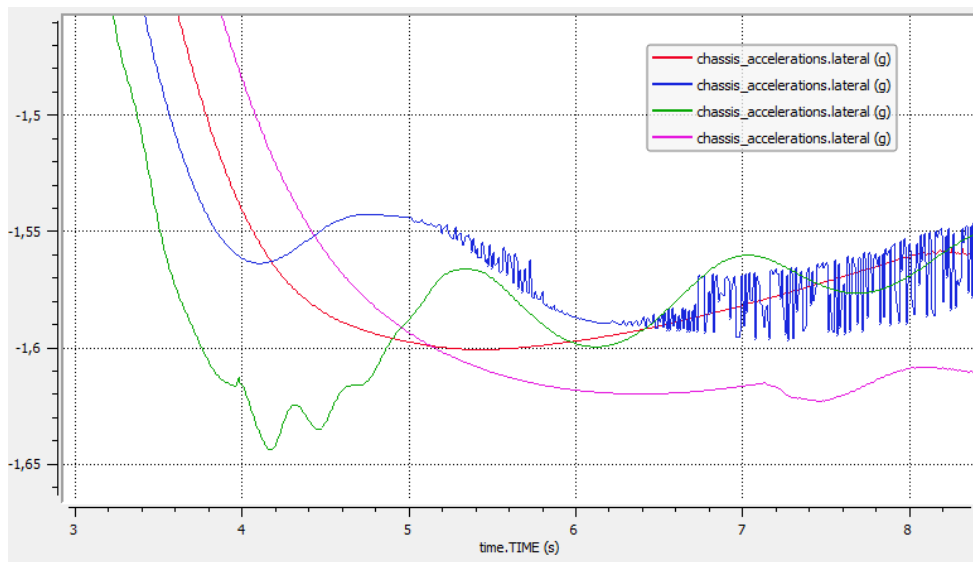
- 609 mm [----]
- 809 mm [----]
- 1009 mm [----]
- 1209 mm [----]



In the above graphs, the ramp steer manoeuvre carried out to analyse the effects of the variation of the centre of gravity is described. It is described by a steering curve, which, starting from the second 1, grows steadily over time by 10 degrees flying for each second. Below, the driver action on the throttle is described to maintain the constant speed that has been set.

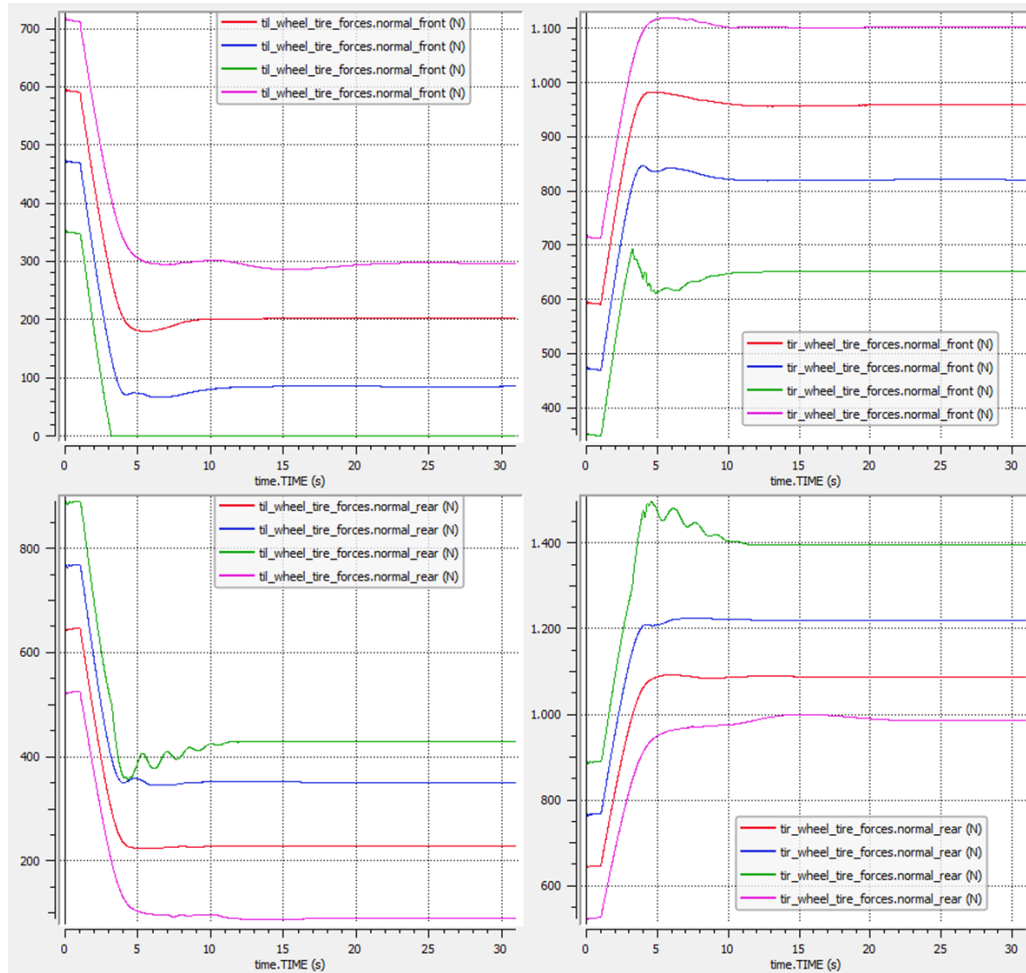


In the graph above, you can see the speed signal, set to cruise control at 54 km/h, go down at the beginning of the steering input and then return to the constant value, with different behaviors, depending on the configuration. In this case, the different speed loss must be analysed according to the position of the centre of gravity, which therefore leads to an input in a different curve.

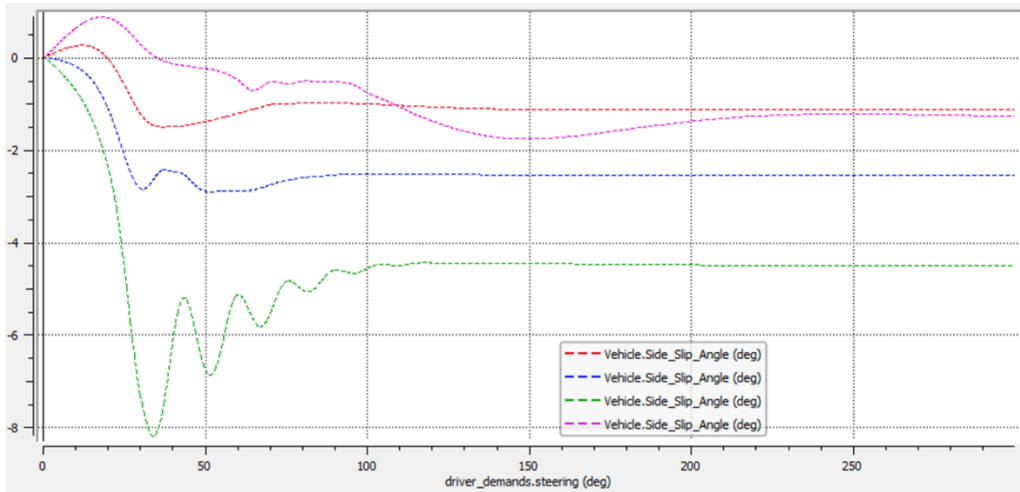


In the detail of the graph, the different curved approach to the ramp steer manoeuvre is analysed with regard to the course of lateral acceleration,

immediately reaching a high peak for the green configuration, which then has a decreasing oscillatory course, while the fuchsia configuration, reaches its peak more slowly but then manages to maintain it.

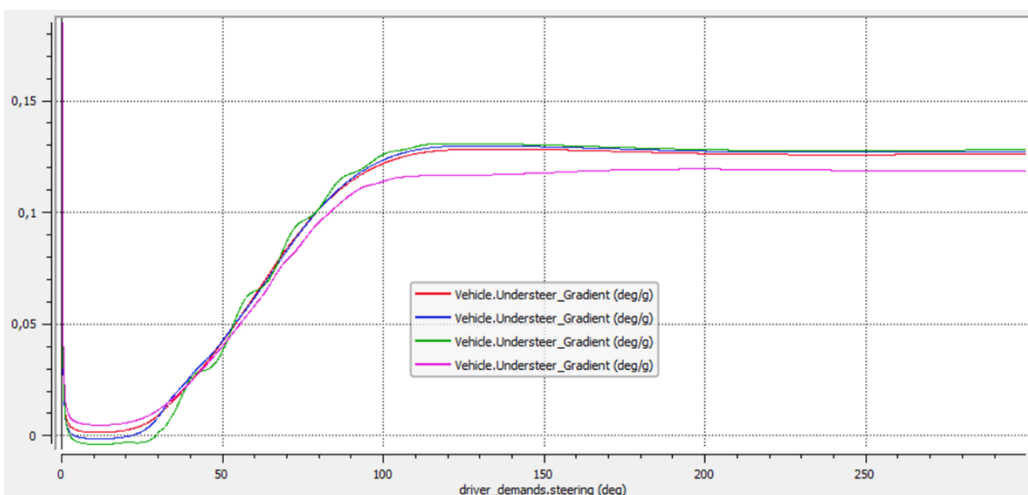


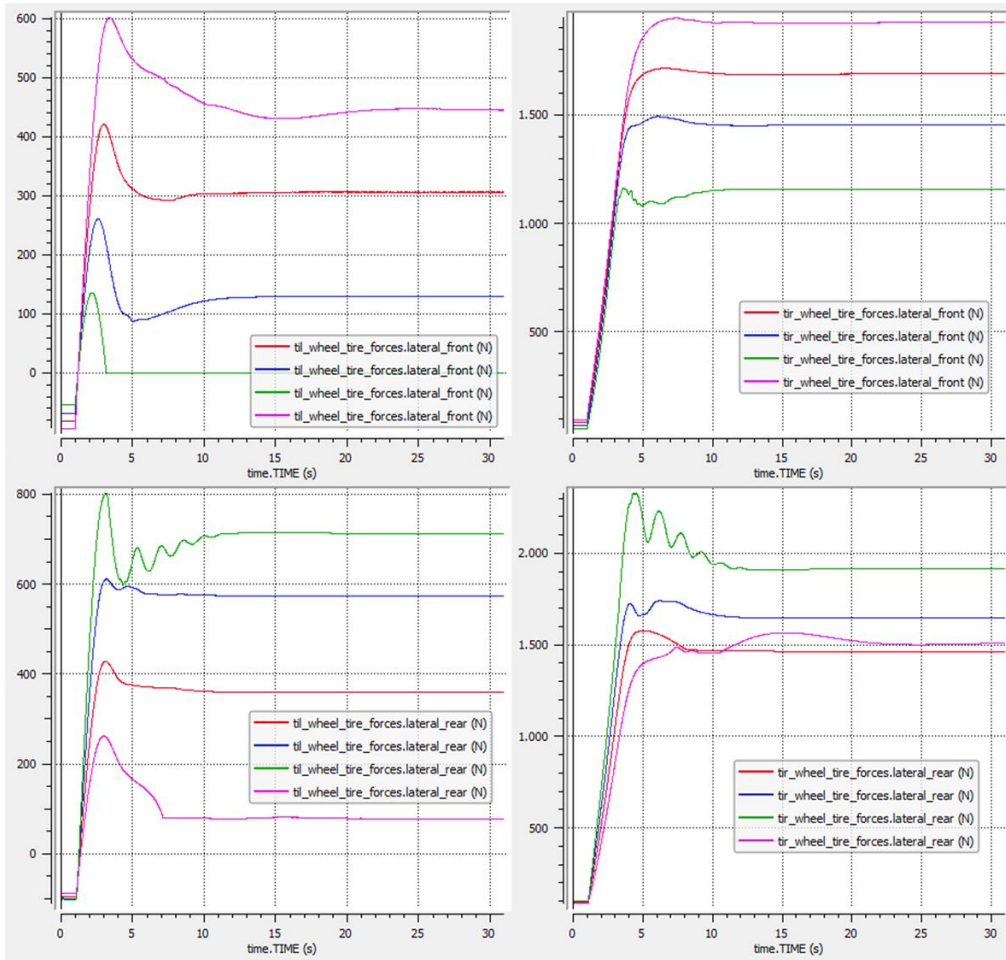
The four graphs above, analyze the trends of normal forces at 4 wheels. This is the initial basis for assessing the correct balance of the vehicle and thus be able to make the best possible use of the most heavily loaded tyre, bearing in mind also its limit. As you can see, the tyre outside the curve is the most loaded, while the interiors are the least, a phenomenon due to the transfer of lateral load in curves. Taking this concept as a starting point, it is possible to analyse the differences that the positions of the centre of gravity can generate, by going to load the front or rear wheel more. In the case of the green curve, unlike in the past, we have the front inner wheel that has practically reached the zero load condition, and this is the reason why the vehicle loses speed and therefore performance.



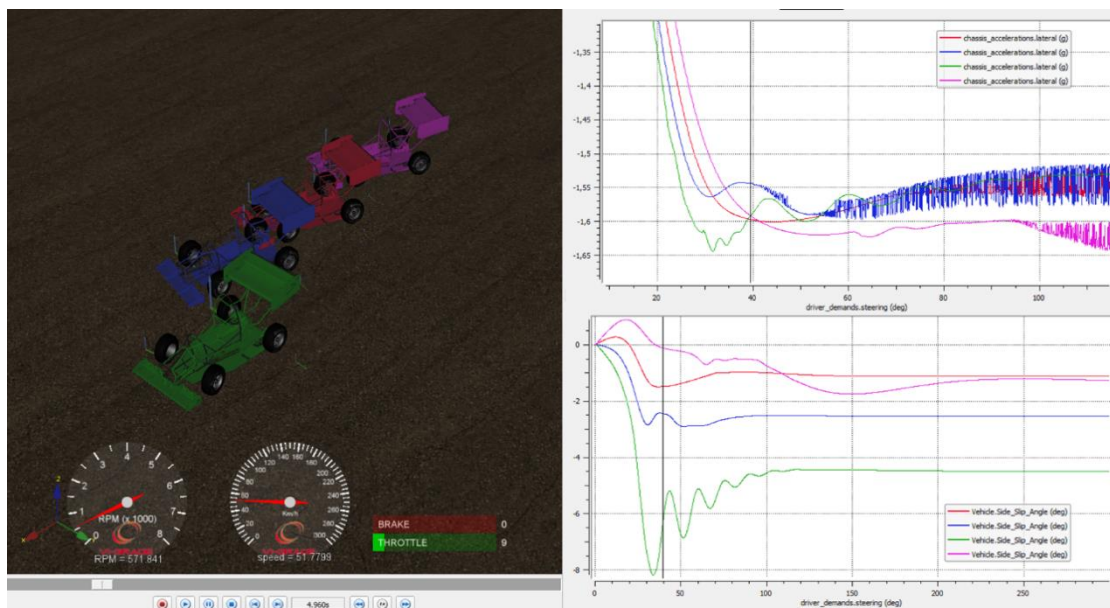
Represented above, the trend of the sideslip angle, with oscillatory behavior for the green curve, while markedly different, especially in the input phase where it reverses the sign, for the fuchsia curve.

Below, instead, is represented the trend of the Understeer Gradient, parameter that allows to evaluate the under-steering behavior of the vehicle, with an index. It is possible to notice the less under-steering trend of the fuchsia curve compared to other analyzed cases.



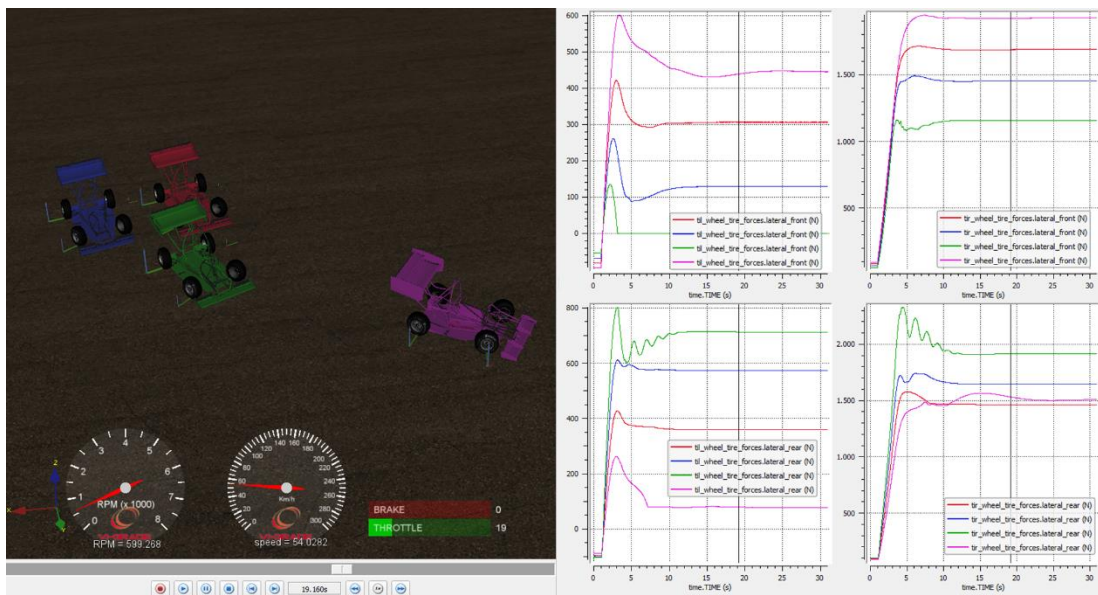


In the graph, the 4 lateral forces exerted by the tyres on the ground, highlight the different approach of the steering ramp. Below, the curved approach is highlighted, corresponding to the beginning of the steering ramp, where the



green vehicle achieves greater lateral acceleration and therefore seems to be ahead of other vehicles. However, this behavior will then be frustrated during the journey of the ramp, as can be seen in the image following.

Once the stability condition is reached, in fact, the fuchsia vehicle is able to maintain a greater lateral acceleration, thus driving along the curve with advantage over the vehicles behind.

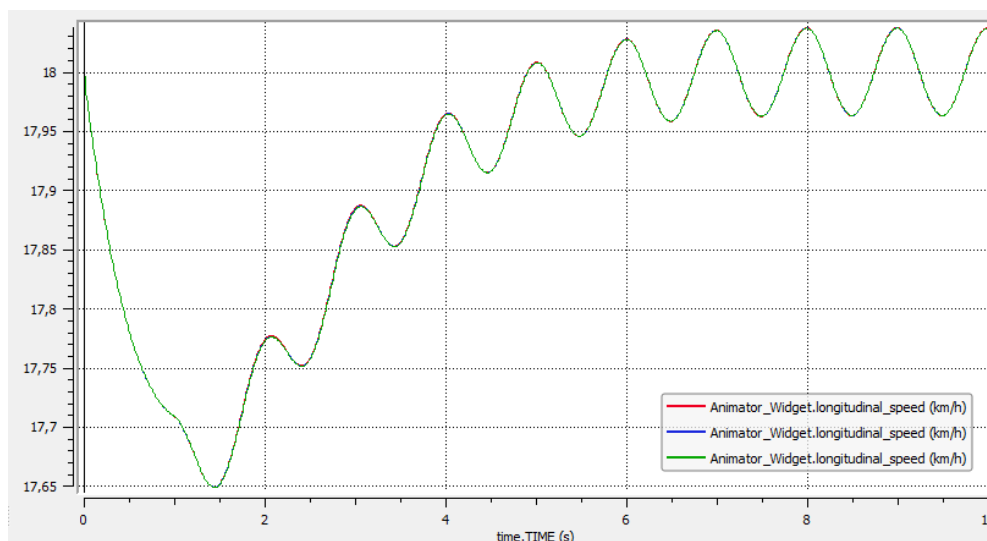


For our type of track, composed of many tight curves, not high speeds, but wide changes of direction, we perform the MaxPerformance manoeuvre to evaluate the differences in the choice of the center of gravity, and choosing the suited ones, in terms of better performance. This is an evaluation given in the next chapter.

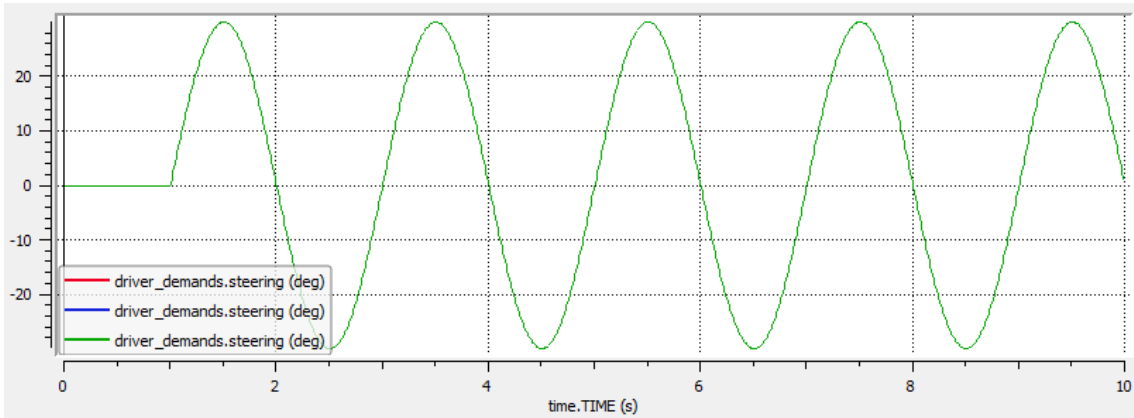
5.3 Wheelbase Length Optimization

The locations of the tires play a key role in how the vehicle behaves dynamically. Certain minimums are established in the rules to ensure stability and thus safety of the vehicle. A minimum wheelbase of 1525 mm is simply stated. The minimum measurement of track width is intrinsically defined by the rollover prevention requirements. The necessary track width is thus a function of the height of the center of gravity of the vehicle and the rollover stability requirement. To eliminate the possibility of trike concept vehicles the smaller track width must be at least 75% of the length of the larger track. There are no maximum values for wheelbase or track explicitly stated. Due to stipulations in dynamic event course layouts, as vehicle overall dimensions become larger due to increased wheelbase and track the vehicle will consume more of the allocated space between cones. This limits the possible lines to be taken by driver and vehicle. For example, a wider vehicle may have better cornering performance than a narrow vehicle due to normal load sensitivity; the narrow vehicle can attain a better racing line due to coned courses being a confined operating environment. For this reasons, we evaluate a possible optimization of different wheelbase.

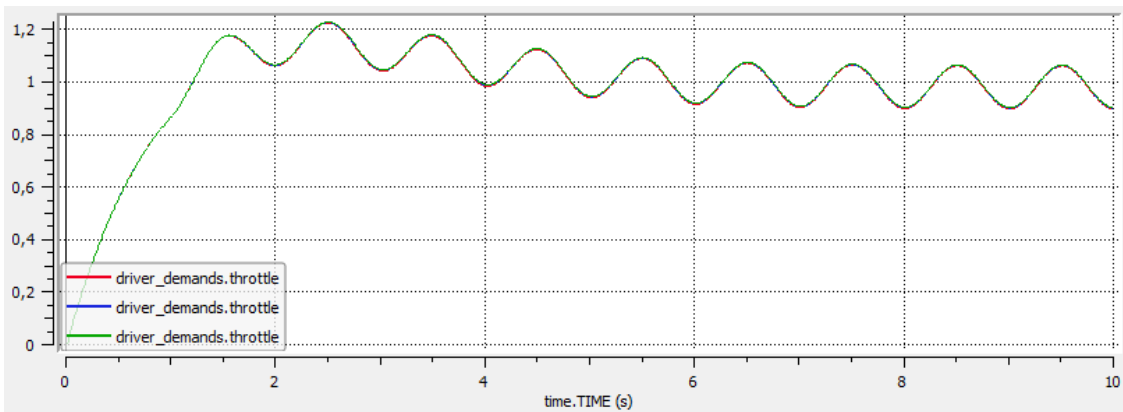
- 1600 mm [----]
- 1550 mm [----]
- 1525 mm (original one) [----]



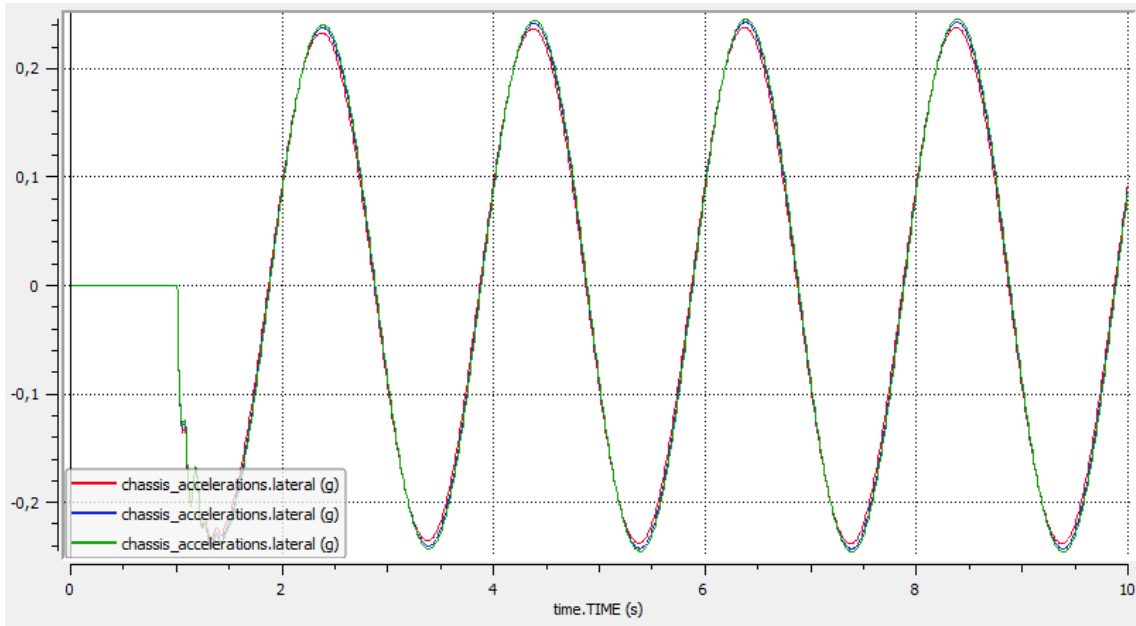
In the above graph, the speed trend during the sine steer manoeuvre is analyzed, in which the driver performs steering defined on the right and left, with a certain frequency. The steering request is displayed in the graph below.



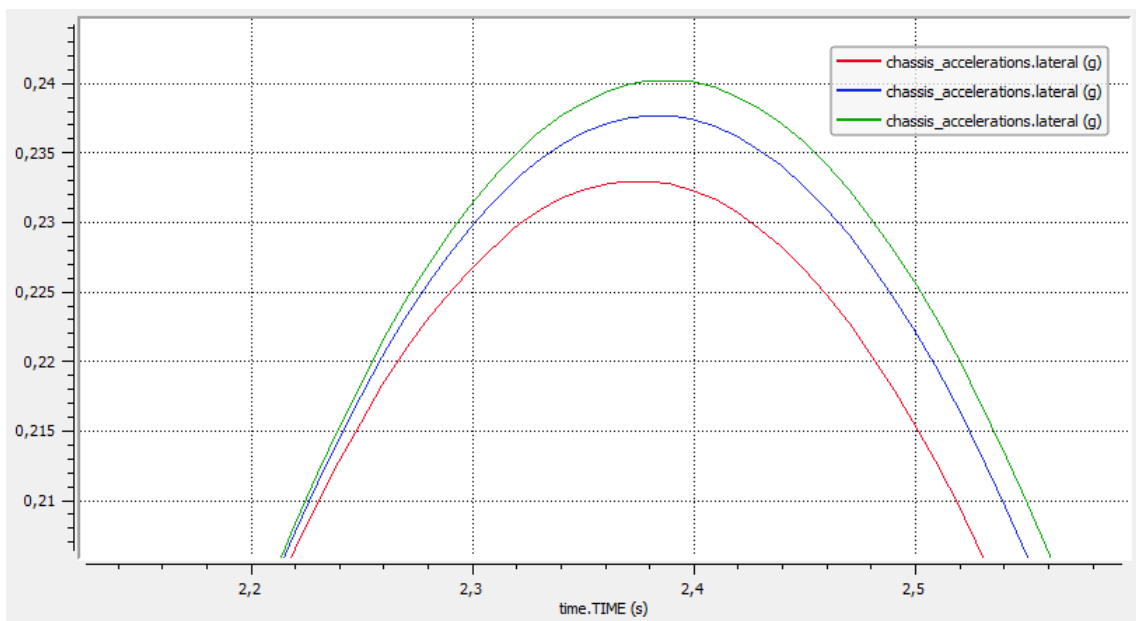
In the same way, the accelerator pedal trend is represented, with the driver's requests to maintain the desired speed. In this case, it is already possible to analyze how the driver inputs to maintain the requests are superimposed. This is already an indication that wheelbase variations may not be so relevant in the manoeuvre.

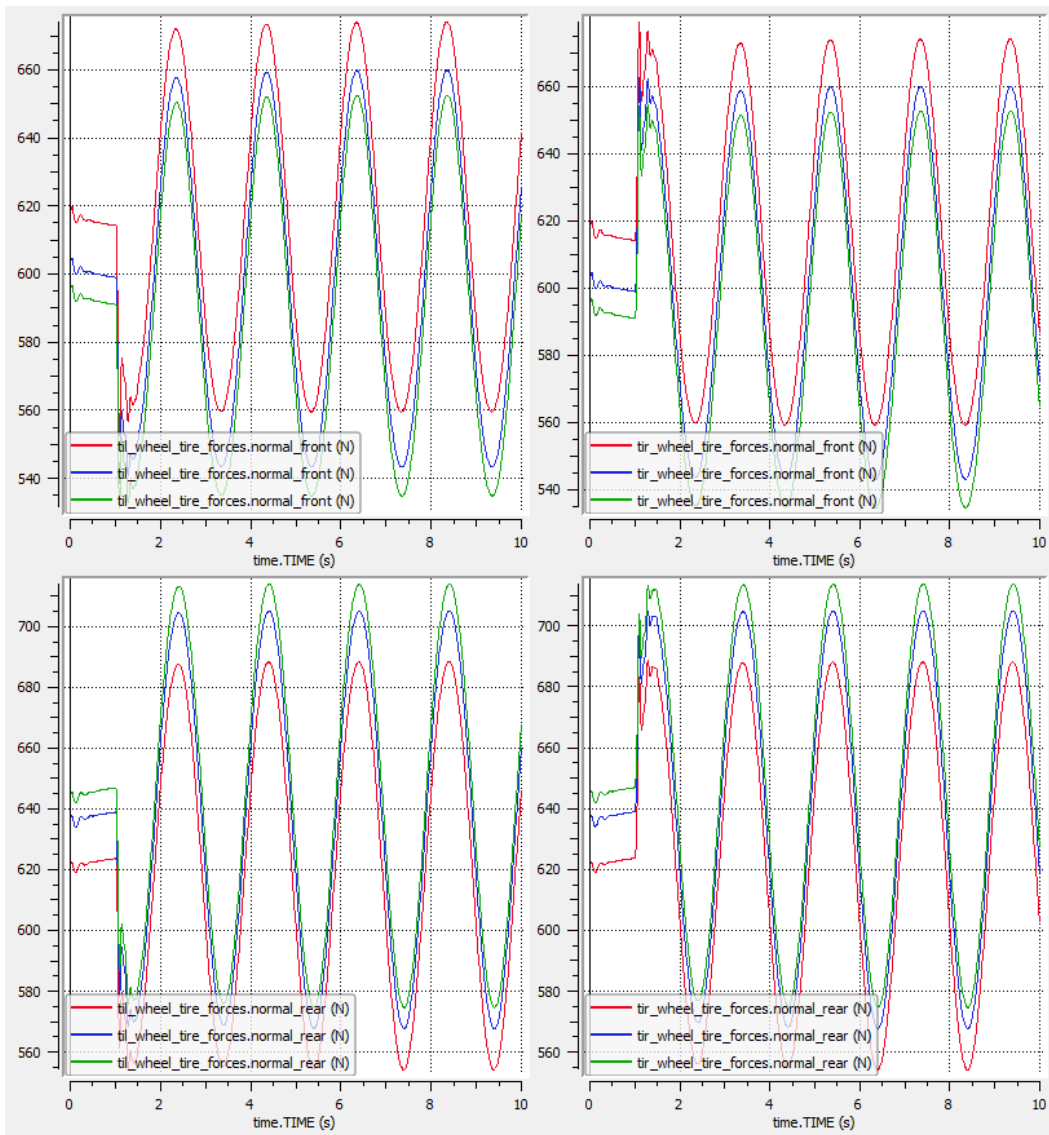
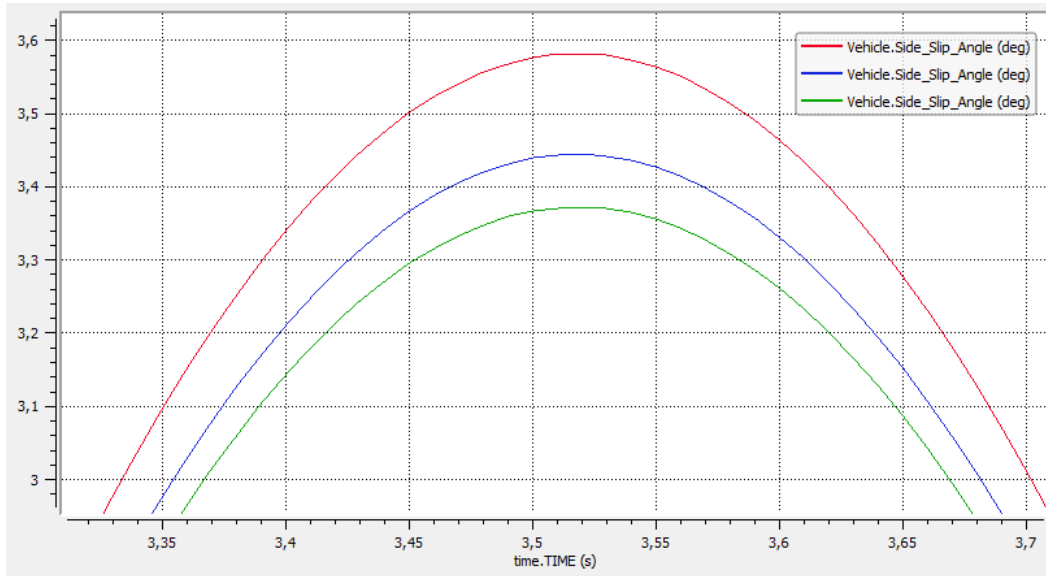


In the graph below, we analyze the trend of lateral acceleration, which in this case too, is not particularly different in the various cases under analysis. We will analyze in the graphs below the detail of the peaks reached.



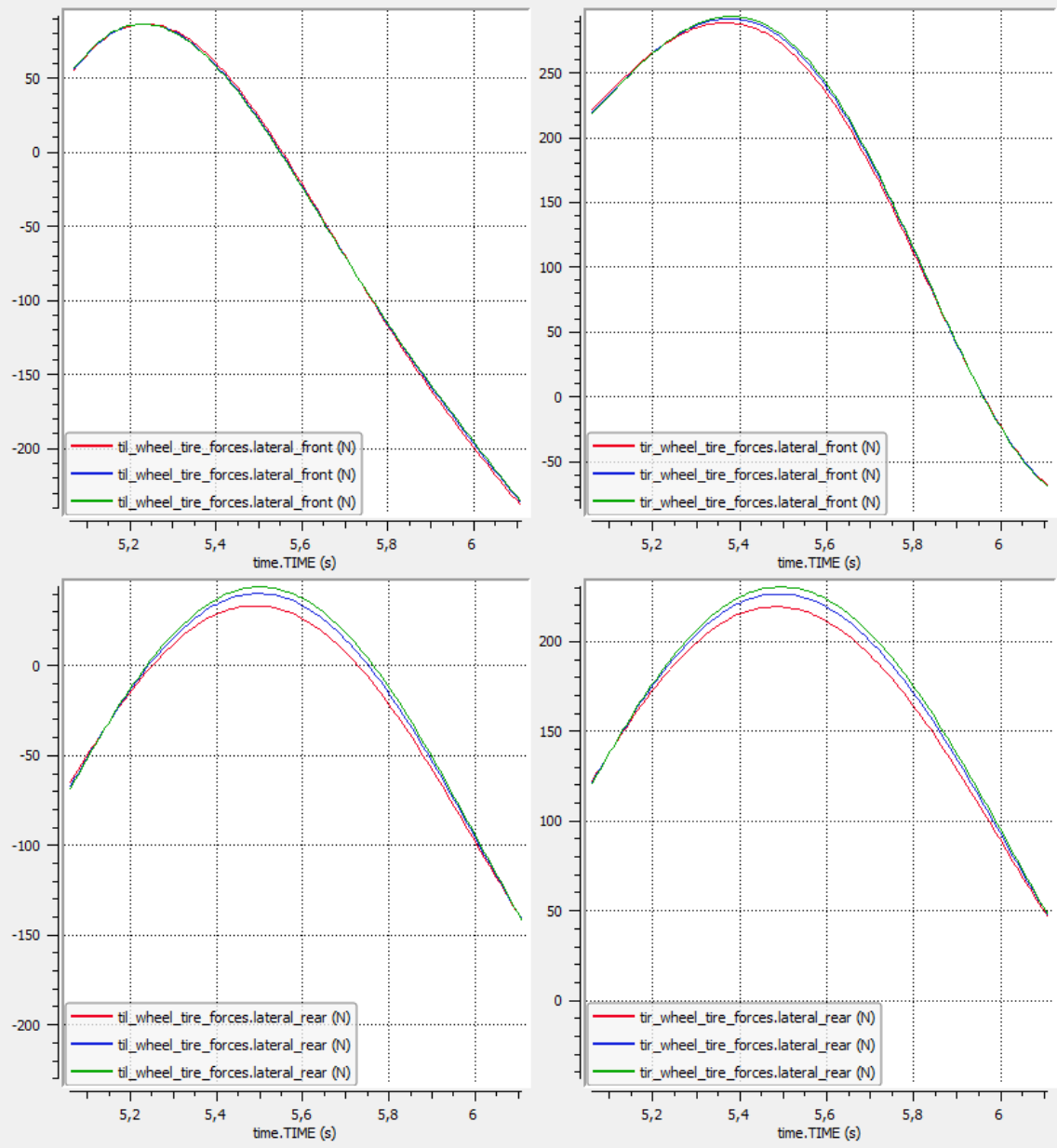
In detail, the subtle difference in behaviour during the sine steer manoeuvre is analysed. It should be noted that we are talking about low lateral accelerations, and therefore the vehicle in this manoeuvre is not pushed to the limit. At the same time, below, the detail of the sideslip angle peak obtained.



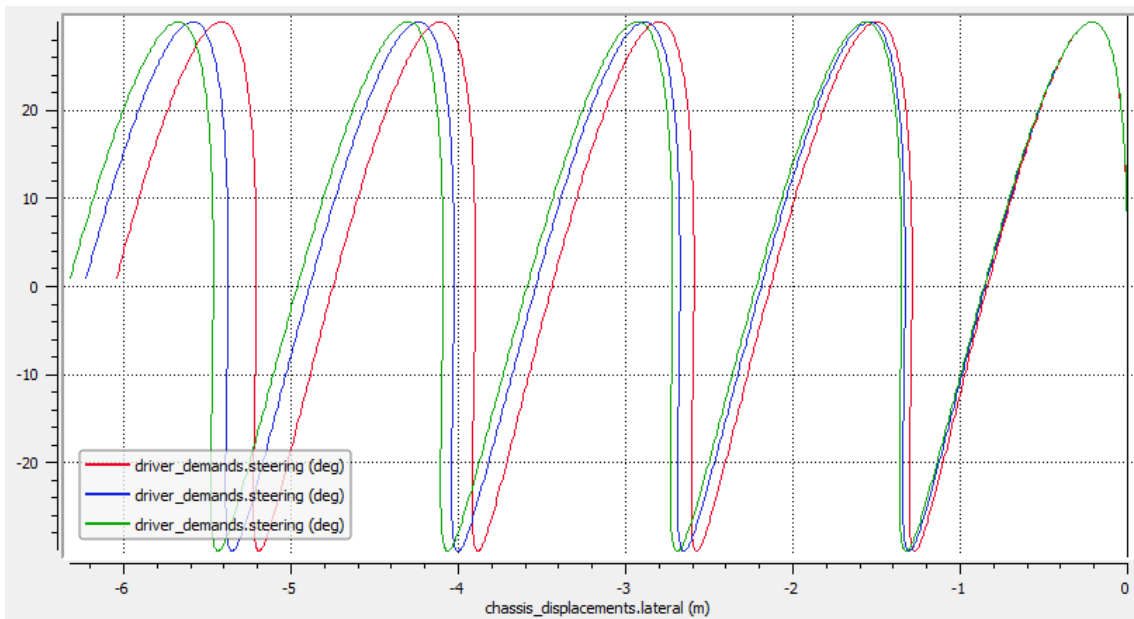


The four graphs above show the development of normal forces on the wheels. In this case, the different distribution of the vertical loads is evident, for the different step lengths taken into consideration.

Below, the same consideration is given to the lateral forces exerted by the tyres.



The difference in behaviour can be made more evident by plotting the required flying angle according to the lateral space covered. Here you can highlight some differences that lead the 3 curves to separate. Further analyses to assess the benefits on the route we have considered will be evaluated in the Max Performance chapter.



where subscripts r and l refer to the right and left wheels respectively and i refers to the i th axle. Consider a vehicle negotiating a bend to the left; the sideslip angle α_i is negative while the side force is positive. The transversal load shift causes an increase of the load on the wheels on the right, the sideslip angle α_i is negative and the side force is positive. If C is the total stiffness of the axle, the cornering force the axle exerts is

$$F_y = -\frac{1}{2} \left[(\alpha_i - \alpha_c) \left(C + \Delta F_z \frac{\partial C}{\partial F_z} \right) + (\alpha_i + \alpha_c) \left(C - \Delta F_z \frac{\partial C}{\partial F_z} \right) \right]$$

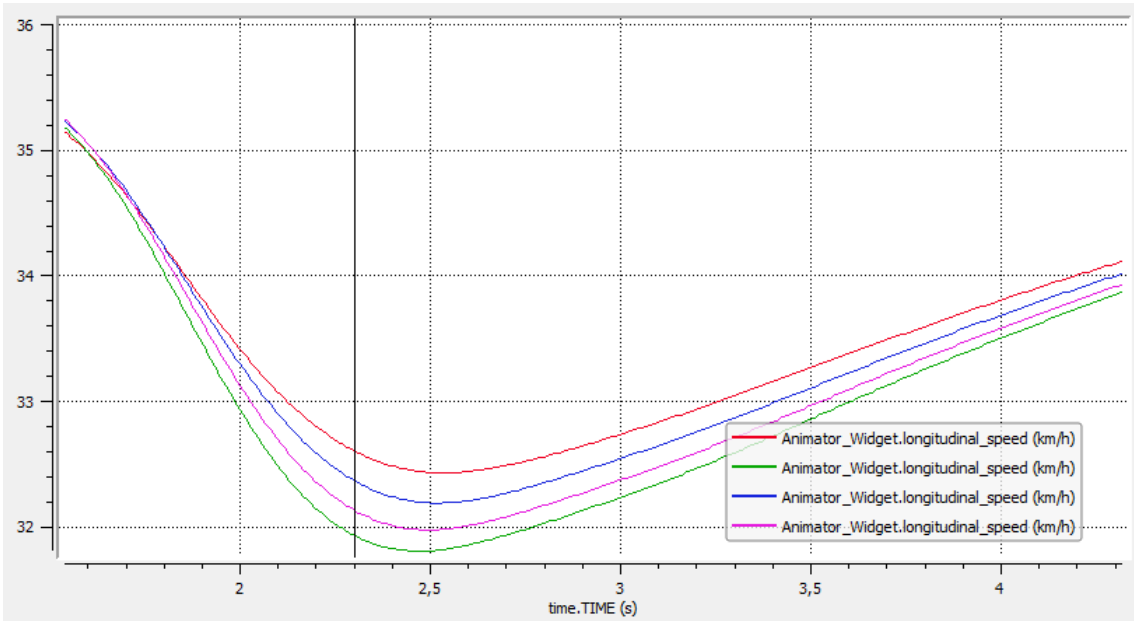
And so:

$$F_y = C|\alpha_i| + \alpha_c \Delta F_z \frac{\partial C}{\partial F_z}$$

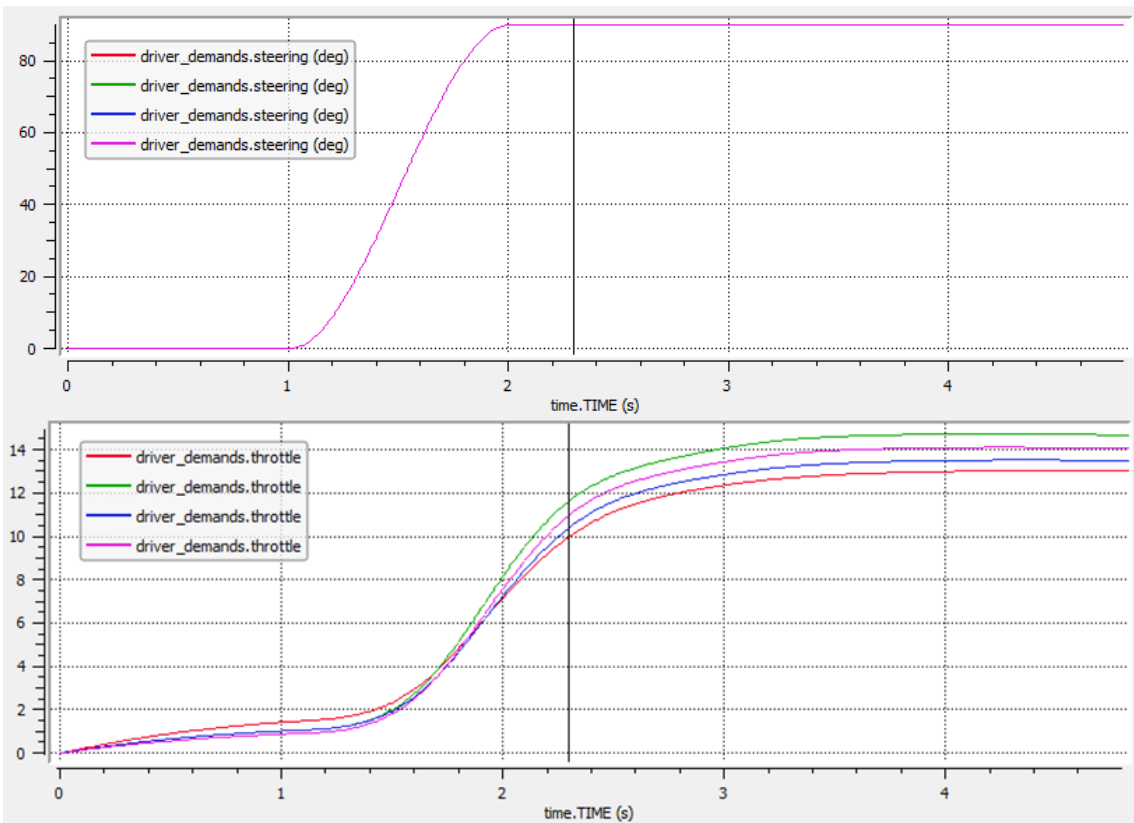
If transversal load shift is not taken into account, and the two wheels have the same cornering stiffness, toe in has no effect within the validity of the linearized model. The situation is different if load shift is included into the model: then toe in causes an increase of the cornering force due to the axle. This has the effect of increasing the cornering stiffness of the axle, depending on the load shift. Toe-in at the front wheels or toe-out of the rear ones thus has an oversteer effect. The effect of toe in is complicated since α_c depends on the steering angle due to steering error, on suspension geometry and on the relative roll stiffness of the suspensions that affect the total shift of the various axles.

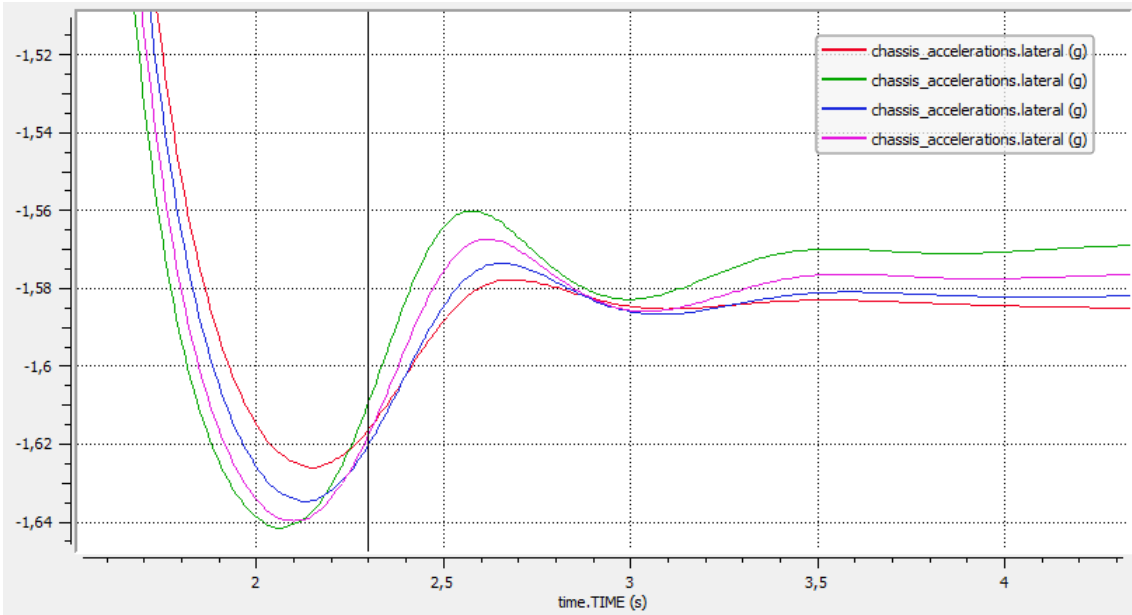
Toe In – Toe Out Configurations:

- Front 0.0 ; Rear 0.0 [deg] [----]
- Front -1.0 ; Rear +1.0 [deg] [----]
- Front -0.5 ; Rear +0.5 [deg] [----]
- Front +0.5 ; Rear -0.5 [deg] [----]

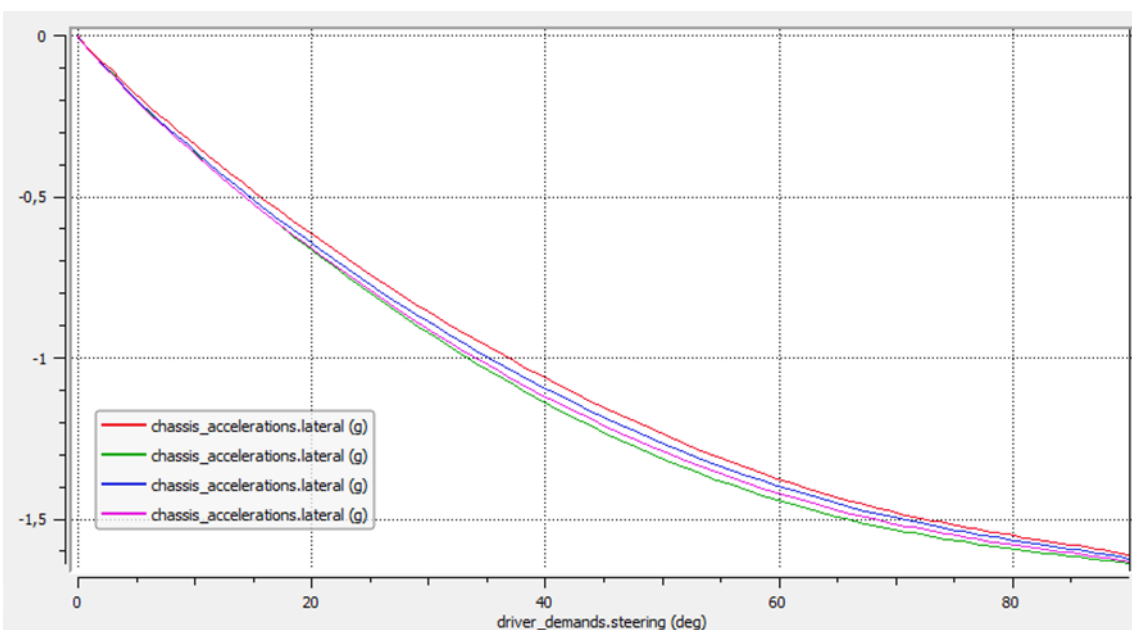


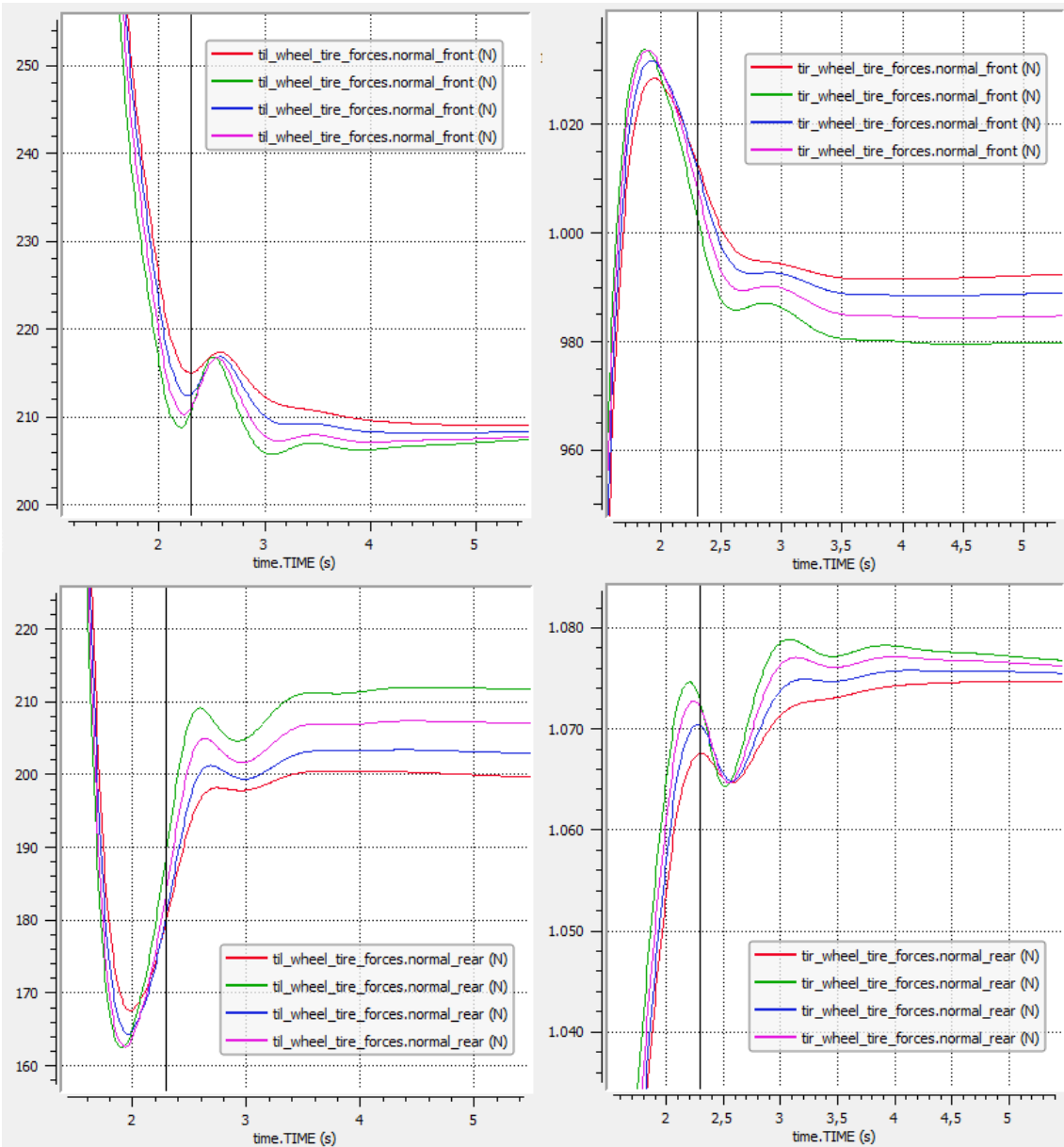
Above is represented the speed maintained during the step steer manoeuvre performed. You can see how, provided a steering input, depending on the angle of toe applied, changes the speed reduction. Below is represented the input of the implemented manoeuvre in steering angle applied and in throttle request to maintain a certain speed.





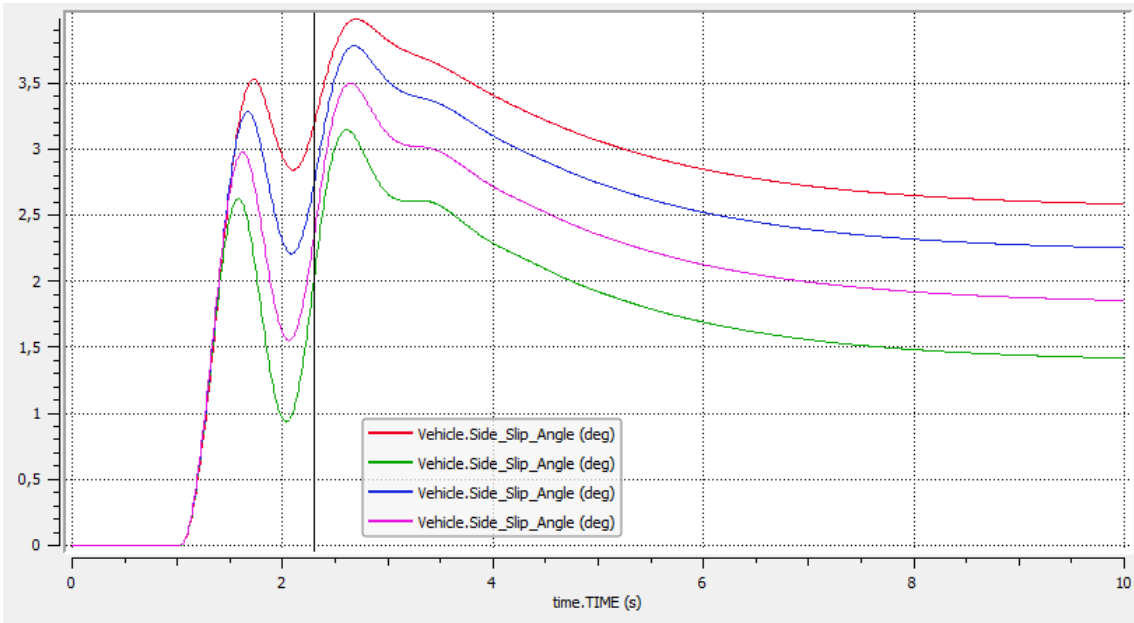
The analysis of the lateral acceleration is carried out both in the time variable and in the required steering variable, so that it is possible to compare, with the same applied steering, what is the lateral acceleration achieved. As you can see, the green curve achieves higher lateral acceleration values than the red curve for a given steering angle.



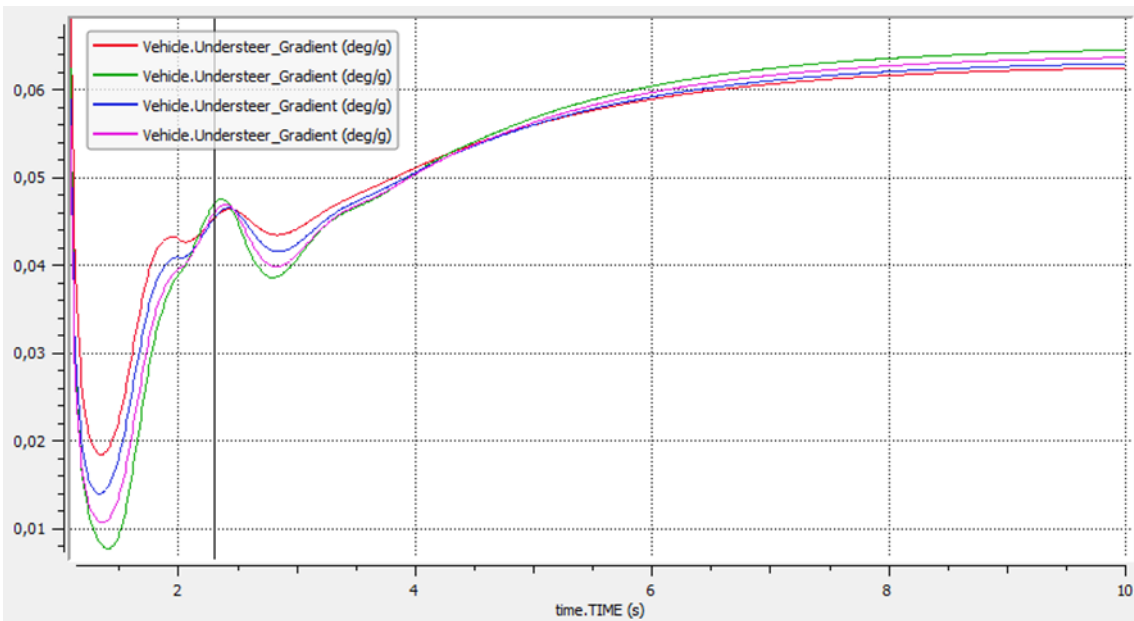


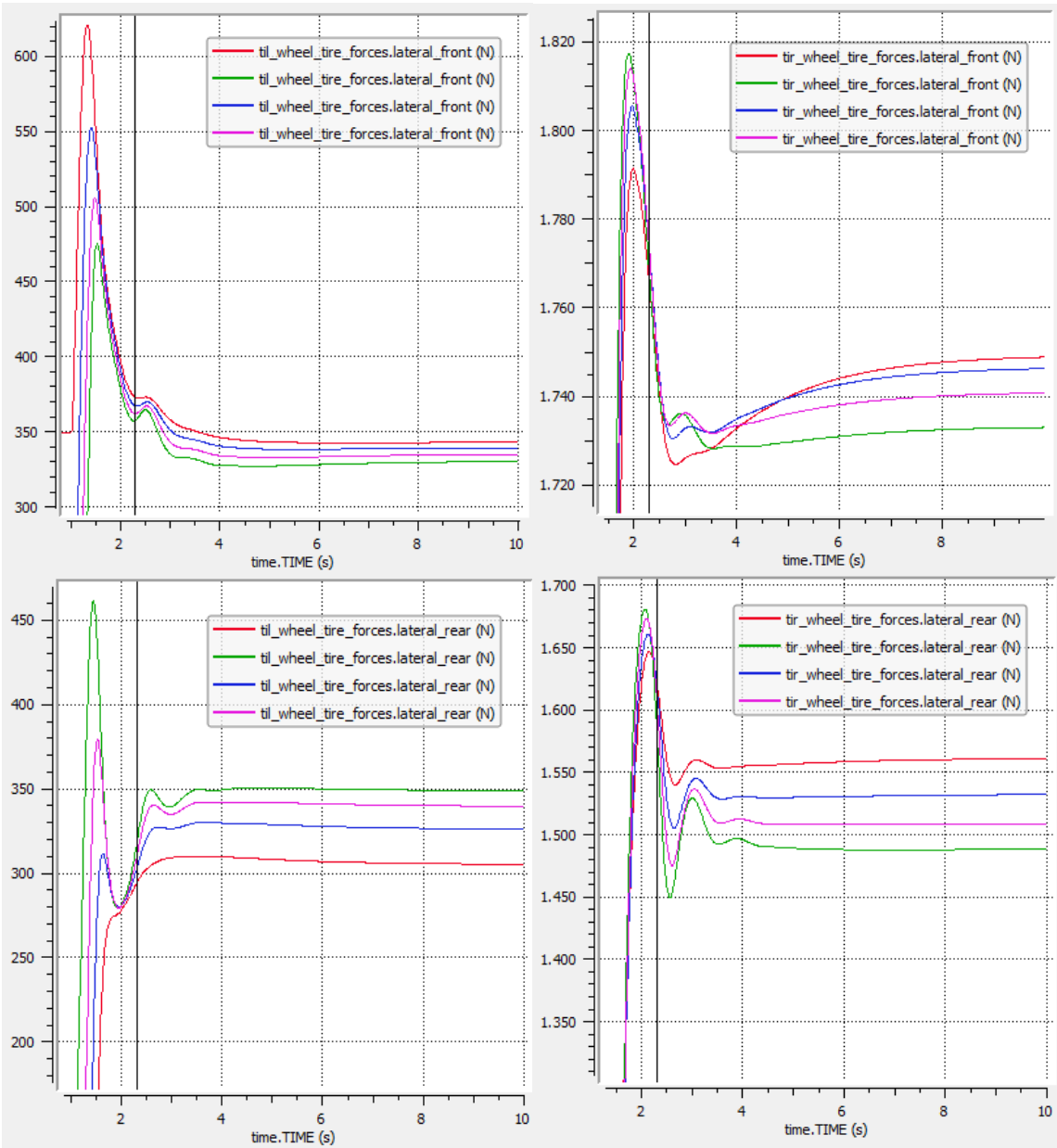
In the 4 graphs above are analyzed the normal forces on the individual wheels to vary the toe in toe out, which can affect, in the order of 10/20 N the behavior of the tire.

In the following graphs are analyzed the side slip angle, which changes significantly depending on the configuration and the understeer gradient, which gives an idea of the more understeer behavior of some selected configurations.



Note above, that the green configuration reaches sideslip values lower than the red configuration and with much less pronounced peaks.





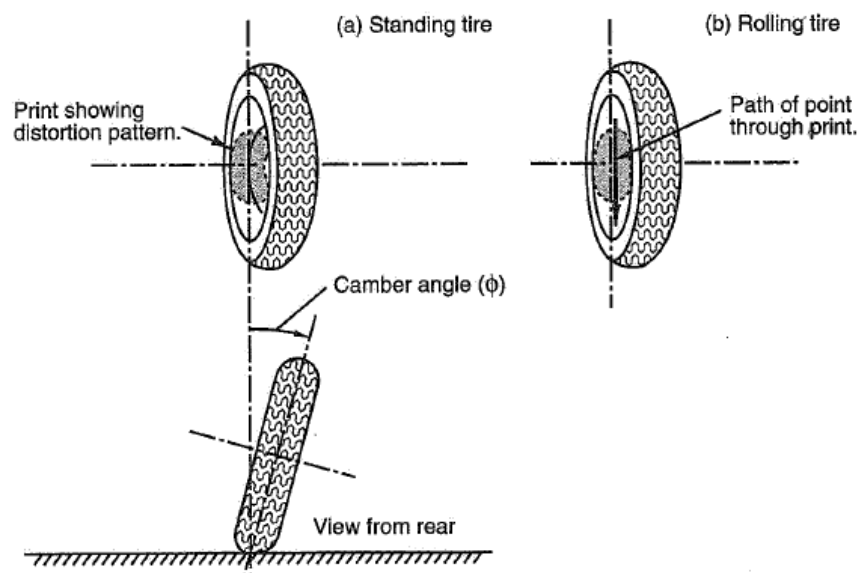
Finally, the course of the lateral forces, plotted in the time of execution of the entire maneuver, which reach a stable course after 4 seconds.

5.5 Camber Angle Optimization

Camber angle, according to SAE terminology, is defined as the angle between a tilted wheel plane and the vertical. The camber is positive if the wheel leans outward at the top relative to the vehicle, or negative if it leans inward. The effect of camber on the tire forces and moments actually depends on the angle between the tire and a perpendicular to the ground – as opposed to the angle between the tire and a chassis reference.

In general, a cambered rolling pneumatic-tired wheel produces a lateral force in the direction of the tilt. When this force occurs at zero slip angle, it is referred to as a camber thrust. A lateral force component due to camber can also occur at slip angles other than zero. Camber force is a function of the tire type, construction, shape, tread, pressure, load, tractive or braking effort and camber and slip angles.

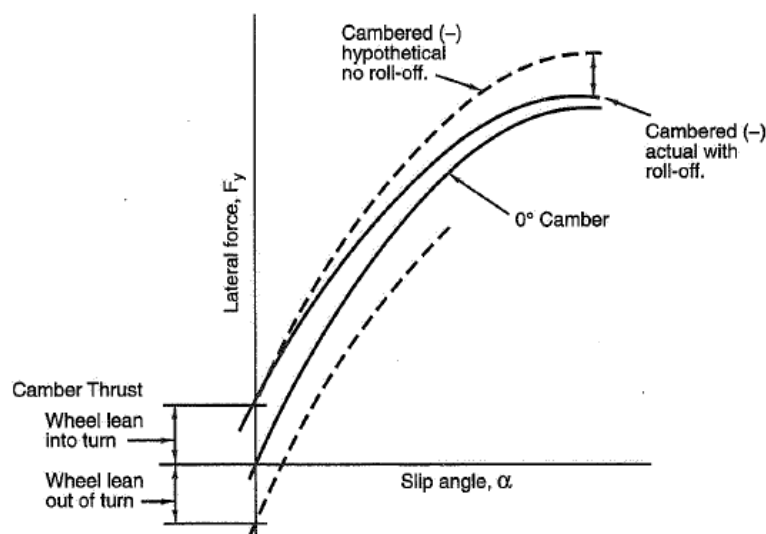
When a stationary tire is pressed down onto the road at a camber angle, the center plane of the print is curved, as showed in figure below.



When the tire is rolled at zero slip angle, a point entering the print is constrained by the road to move through the print on a straight path defined by the direction

of motion. Thus the road applies forces to the tire which tend to remove the curvature in the stationary (nonrolling) tire print. The sum of these forces is the camber thrust. It is also interesting to compare the lateral force produced by camber angle to that produced by slip angle. Because of the shape and size of the print distortion patterns, the lateral force generated in the linear (small angle) range by one degree of slip angle is greater than that generated by one degree of camber. Experimental results highlight that for racing tires, the maximum force due to camber occurs at smaller angles.

In linear range, camber thrust and lateral force due to slip angle are generally viewed as separate effects and are additive. This simply moves the cornering curve (lateral force vs slip angle) up or down parallel to itself, depending on which way the wheel is cambered. As the linear range is exceeded, the additive camber effect decreases or is said to “roll-off”. The figure below shown this effect.

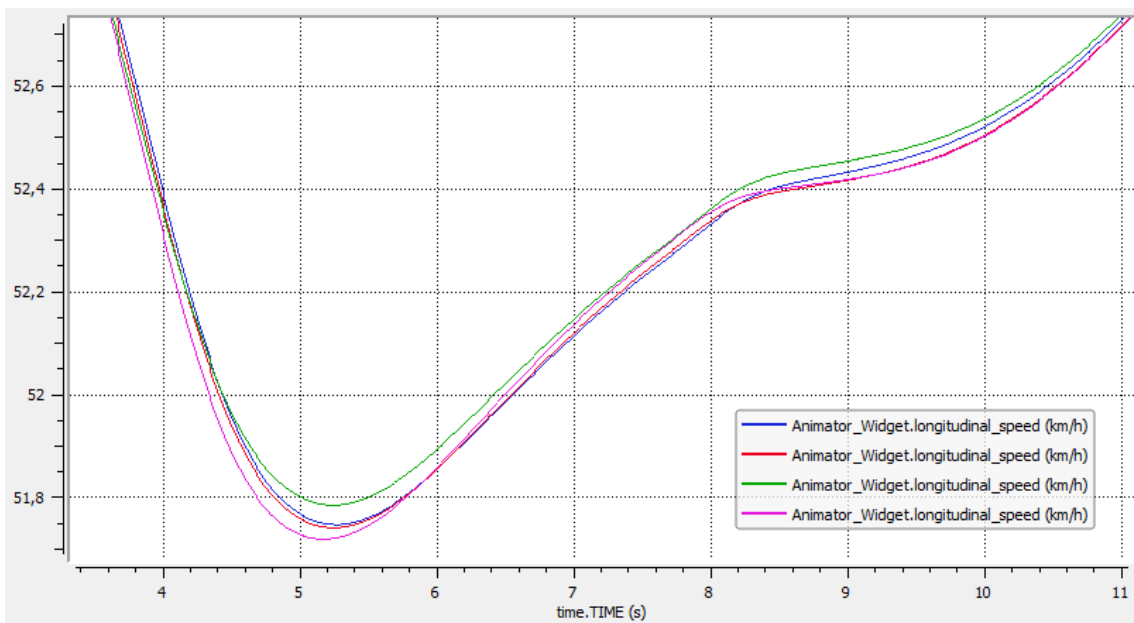


Measurements made on tires, demonstrate that the peak of the cornering curve can move up when the tire is tilted into the turn while the peak generally moves down if the tire is tilted outward. This gain in max lateral force it is not completely explained by the theory, but it is obviously associated with what happens in the print. Road - induced distortion due to slip angle is a maximum toward the rear of the print where local vertical forces are low; the largest distortion in the case of camber is near the center of the print where the local vertical forces are high.

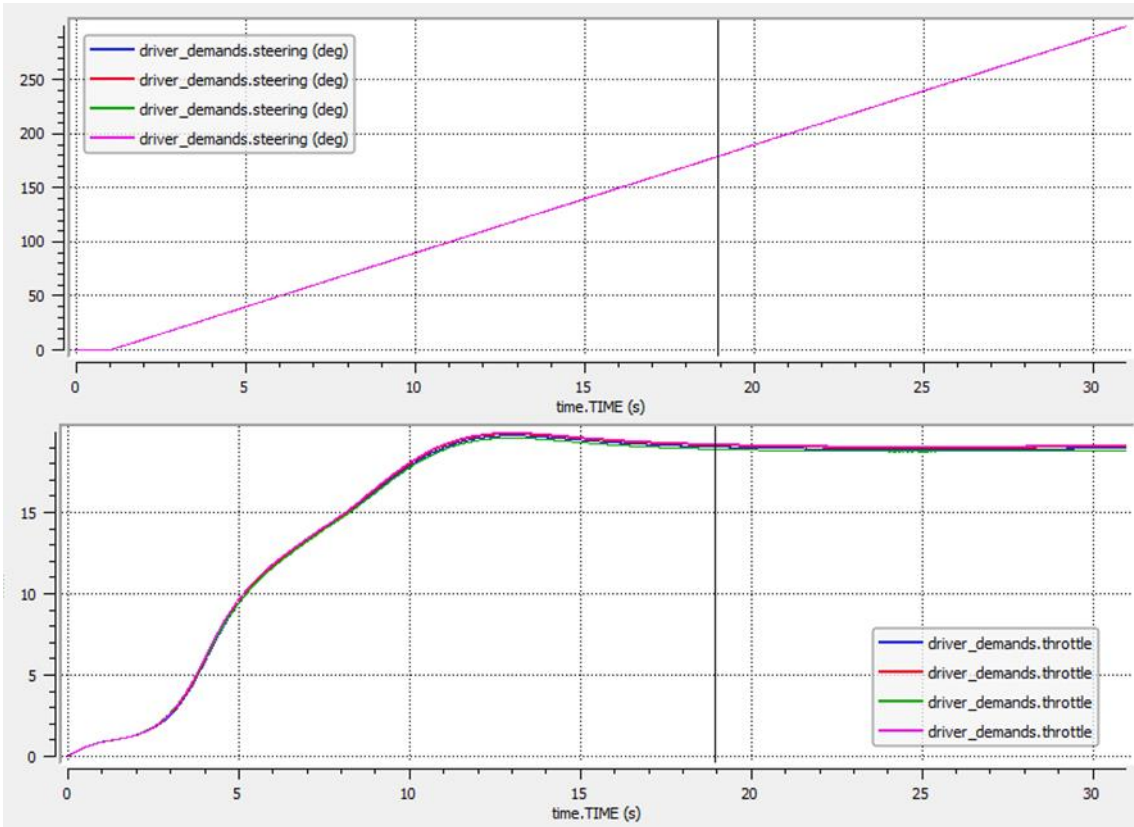
Slippage in the highly loaded center of the print is less likely than at the lightly loaded end of the print. This may help explain why higher lateral force is achieved when “aiding” camber is added to the slip angle. The actual conditions in the print under large slip and camber angles are very complex and not considered in this project.

In order to optimize the camber angles, we have to know the behaviour of the tire under differ loading conditions, evaluating the ration between Lateral and Vertical Forces, in particular for the outside wheel during a corner. In our case, we evaluate different angles in a ramp steer maneuver:

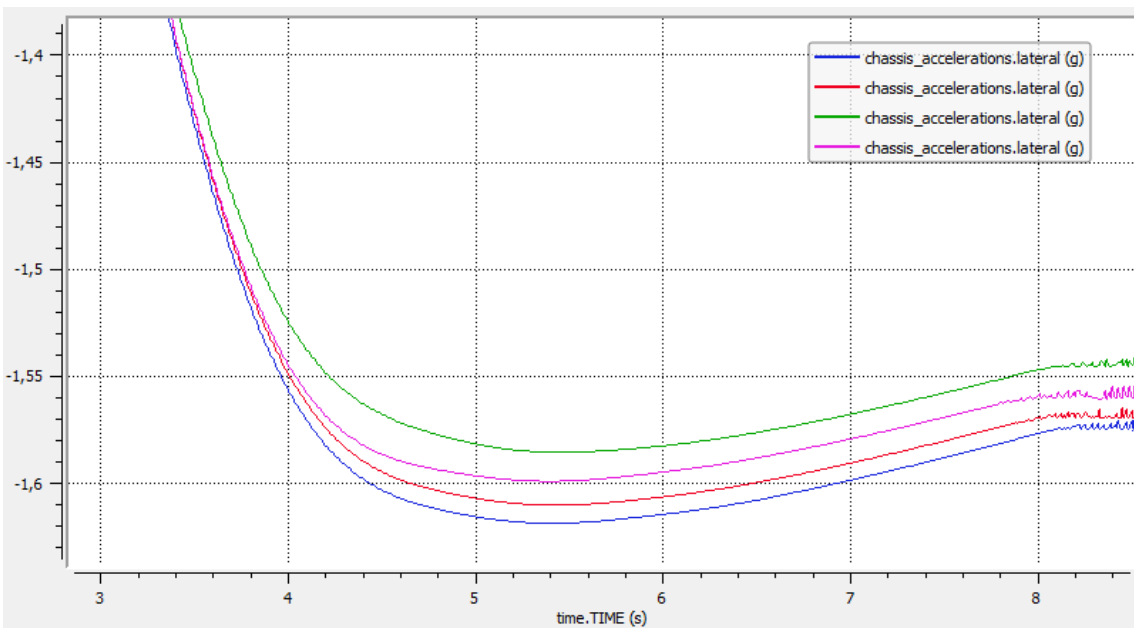
- Front 0.0 ; Rear 0.0 [deg] [----]
- Front -1.0 ; Rear -1.0 [deg] [----]
- Front -2.0 ; Rear -2.0 [deg] [----]
- Front +1.0 ; Rear +1.0 [deg] [----]

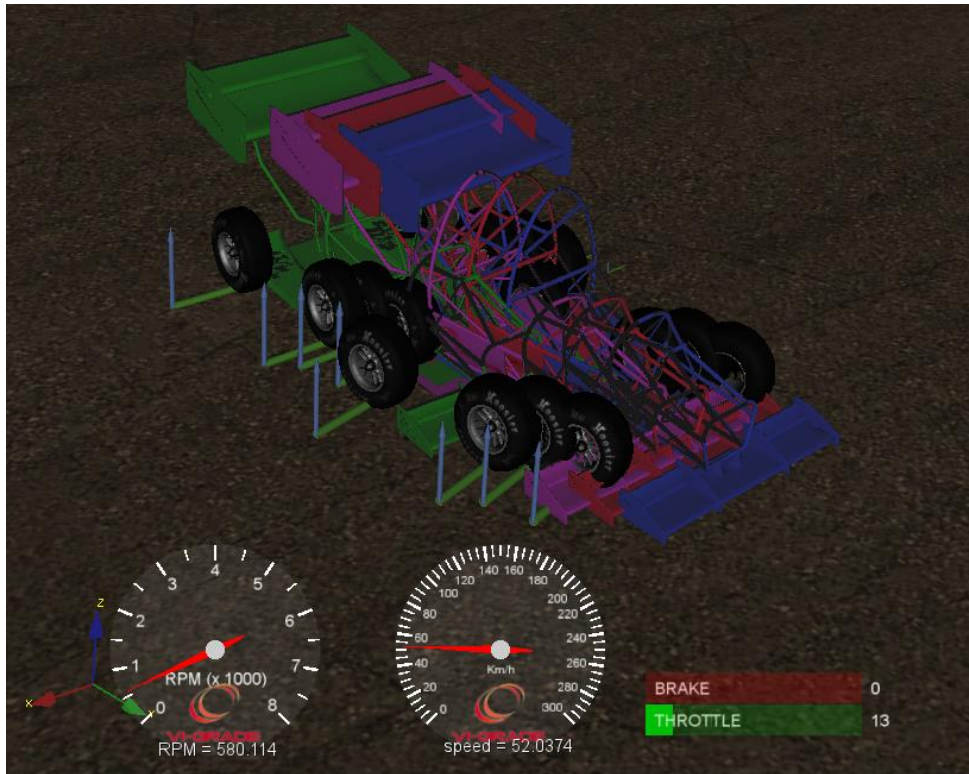


The speed maintained during the ramp steer operation is shown in the graph above. Below are the requests for steering and accelerator inputs, which can be considered very similar for all tested configurations.

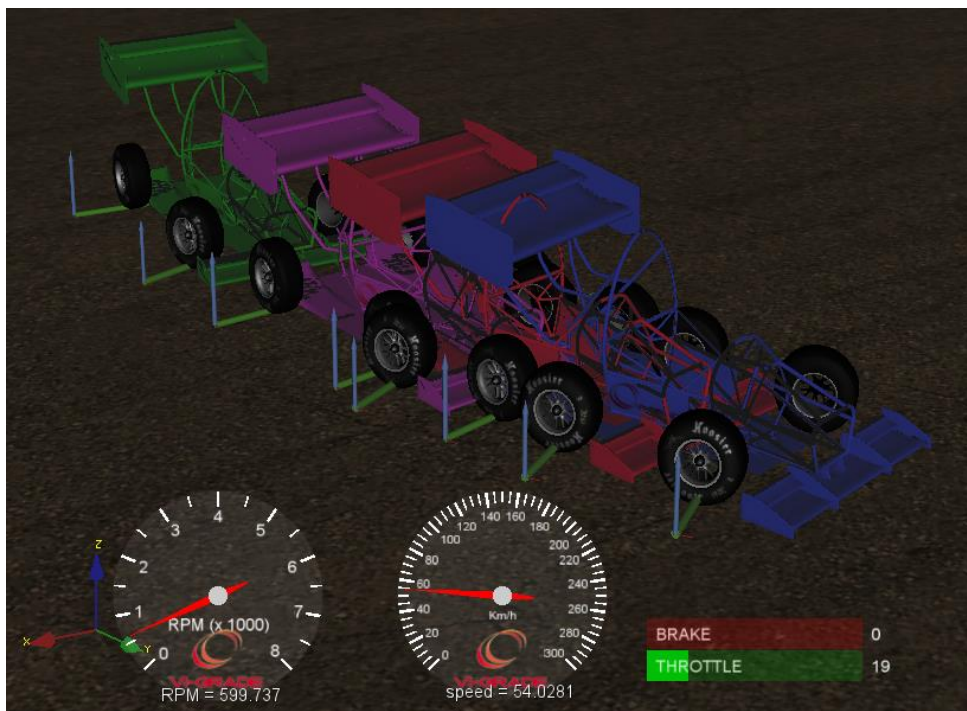


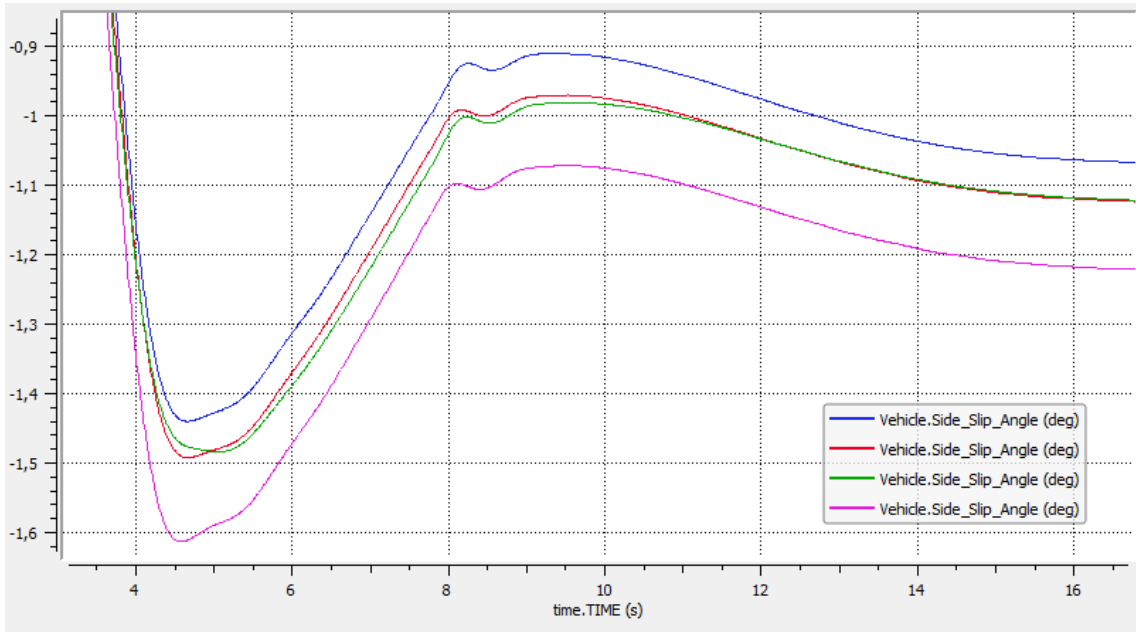
The first interesting analysis is the evaluation of the lateral acceleration achieved by the vehicle in the manoeuvre, with a substantial difference that can be evaluated directly from the images of the simulation on the next page.





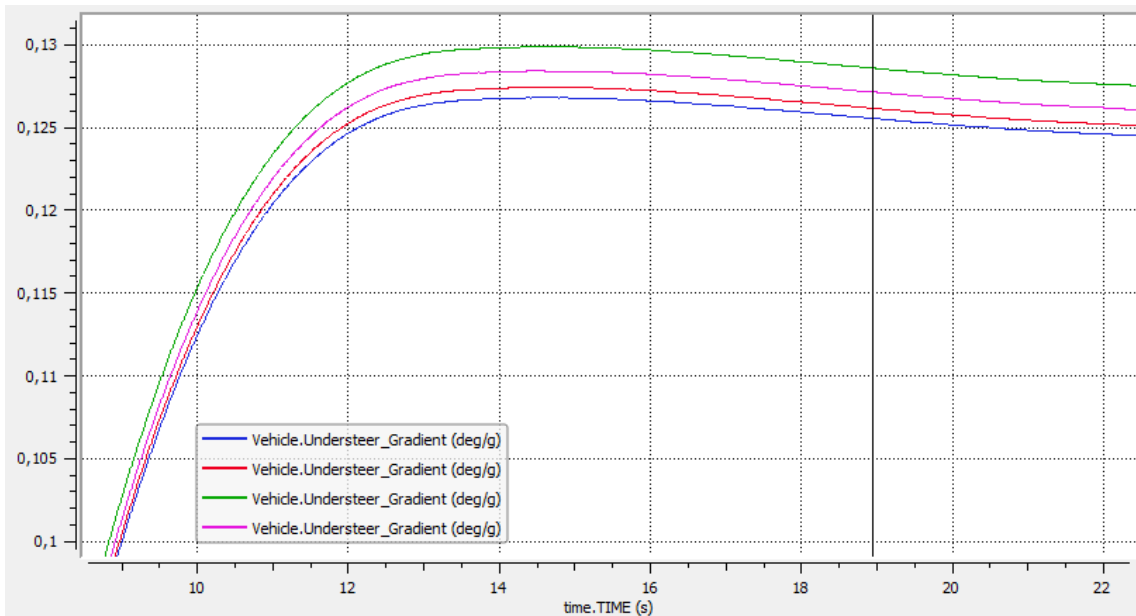
It is in fact clear how the blue vehicle can achieve a greater lateral acceleration, which in the course of the simulation, leads to a clear advantage in cornering compared to the other configurations behind him. All this translates into less time and better performance.

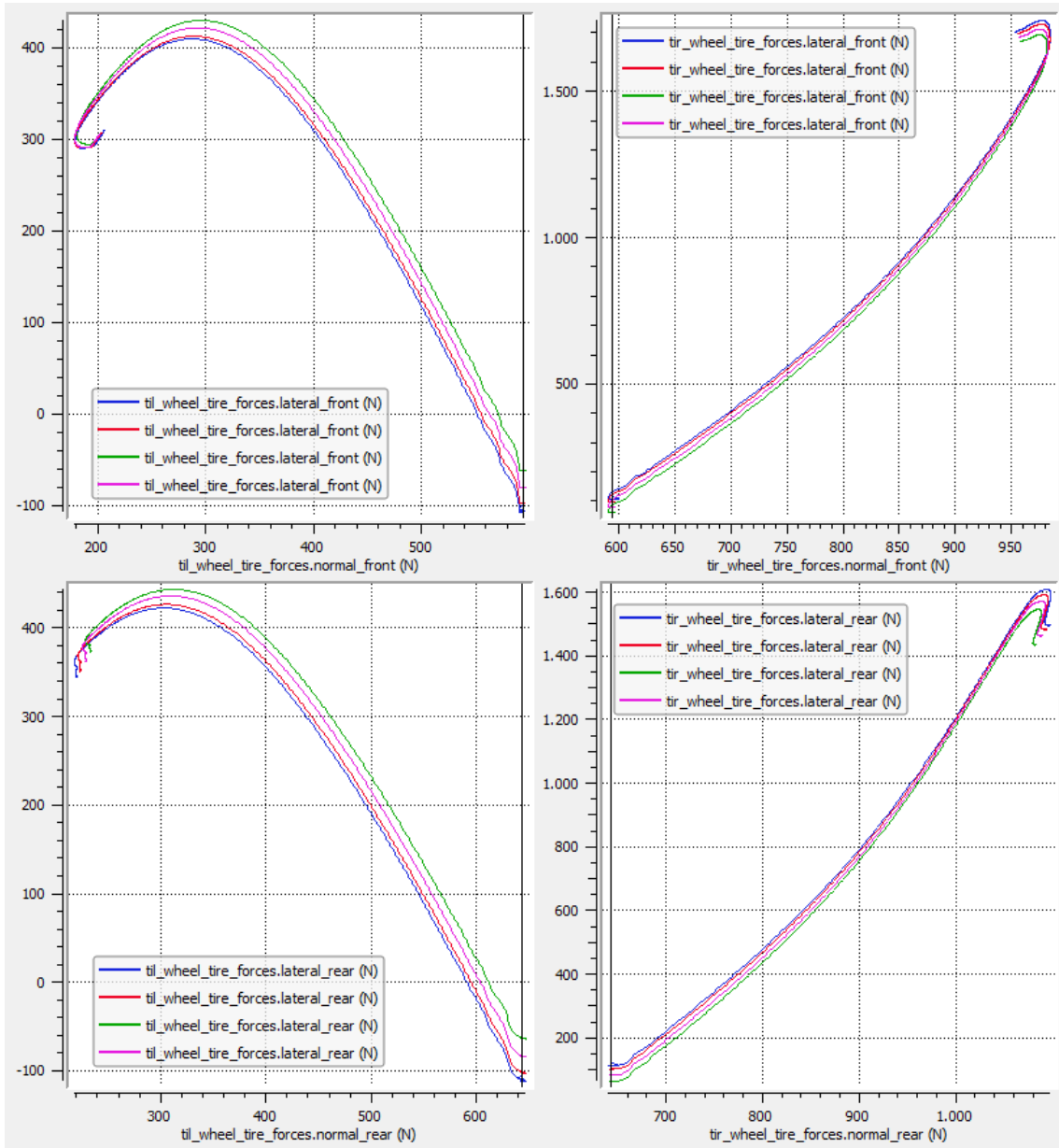




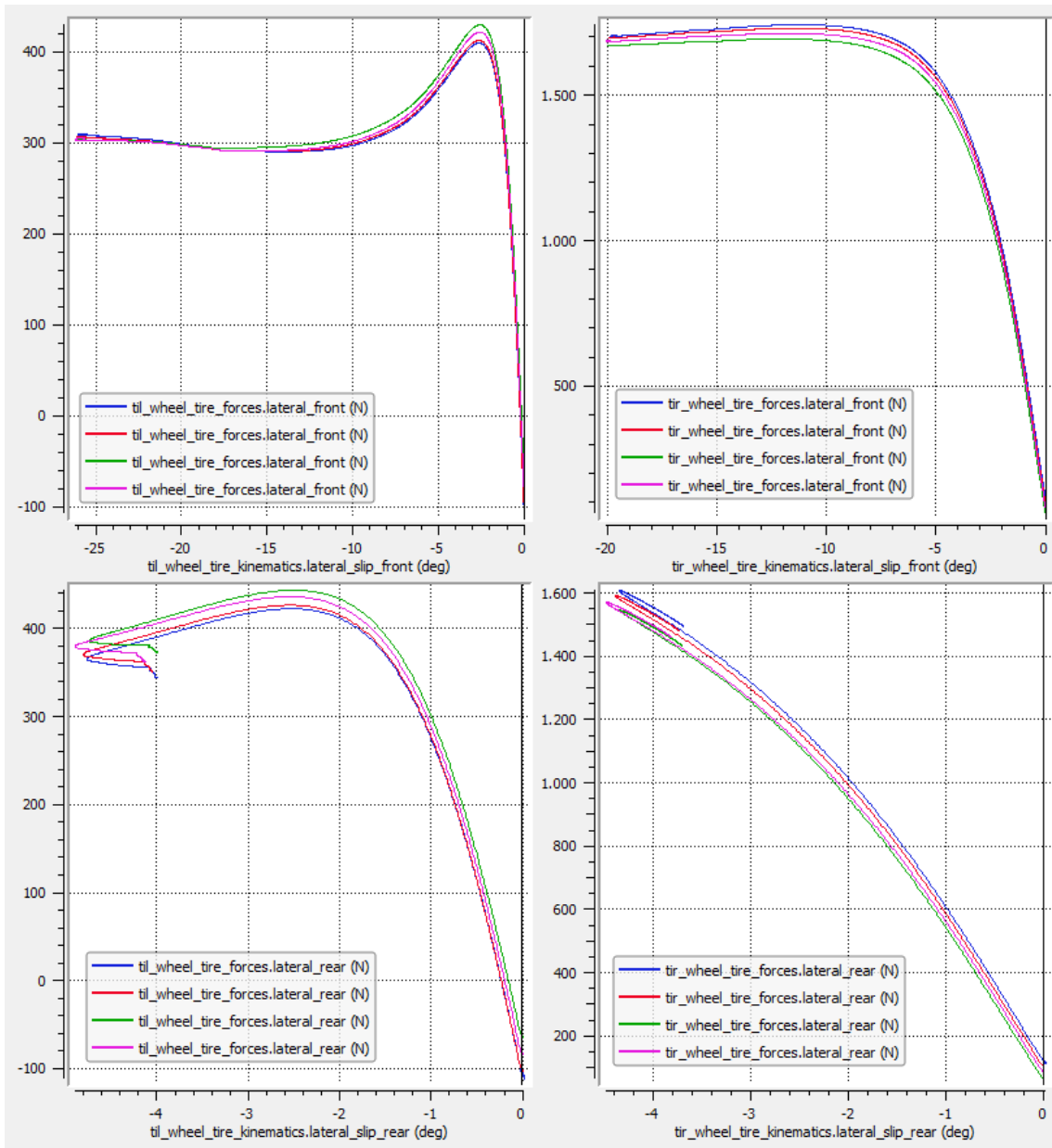
Represented in the graph above, the comparison between the trend of the sideslip angle.

As in previous cases, the assessment was also made for the understeer gradient.





In the evaluation of the camber, not only the single forces one by one, but also the ratio between the lateral forces and the normal forces applied on each wheel axle were taken into consideration, in order to evaluate the behaviour of the wheel in the best possible way.



In the same way as in the previous graph, the lateral force of each individual wheel is evaluated according to the lateral slip, providing more precise and detailed indications of the most suitable camber to meet the requirements considered.

Once these analyses have been carried out, we can move on to evaluation on the built track, with the Max Performance event.

Chapter 6

Max Performance Simulation

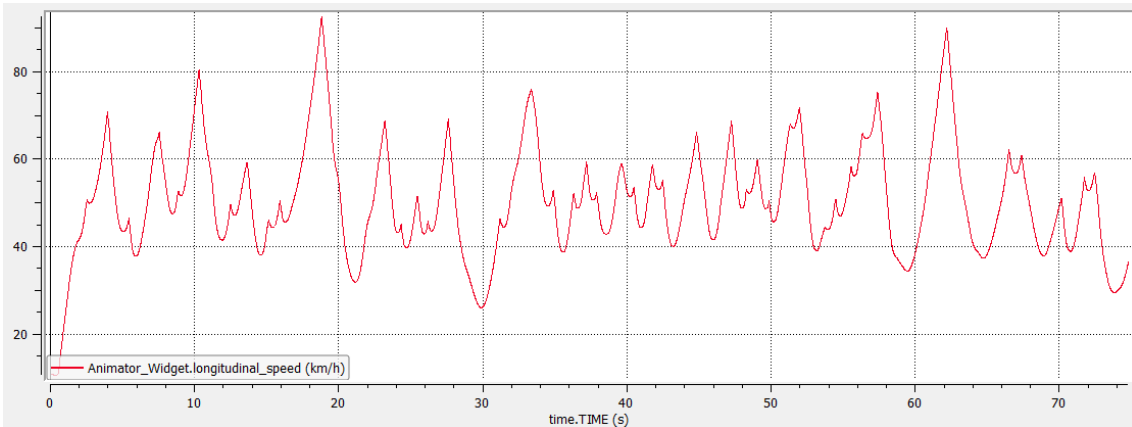
6.1 Max Performance Simulation

Once the dynamic vehicle studies have been carried out to choose the most suitable solution for our case, this solution is tested directly on the track, going to simulate a lap in MaxPerformance. This analysis sees the test of the solution adopted in the race and all the optimizations to follow, one at a time, with the final lap in which we apply all of them.

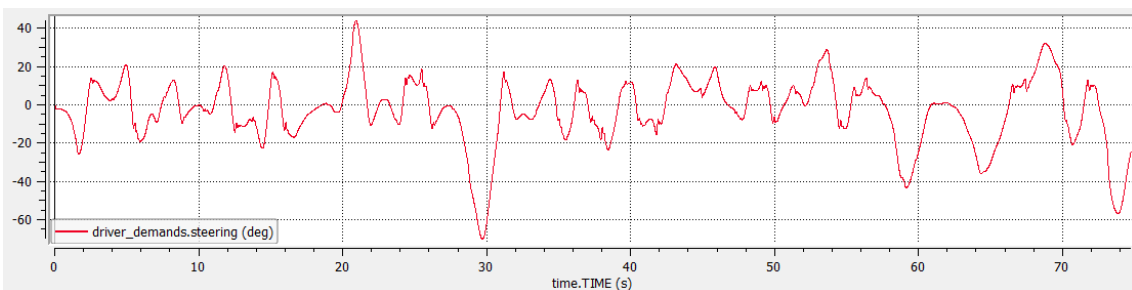
1. MaxPerformance Standard Simulation

First of all we have to simulate the vehicle performing the track with the same condition of the racing. We evaluate these results, comparing it with data acquisition, and we use these datas as the Standard case, to be optimized.

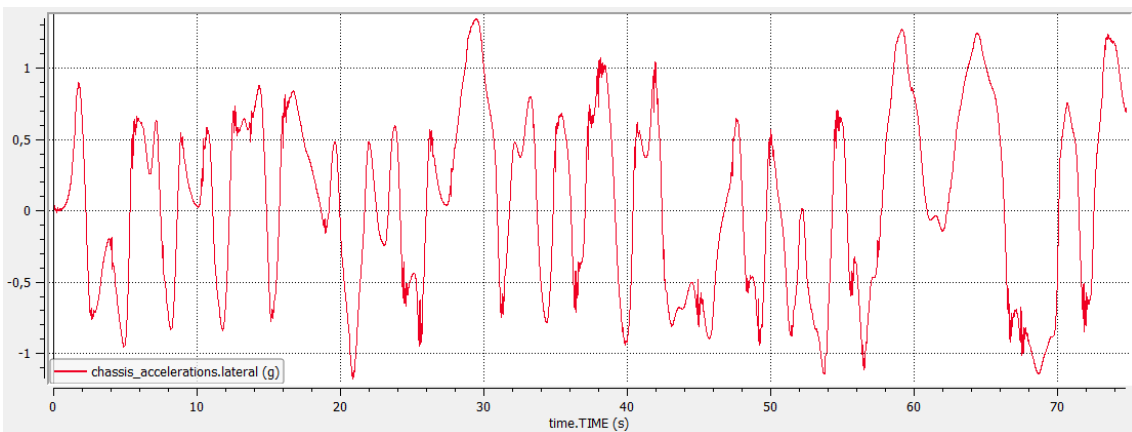
In the following plot, we can see the entire maneuvers and vehicle dynamics behaviour:



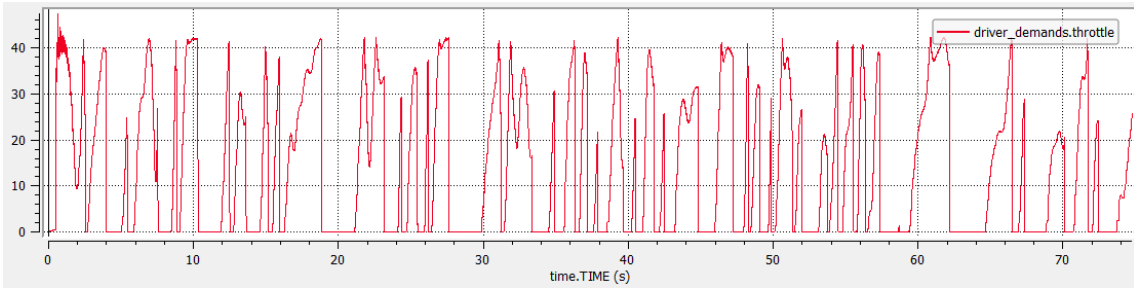
The trend of speed over time, the main index of evaluation to be analyzed.



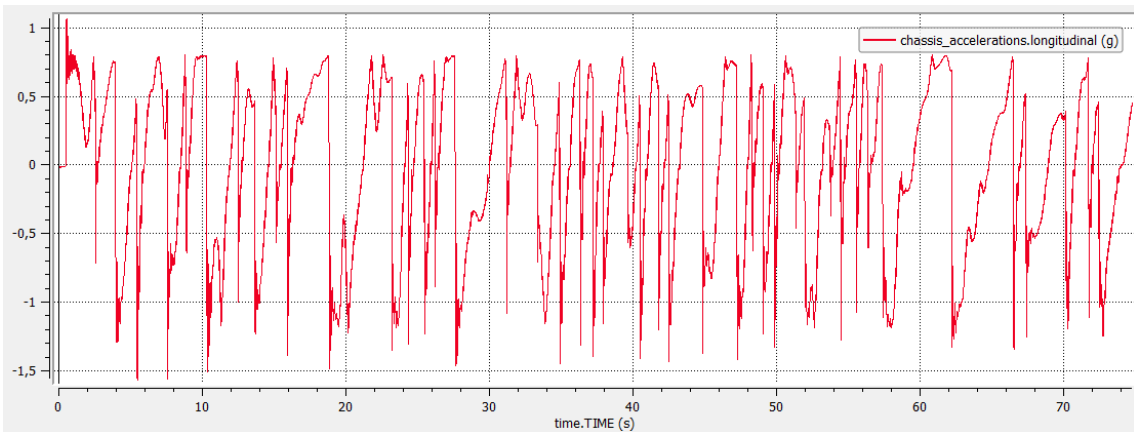
The steering wheel request implemented by the driver during the track



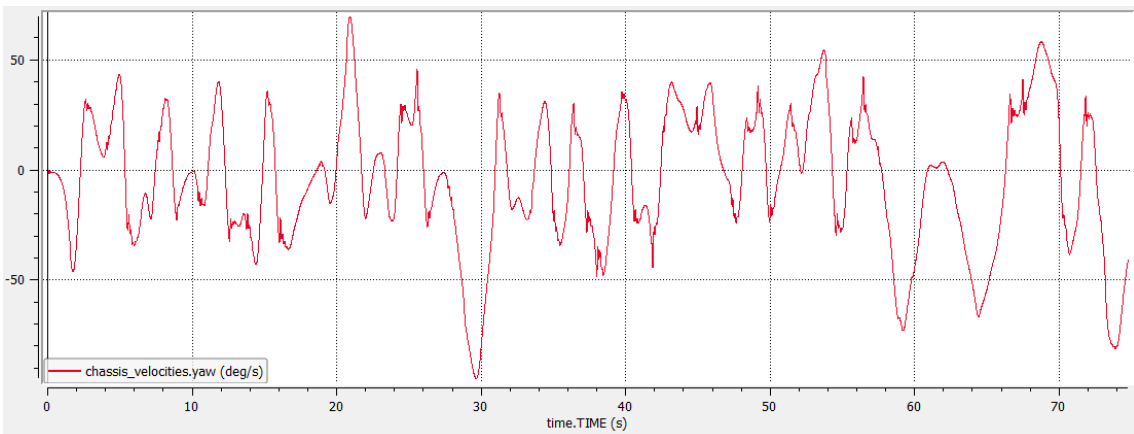
The trend of lateral acceleration, to be evaluated mainly, together with the longitudinal, to reach and maintain the highest peaks in approach and travel curve.



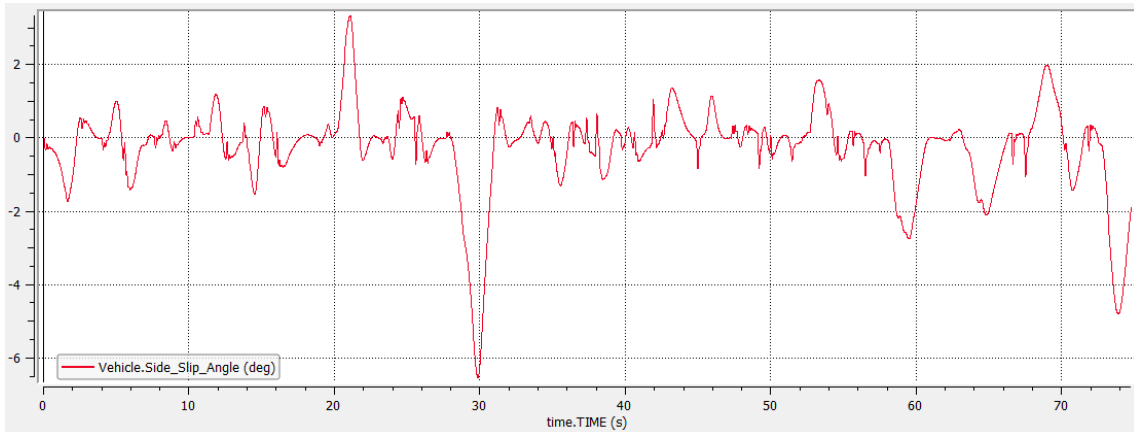
The percentage of throttle required by the driver.



The trend in longitudinal acceleration, which is important in restarts, cornering outtings and braking.



The trend of the Yaw Rate, that gives an idea of the curves carried out and of the intensity of the same curve coupled to the sideslip angle that the vehicle generates.



Once the parameters of the standard configuration have been analysed, it is possible to proceed with the max performance manoeuvre in iteration for each individual parameter considered in hourscedence, evaluating the best configuration to minimise lap time.

2. COG Optimization on Track

Having a reference condition to be evaluated, we can focus on the previous analysis of parameters to understand if is possible to improve the performance of our vehicle in this specific race track. All the conditions previously tested for the variation of the centre of gravity have been evaluated and overlapping MaxPerformance manoeuvres have been started. The result is the need for a slightly forward centre of gravity, which would help the front wheels to acquire greater vertical load, and thus have a better performance when cornering. The position considered suitable for the centre of gravity is therefore 709.0 mm, even if the range between 680 mm and 720 mm is considered valid. It should be noted that if you advance your potion too far (over 609 mm) the positive effect disappears and you fall back into the pressure drop at the rear.

Comparing this analysis to the previous standard case, we can evaluate the corresponding performance gains, according to the following indicators:

| Performance Parameter | Standard Vehicle | COG Optimization | Delta Value |
|-----------------------------------|------------------|------------------|-------------|
| Lap Time [s] | 74.781 | 73.978 | -0.803 |
| Lateral Acceleration Max [g] | 1.312 | 1.321 | +0.009 |
| Longitudinal Acceleration Max [g] | 1.560 | 1.626 | +0.166 |
| Longitudinal Speed Max [km/h] | 92.54 | 93.56 | +1.02 |
| Longitudinal Speed Average [km/h] | 50.20 | 50.73 | +0.53 |

3. Wheelbase Optimization on Track

Taking into consideration the wheelbase, after the analyses previously carried out, it is evident that in the following simulated track, there are no particular differences by varying the pitch of a small amount. In fact, by lengthening the wheelbase, the vehicle tends to behave in a more stable way, with a different behavior in the transfer of longitudinal loads, thus improving the performance on the straight. At the same time, this increase in size makes it more difficult for the vehicle to behave in approach to tight curves and, in our specific case, to perform the typical zigzag between cones, present in the FormulaSAE circuits, which we could not implement in the circuit under consideration. For this reason, the advantages provided by having a slightly longer wheelbase are immediately disadvantaged by the greater difficulty in rapid changes of direction. Therefore, since the minimum wheelbase size of a FormulaSAE vehicle is 1525.0 mm, it is considered the best. Below, the table with comparative results:

| Performance Parameter | Standard Vehicle | Wheelbase Optimization | Delta Value |
|-----------------------------------|------------------|------------------------|-------------|
| Lap Time [s] | 74.781 | 74.652 | -0.129 |
| Lateral Acceleration Max [g] | 1.312 | 1.288 | +0.024 |
| Longitudinal Acceleration Max [g] | 1.560 | 1.641 | -0.081 |
| Longitudinal Speed Max [km/h] | 92.54 | 93.44 | +0.90 |
| Longitudinal Speed Average [km/h] | 50.20 | 50.42 | +0.22 |

4. Camber Optimization on Track

With the analysis of the variation of camber angle, it is immediately clear that the parameter difficult to understand in the simulation environment. It is in fact closely dependent on the rubber, and its condition. Parameters such as tyre pressure, asphalt temperature and tread conditions can alter the performance of the same, changing its behavior. According to the analysis and study of the tire used, a negative camber (front and rear) is effective for better wear of the Pirelli tire used and especially to achieve greater lateral acceleration of the vehicle, and increase the performance of the behavior in curves. For this reason, after the evaluations, an ideal value between -1.5 and -2.0 degrees of camber angle was chosen.

| Performance Parameter | Standard Vehicle | Camber Optimization | Delta Value |
|-----------------------------------|------------------|---------------------|-------------|
| Lap Time [s] | 74.781 | 74.531 | -0.250 |
| Lateral Acceleration Max [g] | 1.312 | 1.340 | +0.028 |
| Longitudinal Acceleration Max [g] | 1.560 | 1.556 | -0.004 |

| | | | |
|--|-------|-------|-------|
| Longitudinal Speed Max [km/h] | 92.54 | 92.42 | -0.12 |
| Longitudinal Speed Average [km/h] | 50.20 | 50.16 | -0.04 |

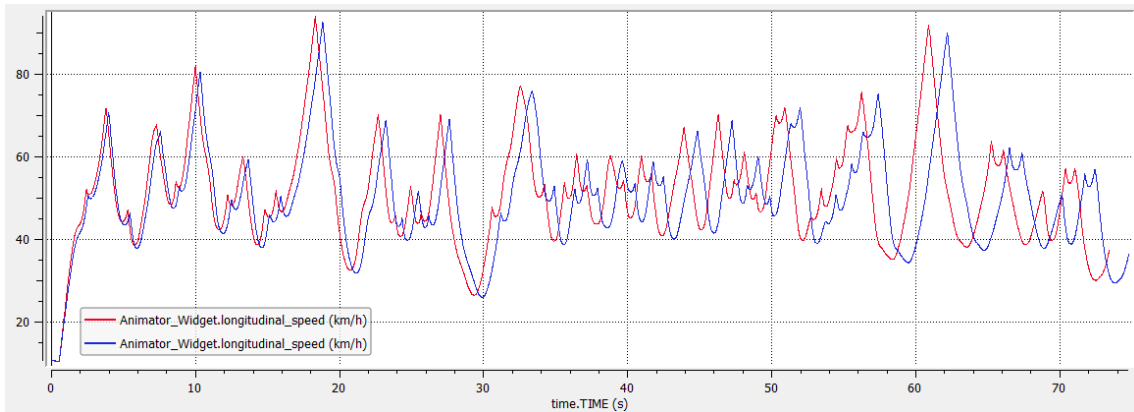
5. Toe in-out Optimization on Track

Like the camber angle, toe angle analysis is difficult and closely related to suspension geometry and rubber. In this case, however, from MaxPerformance simulations and previous analyses, it was evident that a toe out value at the front and toe in at the rear, provides greater performance and a lower lap time. The range considered optimal for is between -0.5 and -1.0 at the front and +0.5 and +1.0 at the rear.

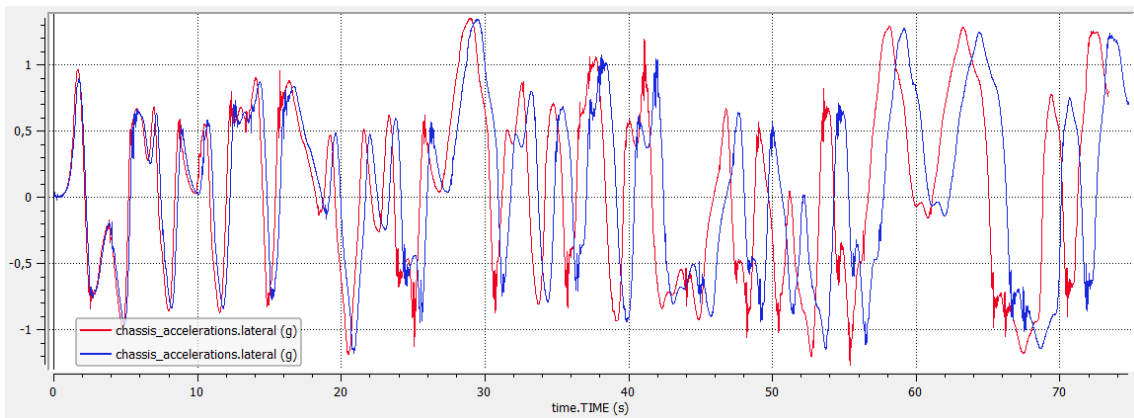
| Performance Parameter | Standard Vehicle | Toe Angle Optimization | Delta Value |
|--|-------------------------|-------------------------------|--------------------|
| Lap Time [s] | 74.781 | 74.541 | -0.240 |
| Lateral Acceleration Max [g] | 1.312 | 1.315 | +0.003 |
| Longitudinal Acceleration Max [g] | 1.560 | 1.600 | +0.004 |
| Longitudinal Speed Max [km/h] | 92.54 | 93.11 | +0.57 |
| Longitudinal Speed Average [km/h] | 50.20 | 50.36 | +0.16 |

6.2 Evaluations and Results

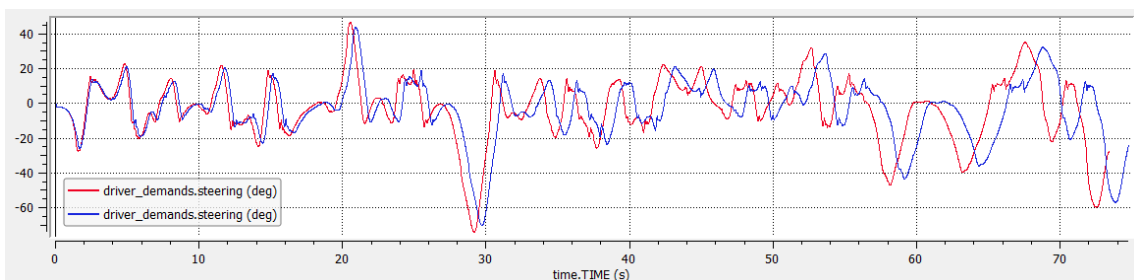
Having obtained the above considerations, it is now possible to simulate in MaxPerformance the vehicle with the modified parameters and evaluate its performance with respect to the previous condition considered standard. Plots with overlapping vehicles are presented below:

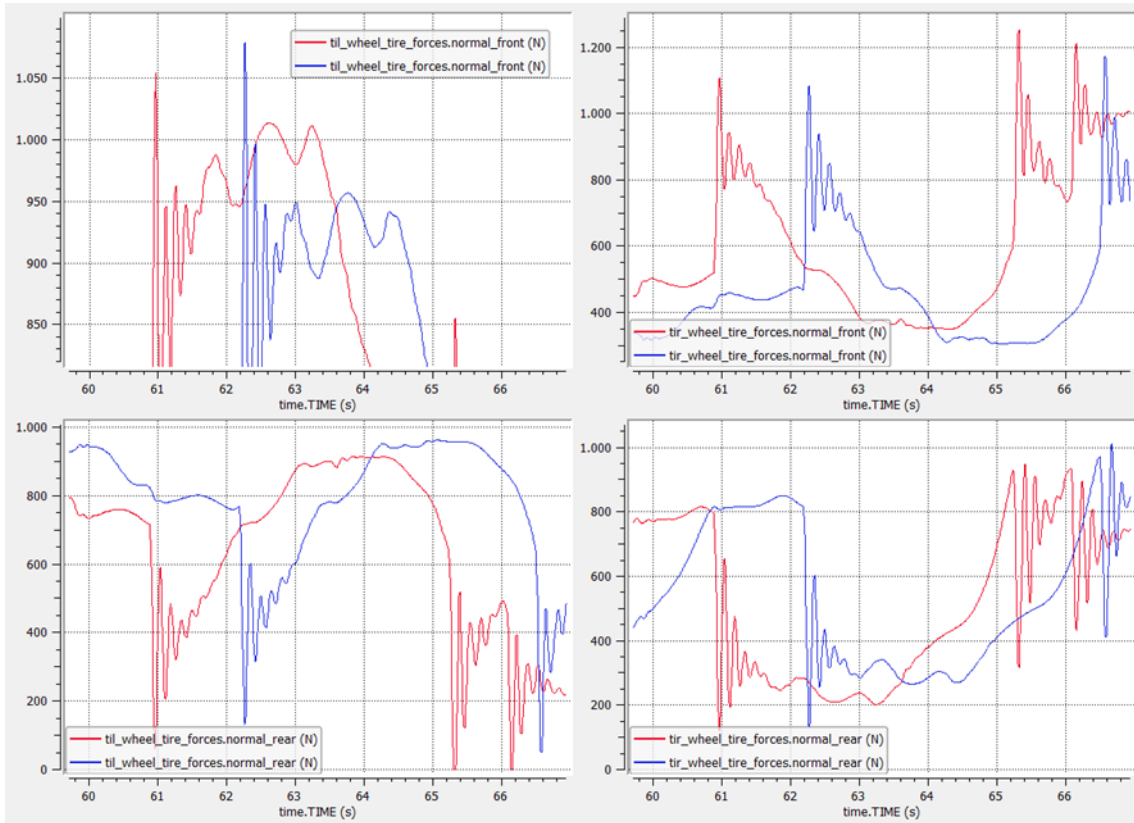


The different speed of the vehicle reached is evaluated, with the evident saving in time on the turn of the optimized curve.



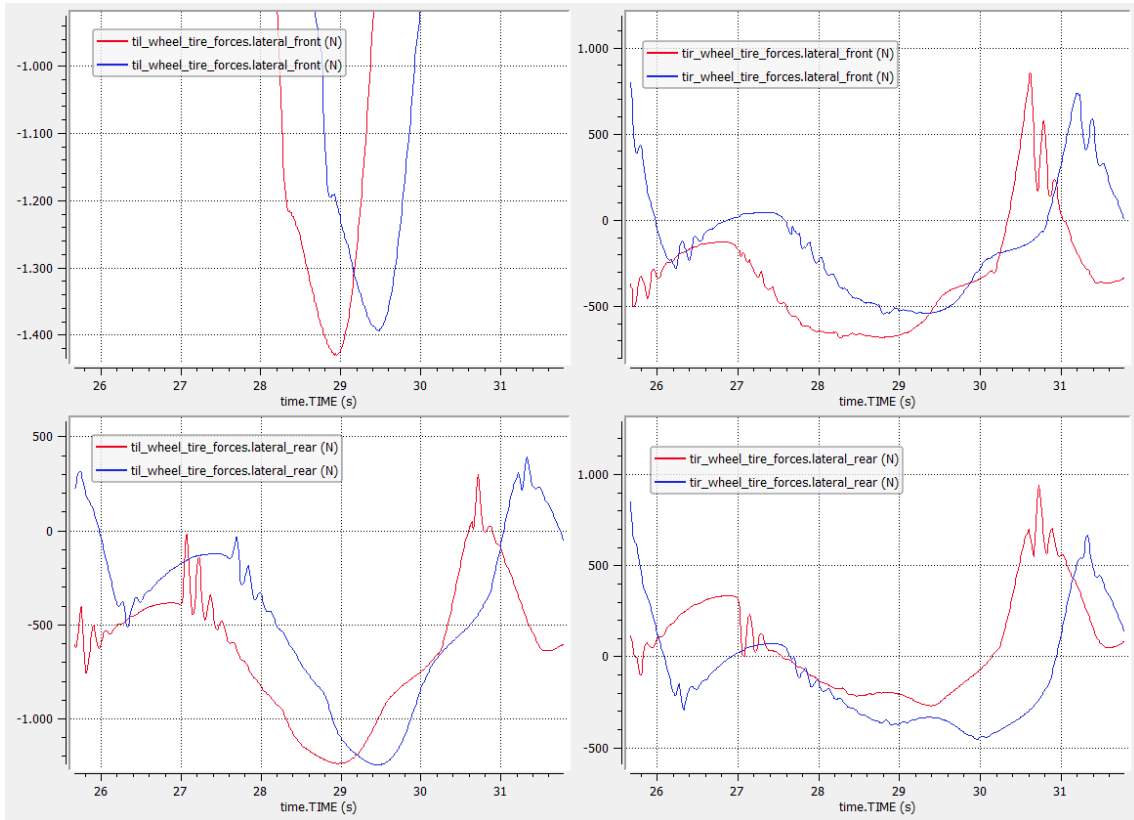
The same consideration is given to the lateral acceleration achieved, although in this case the differences in the peaks are smaller. Underneath is the curve of the request at the steering wheel.





In the graphs above, the normal forces acting on the individual wheels were plotted in detail during the approach and travel of a curve, to assess their trends. The oscillation of the normal force due to the curve input with the oscillations generated by the load transfers is clearly visible.

In the graphs below, at the same motion, it is possible to visualize in detail the lateral forces produced, during the curve with the greatest acceleration peak of the track. The outer wheels, in this case on the left, reach force peaks of more than 1400 N in the optimized configuration.



Finally, the performance parameters of the optimized final solution can be evaluated.

| Performance Parameter | Standard Vehicle | Max Performance Optimization | Delta Value |
|-----------------------------------|------------------|------------------------------|-------------|
| Lap Time [s] | 74.781 | 73.242 | -1.539 |
| Lateral Acceleration Max [g] | 1.312 | 1.354 | +0.042 |
| Longitudinal Acceleration Max [g] | 1.560 | 1.608 | +0.048 |
| Longitudinal Speed Max [km/h] | 92.54 | 93.95 | +1.41 |
| Longitudinal Speed Average [km/h] | 50.20 | 51.12 | +0.92 |

Chapter 7

7.1 Conclusions

To sum up, focusing on 4 parameters typical of dynamics, the performance of the vehicle has been optimized, reducing lap time and increasing the handling characteristics. All this only makes sense, of course, if the vehicle model considered is validated on the track, and this will be part of a future thesis. Nevertheless, the simulation gives a clear idea of the parameters on which you can act to make your vehicle more performing in Formula SAE races. Often the tendency is in fact to set the vehicle with a single configuration, from Trade Off to the 4 tests (very different from each other) with different needs between them, although instead, acting on the vehicle with small corrections, you can get a great final performance. This thesis, in addition to providing evidence of an improvement in vehicle performance in numerical terms, is also intended to be an idea for a standard method to be applied in the future, for the design of new FormulaSAE vehicles or for the analysis and adaptation of your vehicle (already built) before a race test.

7.2 Acknowledgements

Testing a vehicle, measuring it, understanding its behaviour, analysing it, first with the eyes and then with the graphs, understanding its operation, finding the specific point where it could be better and optimizing it was something I discovered with Formula SAE and that has led me to do this for the sake of my job, every day.

I owe all this to the passion for vehicles and technology that this university course has given birth to and grown in me. The contribution of Formula SAE and my friends from the Racing Team was essential and indispensable. I thank all of them, starting with Professor Andrea Tonoli, the team manager, who has always supported me, helped me and made me grow, taking inspiration from him as an excellent engineer and exceptional person. I would like to thank in particular the vehicle dynamics team including Andrea and Stefano, who taught me everything I didn't know yet, and Luca and Marco, who helped me a lot in the development of this thesis, while I was already working. I thank Federico, Ettore and Alessio with whom I shared all the best and worst moments in the team and outside the team, who were colleagues and have become great friends.

I must not forget to thank my employer Andrea, who allowed me to be here today, and continues to pass on to me the same passions for automotive and engineering, which I began to glimpse at the beginning of my career. A special thanks to Nikita, who supported and took great care of me, especially washing my dishes and dirty clothes, every night, for too long now.

Finally, but more important than anyone else, I thank my parents, my sister, my grandparents and uncles, who from behind the curtain, almost invisible to the scene but always present, are the driving force behind all this.

Thank you.

Bibliography

- [1] Genta, G., Morello, L., 2009, "*The Automotive Chassis*", Springer Netherlands
- [2] Milliken W. F., Milliken D.L., 1995, "*Race Car Vehicle Dynamics*", SAE International
- [3] Vi-grade, 2018, "*Vi-CarRealTime 18.2 Documentation*", Vi-grade GmbH
- [4] Schommer A., Soliman P., Farias L. T., Martins M., 2015, "*Analysis of a Formula SAE Vehicle Suspension: Chassis Tuning*", SAE International
- [5] Fredrick J., Randall A., 2006, "*Simplified Tools and Methods for Chassis and Vehicle Dynamics Development for FSAE Vehicles*", University of Cincinnati
- [6] Galanti A., 2005, "Reti E Sistemi Per L'automazione", Università di Parma
- [7] Barsacchi S., 2015, "*Analisi di test dinamici da telemetria di una vettura formula SAE*", Università di Trento

APPENDIX

PIRELLI FSAE TIRE CHARACTERISTICS

[MDI_HEADER]

```
FILE_TYPE      ='tir'  
FILE_VERSION   =3.0  
FILE_FORMAT    ='ASCII'  
!: FILE_NAME : 3Z457.mat  
!: TIRE_VERSION : MF-Tyre 5.2  
!: MF-TOOL TEMPLATE : acar12_mftyre52    $Revision: 1.3 $  
!: COMMENT :   Tire          SlickDM  
!: COMMENT :   Manufacturer  Pirelli  
!: COMMENT :   Nom. section width (m) 0.18  
!: COMMENT :   Nom. aspect ratio (-) 0.53  
!: COMMENT :   Infl. pressure (Pa) 100000  
!: COMMENT :   Rim radius (m) 0.1651  
!: COMMENT :   Test speed (m/s) 22.2222  
!: COMMENT :   Road surface  
!: COMMENT :   Road condition  
!: FILE_FORMAT : ASCII  
!: DATESTAMP : Feb-02-2016 - 03:39:18 PM  
!: USER : MF-Tool 6.1  
!: Copyright TNO, Feb-02-2016 - 03:39:18 PM
```

! USE_MODE specifies the type of calculation performed:

```
! 0: Fz only, no Magic Formula evaluation  
! 1: Fx,My only  
! 2: Fy,Mx,Mz only  
! 3: Fx,Fy,Mx,My,Mz uncombined force/moment calculation  
! 4: Fx,Fy,Mx,My,Mz combined force/moment calculation  
! +10: including relaxation behaviour  
! *-1: mirroring of tyre characteristics  
!  
! example: USE_MODE = 4 implies:  
! -calculation of Fy,Mx,Mz only  
! -including relaxation effects  
! -mirrored tyre characteristics
```

\$-----units

[UNITS]

```
LENGTH      ='meter'  
FORCE       ='newton'  
ANGLE       ='radians'  
MASS        ='kg'  
TIME        ='second'
```

\$-----model

[MODEL]

```
PROPERTY_FILE_FORMAT ='MF-TYRE'  
TYPE                 ='CAR'  
FITTYP               = 6          $Magic Formula Version number  
USE_MODE              = 14        $Tyre use switch (IUSED)  
MFSAFE1               = 99  
MFSAFE2               = 99
```

```

MFSAFE3      =
VXLOW        = 1
LONGVL       = 22.2222      $Measurement speed
$-----dimensions
[DIMENSION]
UNLOADED_RADIUS = 0.26286      $Free tyre radius
WIDTH          = 0.18         $Nominal section width of the tyre
ASPECT_RATIO   = 0.53         $Nominal aspect ratio
RIM_RADIUS     = 0.1651       $Nominal rim radius
RIM_WIDTH      = 0.1778       $Rim width
$-----shape
[SHAPE]
{radial width}
1.0 0.0
1.0 0.4
1.0 0.9
0.9 1.0
$-----parameter
[VERTICAL]
VERTICAL_STIFFNESS = 143087      $Tyre vertical stiffness
VERTICAL_DAMPING   = 500        $Tyre vertical damping
BREFF              = 8.2791      $Low load stiffness e.r.r.
DREFF              = 0          $Peak value of e.r.r.
FREFF              = 0.029319    $High load stiffness e.r.r.
FNOMIN             = 1200        $Nominal wheel load
$-----long_slip_range
[LONG_SLIP_RANGE]
KPUMIN             = -1         $Minimum valid wheel slip
KPUMAX             = 1         $Maximum valid wheel slip
$-----slip_angle_range
[SLIP_ANGLE_RANGE]
ALPMIN             = -3.15      $Minimum valid slip angle
ALPMAX             = 3.15      $Maximum valid slip angle
$-----inclination_slip_range
[INCLINATION_ANGLE_RANGE]
CAMMIN             = -3.15      $Minimum valid camber angle
CAMMAX             = 3.15      $Maximum valid camber angle
$-----vertical_force_range
[VERTICAL_FORCE_RANGE]
FZMIN              = 0          $Minimum allowed wheel load
FZMAX              = 8000       $Maximum allowed wheel load
$-----scaling
[SCALING_COEFFICIENTS]
LFZO               = 1          $Scale factor of nominal (rated) load
LCX                = 1          $Scale factor of Fx shape factor
LMUX               = 1          $Scale factor of Fx peak friction coefficient
LEX                = 1          $Scale factor of Fx curvature factor
LKX                = 1          $Scale factor of Fx slip stiffness
LHX                = 1          $Scale factor of Fx horizontal shift
LVX                = 1          $Scale factor of Fx vertical shift
LGAX               = 1          $Scale factor of camber for Fx
LCY                = 1          $Scale factor of Fy shape factor
LMUY               = 1          $Scale factor of Fy peak friction coefficient
LEY                = 1          $Scale factor of Fy curvature factor
LKY                = 1          $Scale factor of Fy cornering stiffness
LHY                = 1          $Scale factor of Fy horizontal shift
LVY                = 1          $Scale factor of Fy vertical shift
LGAY               = 1          $Scale factor of camber for Fy

```

| | | |
|-----------------------------|---------------|---|
| LTR | = 1 | \$Scale factor of Peak of pneumatic trail |
| LRES | = 1 | \$Scale factor for offset of residual torque |
| LGAZ | = 1 | \$Scale factor of camber for Mz |
| LXAL | = 1 | \$Scale factor of alpha influence on Fx |
| LYKA | = 1 | \$Scale factor of alpha influence on Fx |
| LVIKA | = 1 | \$Scale factor of kappa induced Fy |
| LS | = 1 | \$Scale factor of Moment arm of Fx |
| LSGKP | = 1 | \$Scale factor of Relaxation length of Fx |
| LSGAL | = 1 | \$Scale factor of Relaxation length of Fy |
| LGYR | = 1 | \$Scale factor of gyroscopic torque |
| LMX | = 1 | \$Scale factor of overturning couple |
| LVMX | = 1 | \$Scale factor of Mx vertical shift |
| LMY | = 1 | \$Scale factor of rolling resistance torque |
| \$-----longitudinal | | |
| [LONGITUDINAL_COEFFICIENTS] | | |
| PCX1 | = 1.1 | \$Shape factor Cfx for longitudinal force |
| PDX1 | = 1.9046 | \$Longitudinal friction Mux at Fznom |
| PDX2 | = -1.0919e-05 | \$Variation of friction Mux with load |
| PDX3 | = -0.0023968 | \$Variation of friction Mux with camber |
| PEX1 | = -1.7839 | \$Longitudinal curvature Efx at Fznom |
| PEX2 | = -2.9831 | \$Variation of curvature Efx with load |
| PEX3 | = -0.59976 | \$Variation of curvature Efx with load squared |
| PEX4 | = -0.87799 | \$Factor in curvature Efx while driving |
| PKX1 | = 84.2926 | \$Longitudinal slip stiffness Kfx/Fz at Fznom |
| PKX2 | = 7.2266 | \$Variation of slip stiffness Kfx/Fz with load |
| PKX3 | = 0 | \$Exponent in slip stiffness Kfx/Fz with load |
| PHX1 | = -0.00097729 | \$Horizontal shift Shx at Fznom |
| PHX2 | = -0.0036579 | \$Variation of shift Shx with load |
| PVX1 | = 0.041326 | \$Vertical shift Svz/Fz at Fznom |
| PVX2 | = -0.099969 | \$Variation of shift Svz/Fz with load |
| RBX1 | = 27.9734 | \$Slope factor for combined slip Fx reduction |
| RBX2 | = 49.6462 | \$Variation of slope Fx reduction with kappa |
| RCX1 | = 0.88549 | \$Shape factor for combined slip Fx reduction |
| REX1 | = -4.8907 | \$Curvature factor of combined Fx |
| REX2 | = 0 | \$Curvature factor of combined Fx with load |
| RHX1 | = 0 | \$Shift factor for combined slip Fx reduction |
| PTX1 | = 2.4029 | \$Relaxation length SigKap0/Fz at Fznom |
| PTX2 | = 2.6901 | \$Variation of SigKap0/Fz with load |
| PTX3 | = 1.1237 | \$Variation of SigKap0/Fz with exponent of load |
| \$-----overturning | | |
| [OVERTURNING_COEFFICIENTS] | | |
| QSX1 | = -0.1 | \$Lateral force induced overturning moment |
| QSX2 | = 0.99986 | \$Camber induced overturning couple |
| QSX3 | = 0.012484 | \$Fy induced overturning couple |
| \$-----lateral | | |
| [LATERAL_COEFFICIENTS] | | |
| PCY1 | = 1.5224 | \$Shape factor Cfy for lateral forces |
| PDY1 | = 1.7027 | \$Lateral friction Muy |
| PDY2 | = -0.21677 | \$Variation of friction Muy with load |
| PDY3 | = -2.1986 | \$Variation of friction Muy with squared camber |
| PEY1 | = -0.3375 | \$Lateral curvature Efy at Fznom |
| PEY2 | = -0.86215 | \$Variation of curvature Efy with load |
| PEY3 | = -0.41158 | \$Zero order camber dependency of curvature Efy |
| PEY4 | = -3.1195 | \$Variation of curvature Efy with camber |
| PKY1 | = -55.9878 | \$Maximum value of stiffness Kfy/Fznom |
| PKY2 | = 1.1877 | \$Load at which Kfy reaches maximum value |
| PKY3 | = 0.002871 | \$Variation of Kfy/Fznom with camber |
| PHY1 | = 0.0018126 | \$Horizontal shift Shy at Fznom |

| | | |
|------|---------------|---|
| PHY2 | = 0.0014139 | \$Variation of shift S _{hy} with load |
| PHY3 | = 0.0099991 | \$Variation of shift S _{hy} with camber |
| PVY1 | = -0.061725 | \$Vertical shift in S _{vy} /F _z at F _{znom} |
| PVY2 | = 0.049626 | \$Variation of shift S _{vy} /F _z with load |
| PVY3 | = -2.3689 | \$Variation of shift S _{vy} /F _z with camber |
| PVY4 | = -1.1691 | \$Variation of shift S _{vy} /F _z with camber and load |
| RBY1 | = 29.4898 | \$Slope factor for combined F _y reduction |
| RBY2 | = 35.2338 | \$Variation of slope F _y reduction with alpha |
| RBY3 | = -0.0010285 | \$Shift term for alpha in slope F _y reduction |
| RCY1 | = 0.998 | \$Shape factor for combined F _y reduction |
| REY1 | = -0.20747 | \$Curvature factor of combined F _y |
| REY2 | = 0.57275 | \$Curvature factor of combined F _y with load |
| RHY1 | = -0.00092886 | \$Shift factor for combined F _y reduction |
| RHY2 | = -2.9967e-09 | \$Shift factor for combined F _y reduction with load |
| RVY1 | = -0.032069 | \$Kappa induced side force S _{vyk} /M _{uy} *F _z at F _{znom} |
| RVY2 | = -0.05585 | \$Variation of S _{vyk} /M _{uy} *F _z with load |
| RVY3 | = 1.7625 | \$Variation of S _{vyk} /M _{uy} *F _z with camber |
| RVY4 | = 27.0998 | \$Variation of S _{vyk} /M _{uy} *F _z with alpha |
| RVY5 | = 2.1199 | \$Variation of S _{vyk} /M _{uy} *F _z with kappa |
| RVY6 | = 16.8489 | \$Variation of S _{vyk} /M _{uy} *F _z with atan(kappa) |
| PTY1 | = 2.8955 | \$Peak value of relaxation length SigAlp0/R0 |
| PTY2 | = 1.4795 | \$Value of F _z /F _{znom} where SigAlp0 is extreme |

\$-----rolling resistance

[ROLLING_COEFFICIENTS]

| | | |
|------|--------|---|
| QSY1 | = 0.01 | \$Rolling resistance torque coefficient |
| QSY2 | = 0.1 | \$Rolling resistance torque depending on F _x |
| QSY3 | = 0 | \$Rolling resistance torque depending on speed |
| QSY4 | = 0 | \$Rolling resistance torque depending on speed ^4 |

\$-----aligning

[ALIGNING_COEFFICIENTS]

| | | |
|-------|--------------|---|
| QBZ1 | = 20.5623 | \$Trail slope factor for trail B _{pt} at F _{znom} |
| QBZ2 | = -9.7942 | \$Variation of slope B _{pt} with load |
| QBZ3 | = -6.8393 | \$Variation of slope B _{pt} with load squared |
| QBZ4 | = 0.084553 | \$Variation of slope B _{pt} with camber |
| QBZ5 | = 1.0902 | \$Variation of slope B _{pt} with absolute camber |
| QBZ9 | = 36.2535 | \$Slope factor Br of residual torque M _{zr} |
| QBZ10 | = 2.6633 | \$Slope factor Br of residual torque M _{zr} |
| QCZ1 | = 1.1851 | \$Shape factor C _{pt} for pneumatic trail |
| QDZ1 | = 0.11243 | \$Peak trail D _{pt} " = D _{pt} *(F _z /F _{znom} *R0) |
| QDZ2 | = 0.028435 | \$Variation of peak D _{pt} " with load |
| QDZ3 | = 0.49635 | \$Variation of peak D _{pt} " with camber |
| QDZ4 | = -18.7256 | \$Variation of peak D _{pt} " with camber squared |
| QDZ6 | = 0.0018402 | \$Peak residual torque D _{mr} " = D _{mr} /(F _z *R0) |
| QDZ7 | = 0.0026923 | \$Variation of peak factor D _{mr} " with load |
| QDZ8 | = -1.2749 | \$Variation of peak factor D _{mr} " with camber |
| QDZ9 | = -0.12722 | \$Variation of peak factor D _{mr} " with camber and load |
| QEZ1 | = -1.7611 | \$Trail curvature E _{pt} at F _{znom} |
| QEZ2 | = -4.3901 | \$Variation of curvature E _{pt} with load |
| QEZ3 | = -16.2689 | \$Variation of curvature E _{pt} with load squared |
| QEZ4 | = 0.79028 | \$Variation of curvature E _{pt} with sign of Alpha-t |
| QEZ5 | = -1.353 | \$Variation of E _{pt} with camber and sign Alpha-t |
| QHZ1 | = 0.004522 | \$Trail horizontal shift S _{ht} at F _{znom} |
| QHZ2 | = -0.0011535 | \$Variation of shift S _{ht} with load |
| QHZ3 | = 0.094433 | \$Variation of shift S _{ht} with camber |
| QHZ4 | = -0.21893 | \$Variation of shift S _{ht} with camber and load |
| SSZ1 | = 0.1 | \$Nominal value of s/R0: effect of F _x on M _z |
| SSZ2 | = 0.039173 | \$Variation of distance s/R0 with F _y /F _{znom} |
| SSZ3 | = 1.0648 | \$Variation of distance s/R0 with camber |

SSZ4 = -2.9347 \$Variation of distance s/R0 with load and camber
 QTZ1 = 0 \$Gyration torque constant
 MBELT = 0 \$Belt mass of the wheel

Parametri Aerodinamica Vi-CRT

k = front downforce Scale factor taken from Modifiers block of Aerodynamic Force panel
 k_ρ = reference density scaling factor, REFERENCE_DENSITY parameter in aer property file
 F_z^{table} = force value interpolated from [FRONT_DOWNFORCE] block of aer property file
 k_{shift}^f = front downforce Shift factor taken from Modifiers block of Aerodynamic Force panel
 V = actual vehicle longitudinal speed
 V_{ref} = reference speed at which the maps have been calculated; REFERENCE_VELOCITY parameter in aer property file

k = rear downforce Scale factor taken from Modifiers block of Aerodynamic Force panel
 k_ρ = reference density scaling factor, REFERENCE_DENSITY parameter in aer property file
 F_z^{table} = rear value interpolated from [REAR_DOWNFORCE] block of aer property file
 k_{shift}^r = rear downforce Shift factor taken from Modifiers block of Aerodynamic Force panel
 V = actual vehicle longitudinal speed
 V_{ref} = reference speed at which the maps have been calculated; REFERENCE_VELOCITY parameter in aer property file

k = center drag force Scale factor taken from Modifiers block of Aerodynamic Force panel
 k_ρ = reference density scaling factor, REFERENCE_DENSITY parameter in aer property file
 F_d^{table} = drag force value interpolated from [DRAG] block of aer property file
 k_{shift}^d = center drag force Shift factor taken from Modifiers block of Aerodynamic Force panel
 V = actual vehicle longitudinal speed
 V_{ref} = reference speed at which the maps have been calculated; REFERENCE_VELOCITY parameter in aer property file